

University of Windsor

Scholarship at UWindor

Electronic Theses and Dissertations

Theses, Dissertations, and Major Papers

2010

Instrumentation and Modal Modeling of a Commercial Wind Turbine

Adam Mourad
University of Windsor

Follow this and additional works at: <https://scholar.uwindsor.ca/etd>

Recommended Citation

Mourad, Adam, "Instrumentation and Modal Modeling of a Commercial Wind Turbine" (2010). *Electronic Theses and Dissertations*. 8072.

<https://scholar.uwindsor.ca/etd/8072>

This online database contains the full-text of PhD dissertations and Masters' theses of University of Windsor students from 1954 forward. These documents are made available for personal study and research purposes only, in accordance with the Canadian Copyright Act and the Creative Commons license—CC BY-NC-ND (Attribution, Non-Commercial, No Derivative Works). Under this license, works must always be attributed to the copyright holder (original author), cannot be used for any commercial purposes, and may not be altered. Any other use would require the permission of the copyright holder. Students may inquire about withdrawing their dissertation and/or thesis from this database. For additional inquiries, please contact the repository administrator via email (scholarship@uwindsor.ca) or by telephone at 519-253-3000ext. 3208.

Instrumentation and Modal Modeling of a Commercial Wind Turbine

By

Adam Mourad

A Thesis

**Submitted to the Faculty of Graduate Studies
through Civil Engineering
in Partial Fulfillment of the Requirements for
the Degree of Master of Applied Science at the
University of Windsor**

Windsor, Ontario, Canada

2010

© 2010 Adam Mourad



Library and Archives
Canada

Published Heritage
Branch

395 Wellington Street
Ottawa ON K1A 0N4
Canada

Bibliothèque et
Archives Canada

Direction du
Patrimoine de l'édition

395, rue Wellington
Ottawa ON K1A 0N4
Canada

Your file *Votre référence*
ISBN: 978-0-494-70583-4
Our file *Notre référence*
ISBN: 978-0-494-70583-4

NOTICE:

The author has granted a non-exclusive license allowing Library and Archives Canada to reproduce, publish, archive, preserve, conserve, communicate to the public by telecommunication or on the Internet, loan, distribute and sell theses worldwide, for commercial or non-commercial purposes, in microform, paper, electronic and/or any other formats.

The author retains copyright ownership and moral rights in this thesis. Neither the thesis nor substantial extracts from it may be printed or otherwise reproduced without the author's permission.

In compliance with the Canadian Privacy Act some supporting forms may have been removed from this thesis.

While these forms may be included in the document page count, their removal does not represent any loss of content from the thesis.

AVIS:

L'auteur a accordé une licence non exclusive permettant à la Bibliothèque et Archives Canada de reproduire, publier, archiver, sauvegarder, conserver, transmettre au public par télécommunication ou par l'Internet, prêter, distribuer et vendre des thèses partout dans le monde, à des fins commerciales ou autres, sur support microforme, papier, électronique et/ou autres formats.

L'auteur conserve la propriété du droit d'auteur et des droits moraux qui protègent cette thèse. Ni la thèse ni des extraits substantiels de celle-ci ne doivent être imprimés ou autrement reproduits sans son autorisation.

Conformément à la loi canadienne sur la protection de la vie privée, quelques formulaires secondaires ont été enlevés de cette thèse.

Bien que ces formulaires aient inclus dans la pagination, il n'y aura aucun contenu manquant.


Canada

Author's Declaration of Originality

I hereby certify that I am the sole author of this thesis and that no part of this thesis has been published or submitted for publication.

I certify that, to the best of my knowledge, my thesis does not infringe upon anyone's copyright nor violate any proprietary rights and that any ideas, techniques, quotations, or any other material from the work of other people included in my thesis, published or otherwise, are fully acknowledged in accordance with the standard referencing practices. Furthermore, to the extent that I have included copyrighted material that surpasses the bounds of fair dealing within the meaning of the Canada Copyright Act, I certify that I have obtained a written permission from the copyright owner(s) to include such material(s) in my thesis and have included copies of such copyright clearances to my appendix.

I declare that this is a true copy of my thesis, including any final revisions, as approved by my thesis committee and the Graduate Studies office, and that this thesis has not been submitted for a higher degree to any other University or Institution.

Abstract

With commercial wind power generation coming of age, the majority of research and development has gone into the design of turbine blades and the components within the nacelle, leaving the turbine mast largely ignored. The author proposes a system for the instrumentation and monitoring the modal properties of a commercial wind turbine, as well as the design and creation of a model suitable for use in wind tunnel tests. This is accomplished via a combination of experimental and theoretical methods. A system for structural monitoring of the turbine will allow for early warning and preventive maintenance of masts in the field. The model will focus on conditions where failure of the mast is most likely to occur, such as severe weather events. These tools will prove valuable in the design of masts as well as siting for wind farms.

Dedication

To my colleagues in the office, the boys around the table who still think I'm milling grain, and above all, to the one person who walked the fine line between encouragement and harassment.

Acknowledgements

My thanks goes out to all the people who offered their help, support, and patience throughout this project. I would first like to acknowledge my advisors Dr. Carriveau and Dr. Ting whose abilities as teachers, mentors and sounding boards, made this project a success. Also, I would like to express my gratitude to the University's technical staff, whose formidable skills turned ink into steel and ideas into reality.

Additionally I would like to thank Dr. Cheng and Dr. Zamani for their insights and agreeing to sit on my committee.

Finally I would like to thank my family and my fiancé who have always been by my side.

Table of Contents

Author's Declaration of Originality	iii
Abstract	iv
Dedication	v
Acknowledgements	vi
List of Tables	ix
List of Figures	x
List of Appendices	xi
List of Symbols and Abbreviations.....	xii
1.0 Introduction.....	1
2.0 Literature Review.....	2
2.1 Significance of Research.....	2
2.2 Structural Health Monitoring	3
2.3 Data Acquisition Systems	5
2.3.1 34 m Test Bed.....	7
2.3.2 ATLAS	8
2.3.3 Meteorological Equipment.....	11
2.3.4 Strain Gauges	12
2.4 Computational Modeling.....	14
2.5 Modal Modeling.....	17
3.0 Objectives.....	21
4.0 Data Acquisition System.....	22
4.1 Short Term Data Acquisition System.....	22
4.1.1 Objectives	22
4.1.2 Methodology.....	22
4.1.3 Procedure	23
4.1.4 Results	27
4.2 Long Term Data Acquisition System.....	31
4.2.1 Objectives	32
4.2.2 Methodology.....	32
4.2.3 Procedure	32
4.2.4 Results	33
5.0 Computational Modeling	36
5.1 Objectives.....	36
5.2 Methodology	36
5.3 Procedure.....	39
5.3.1 Matlab	40
5.3.2 ANSYS	40
5.4 Results	40
5.4.1 Matlab.....	40

6.0 Aero-Elastic Model	42
6.1 Objectives	42
6.2 Methodology	42
6.3 Results	45
7.0 Results	46
7.1 Validation of Computational Modeling	46
7.2 Modeling of the Full Scale Wind Turbine.....	47
7.2.1 Data Acquisition System	49
7.3 Modal Model	54
8.0 Future Work	55
9.0 Concluding Remarks.....	57
References	58
Vita Auctoris	95

List of Tables

Table 1: Modal Frequencies and Damping Ratios for a Stationary and a Rotating Darrieus Wind

Turbine

Table 2: Accelerometer Locations on Wind Turbine

Table 3: Modal Assurance Criterion for Wind Turbine

Table 4: Computed Resonance Frequencies of Model and Field Turbine

Table 5: Modal Properties of Stainless Steel Test Specimen

Table 6: Comparison of Results for Resonance Frequencies

Table 7: Comparison of Results for Resonance frequencies for the Wind Turbine

Table 8: Sensor Positions for Detection of Resonance

List of Figures

- Figure 1: Lead-lag Response in 17 m/s winds
- Figure 2: Schematic of a Typical ATLAS Setup
- Figure 3: LIST Turbine in Bushland, TX
- Figure 4: Regression of Priority Inflow on Edgewise Bending in a Turbine Blade
- Figure 5: Residuals After Removal of Dependence on Primary Inflow Parameters
- Figure 6: Schematic of Jindo Bridge Model
- Figure 7: Location of Accelerometer Positions on Wind Turbine
- Figure 8: Exterior of Field Turbine
- Figure 9: Interior of Field Turbine
- Figure 10: FRF Function for Wind Turbine on Apr. 29, 2009
- Figure 11: FRF Function for Wind Turbine on Aug. 6, 2009
- Figure 12: Modal Assurance Criterion Matrix
- Figure 13: Fig. 11: Comparison of Accelerometer Sensitivity with Perpendicular Axis's
- Figure 14: R.M. Young 81000 Sonic Anemometer
- Figure 15: Assumed Bending Shape of Beam Elements
- Figure 16: Schematic of Model Stiffness Element
- Figure 17: Test Specimen in Free-Free Boundary Condition
- Figure 18: Test Specimen in Fixed-Free Boundary Condition
- Figure 19: Long Term DAQ Schematic
- Figure 10: FRF Curve for Position 5.0 m above Base
- Figure 21: FRF Curve for Position 15.86 m above Base
- Figure 22: FRF Curve for Position 42.44 m above Base
- Figure 23: FRF Curve for Position 66.0 m above Base
- Figure C1: Mode 1: 224 Hz
- Figure C1: Mode 1: 224 Hz
- Figure C2: Mode 2: 607 Hz
- Figure C3: Mode 3: 1158.6 Hz
- Figure C4: Mode 1: 271.37 Hz
- Figure C5: Mode 2: 732.44 Hz
- Figure C6: Mode 3: 1389.62 Hz
- Figure C7: Mode 1: 46.21 Hz
- Figure C8: Mode 2: 285 Hz
- Figure C9: Mode 3: 776.68 Hz
- Figure E1: Resonance Frequencies of Test Specimen in Still Air
- Figure E2: Resonance Frequencies of Test Specimen in 7 m/s Wind
- Figure E3: Mode 1, 12.23 Hz: Still Air
- Figure E4: Mode 1, 12.55 Hz: 7 m/s Wind
- Figure E5: Mode 2, 99.16 Hz: Still Air
- Figure E6: Mode 2, 98.41 Hz: 7 m/s Wind
- Figure E7: Mode 3, 291.71 Hz: Still Air
- Figure E8: Mode 3, 293.61 Hz: 7 m/s Wind

List of Appendices

Appendix A: Calibration and Specification Sheets

Appendix B: ANSYS Reports

Appendix C: Mode Shapes

Appendix D: Matlab Programs

List of Symbols and Abbreviations

Abbreviations

ATLAS- Accurate Time-Linked Data Acquisition System
AWG- American Wire Gauge
BEM- Blade Element Momentum
 C_p - Power Coefficient
DAQ- Data Acquisition System
DOF- Degree of Freedom
DTU- Technical University of Denmark
ENREL- National Renewable Energy Laboratory
FAST- Fatigue, Aerodynamics, Structures, and Turbulence
FEA- Finite Element Analysis
FRF- Frequency Response Function
GPS- Global Positioning system
IEC- International Electrotechnical Commission
IMU- Inertial Measurement Unit
LIST- Long-Term Inflow and Structural Test
MFC- Microfiber Composite
NBU- Nacelle Based Unit
NWTC- National Wind Technology Center
RBU- Rotor Based Unit
SCADAS- Supervisory Control and Data Acquisition System
SNL- Sandia National Laboratories
VAWT- Vertical Axis Wind Turbine

Symbols

E- Modulus of Elasticity
I- Moment of Inertia
k- Stiffness Matrix
K- Stiffness Coefficient
[K]- Generic Stiffness Matrix
L- Length of Element
 l - Characteristic Length
m- Lumped Mass Matrix
 \bar{m} - Mass of Element per Unit Length
[M]- Generic Lumped Mass Matrix
Re- Reynolds Number
 \hat{v} - Vector Representing the Shape of the System
V- Fluid Velocity
x- Distance Along the Beam Element from the Left Hand Side
 ζ - Damping Coefficient
 μ - Fluid Viscosity
 ρ - Fluid Density
 Ψ - Shape function of a Cubic Hermitian Polynomial
 ω - Undamped Natural Frequency
 ω_D - Damped Natural Frequency

1.0 Introduction

In recent years wind power technology has emerged as a competitive and desirable alternative to traditional methods of energy production. As it becomes more feasible, the majority of research has gone towards the design of wind turbine blades and the equipment in the nacelle; as a result, these subjects are discussed heavily in the literature. Far less information is available on the design and analysis of the mast of wind turbines, structures which have failed in the past. The author wishes to investigate one of the failure methods, the excitation of natural frequencies. The excitation of these resonant frequencies is undesirable in structures such as these due to the large forces the resultant displacements exert on the structure.

With this in mind, this paper will cover two subjects regarding the modal properties of the mast of a commercial wind turbine. The first will be the development and implementation of a data acquisition system (DAQ) for use in a commercial wind farm. The main thrust of this exercise is to be able to select the minimum number of locations on the mast of a wind turbine that can be used to indicate if and when resonance is induced in the mast. This is desirable for the sake of preserving the structure by allowing engineers to detect whether or not a turbine is experiencing excitation around its resonance frequencies. If these events are found to occur regularly, steps could then be taken to avoid such occurrences. This is achieved through a combination of theoretical, computational and experimental methods.

The second subject covered in this thesis is the creation of a physical model that exhibits the same modal properties as the wind turbine, and is suitable for use in wind tunnel tests. This will provide a proactive method that will allow engineers to study the effect of severe weather and placement on a potential wind turbine design. Additionally this method could be expanded to the investigation of severe weather events on wind farms as a whole through physical modeling of entire sections of a farm, allowing for exploration of turbine wake interactions on individual units.

2.0 Literature Review

2.1 Significance of Research

Modal analysis in its most basic form is a way of describing a system via the characteristics that determine its natural frequencies. These characteristics are the mass, stiffness, and damping of the structure. The most important result of these qualities relates to what are known as the mode shapes and the natural, or resonant, frequencies. These are the frequencies at which the structure exhibits a greater response in the form of structural deflection and acceleration per unit of force applied to the structure (Avitabile, 2001). Numerous papers have been published on the effects of resonance on structures, usually bridges. The effects on the structure can range from inconvenient, such as the displacements experienced by the Millennium Bridge (Strogatz et al., 2005), to catastrophic, such as the Tacoma Narrows disaster (Billah and Scanlan, 1990). The situation that gave rise to these events occurred when forces acting on the structure oscillate in sync with a resonant frequency of the structure. This allows the force to be amplified over successive oscillations causing the marked increase in amplitude in structural displacement and acceleration (Abdulrehem and Ott, 2009).

Researchers at Riso National Laboratories in Denmark have recently published a paper outlining recent developments and future challenges regarding the design of wind turbines. One specifically mentions the need for greater knowledge of the wind turbine mast. This is important due to the coupling that can occur between the tower and the blades, leading to greater stresses on both (Rasmussen et al., 2003). Driving the need for this knowledge is the current trend of increasing the size of wind turbines to increase energy production. Commercial wind turbines have increased in power output by nearly a factor of ten over the past decade. To enable this level of power extraction the turbines have grown in size by three to four times. As this occurs, the relative stiffness of the tower decreases making its flexibility and damping properties more relevant to the longevity of the turbine. Further exasperating the issue is the fact that as turbine components increase in size, their natural frequencies have the tendency to decrease, bringing them down into the range where they could be more easily excited by

aerodynamic forces and structural interaction (Hansen et al., 2006). Furthermore, as the size increases the financial investment increases as well, making further investigation into previously ignored systems more cost effective.

Recent studies have brought to light evidence that the electrical power systems used in electrical distribution can cause a phenomenon called sub-synchronous resonance, an event in which unintended voltages form in the electrical distribution system can produce a harmonic force within the generator (Varma et al., 2008). When the frequency of this applied force coincides with that of the generator shaft or other components, such as the turbine mast, these modes are excited and failure can occur. This event can excite modes in the low frequency range, about 1 or 2 Hz, and illustrates the importance of studding the natural frequencies of wind turbine masts.

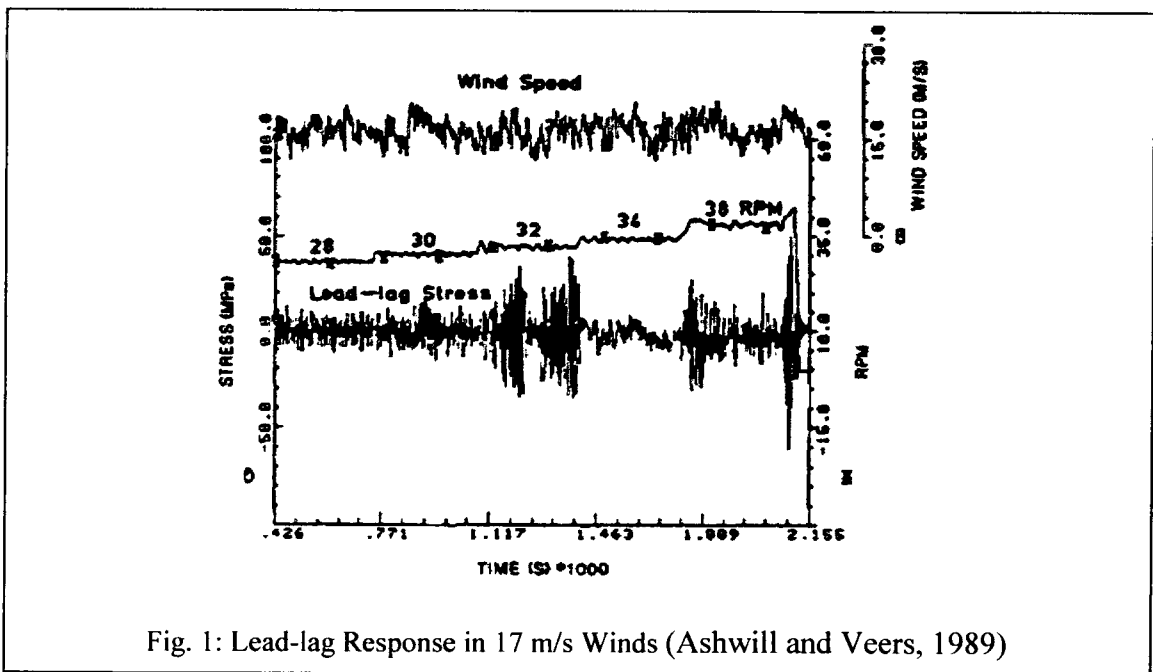
2.2 Structural Health Monitoring

Structural health monitoring is a method by which damage to a structure is detected and, if possible, located through the use of sensors such as strain gauges and accelerometers installed throughout a structure. It is based on the idea of building up a database that makes up a picture of what the response of a new, or “healthy”, structure looks like. Deviation from this baseline is an indication of damage to the structure and ideally, the location and severity of the damage can be ascertained by the system. This has been achieved with varying degrees of success on objects such as composite concrete and steel beams (Chellini et al., 2008). More complex structures such as a highway bridges and the blades of horizontal axis wind turbines have also undergone structural health monitoring and damage localization under controlled conditions (James et al., 1995). This method is dependent on building a healthy state database to use as a datum as well as monitoring the structure for deviation from this baseline.

An approach developed at Sandia National Laboratories (SNL) is used to determine fatigue damage and the subsequent effect of crack growth on the blades of wind turbines. This method is dependent on loads derived from mathematical models or, real loads determined from an operational wind turbine. These values must represent a

lifetime of use for the turbine components and require a long term data acquisition system to provide this information (Veers, 1989).

During a test of the 34 m Test Bed Vertical Axis Wind Turbine (VAWT) at SNL, two unforeseen significant events occurred while this turbine was operating near its resonance frequencies. The first was during a high wind over-speed condition that caused blade resonance. As the wind reached speeds in excess of 20 meters per second, the power production of the turbine exceeded its generator capacity, causing the rotors to rotate faster. As the rotor speed reached 32 rpm, it swept through the first blade edgewise bending mode, causing a subsequent increase in stresses in the structure. As the speed of the turbine further increased to 40 rpm, the first in plane tower bending mode was excited, causing peak to peak stresses of over 100 MPa. The results from this event are graphed in Figure 1.



The second event occurred during a cold day at normal operating speeds. Normally the turbine is operated at a rotational speed above that the resonance frequencies of the guy wires. On this exceptionally cold day, the guy wires underwent thermal contraction, causing an increase in cable tension and subsequently shifting the resonant frequencies

up the spectrum and into the range of the current operating speed of the turbine. This caused excessive vibrations in the cable and a peak to peak strain of nearly 40 MPa in the blades as the cables began affecting the tower. This led to an emergency stop, during which, and for some time after, the cables continued to vibrate excessively (Ashwill and Veers, 1989).

Another approach to structural health monitoring in wind turbines has been the use of impact testing on a healthy wind turbine blade mounted in the field. A comparison is then performed between the initial healthy condition of the blade and that of the blade with simulated damage applied to it by loosening the bolts connecting the blade to the rotor hub. This study was unable to locate or conclusively detect the virtual damage in the blade and the experiment was ruled inconclusive (Gross et al., 1998).

It has been noticed that vibrations in the blades can cause tower vibration. Specifically classical flutter and stall induced vibrations have been investigated. Classical flutter can prove to be problematic in pitch regulated turbines if the blade has been designed with features that make it susceptible to such excitation, or if the tip speed increases beyond its design limit due to over-speed. Stall induced vibration is a problem often seen in stall regulated turbines. As the blade is operated in separated flow conditions, turbulence is generated which acts on the blade. Currently, stall induced vibrations from a deep stall, such as is found in parked turbines, is being looked at due to the large loads that can be exerted upon a machine such as during severe weather (Hansen, 2007).

2.3 Data Acquisition Systems

In the past, field modal analysis has been carried out on many different structures, primarily bridges. As with this paper, the primary goals of these studies have been to determine the dynamic properties and response of the structures conditions found in the field. These studies often use accelerometers placed on the structure to determine its dynamic response, and strain gauges to measure its static response (Sutherland et al., 2001). This is generally satisfactory for structures such as those studied in the past by

SNL and Riso National Laboratories due to their relatively small size of less than 20m in height. When larger structures are tested, a combination of strain gauges and accelerometers used in concert to measure the dynamic response of very low frequency vibrations can yield better results. It has been shown in field tests on the Tsing Yi South Bridge, strain gauges have the ability to display low frequency modes with greater clarity than accelerometers due to the limits on low frequency response that are inherent in these instruments (Ashebo et al., 2007).

In a report by Riso National Laboratories, an applied modal analysis test of wind turbine blades was executed. During selection of excitation methods, they made a decision to use transient excitation supplied via an impact hammer. They cited the difficulties of shaker methods in exciting frequencies below 1.5 Hz as the reason for the decision. In the end they constructed an electrically driven impulse hammer in order to provide repeatability in their measurement campaign (Pendersen and Kristensen, 2003).

It was realized early on during testing of SNL's 17 m VAWT, that full modal testing of a wind turbine was time consuming and labour intensive. It required a team of two people two weeks to adequately characterise the structure. Because of this, the idea of "mini-modal" testing was suggested, the idea that a computational model could be used in conjunction with a modal testing procedure of comparatively small scope could be used to describe the modal properties of the turbine. The theory is that the computational model could be verified and adjusted by this small scale testing. Over the course of this project several methods of structural excitation were investigated including step-relaxation (an excitation method that involves loading the turbine with an anchored cable and then suddenly cutting the cable), human excitation (involving a person physically grabbing and shaking the structure), wind induced or ambient excitation, and impact excitation. It was determined that for small or very flexible structures that a person was capable of moving by hand, human excitation was the most effective and easiest to execute, due to quick set up and ease of implementation. Step excitation was a good second choice, especially for structures that are too stiff or massive to excite by hand (Lauffer et al., 1987).

2.3.1 34 m Test Bed

Early wind turbine tests aimed at characterizing the structural response of a commercial scale wind turbine were carried out by SNL. Their early large scale test turbine was a 34 m VAWT known as the 34-Meter VAWT Test Bed (Carne et al., 1992). The structure initially underwent what they termed substructure modal testing, a method that is used to verify the physical models developed by first testing and then verifying the computational model for each component on its own before testing them together in their installed state. This allows designers to troubleshoot their computational models before the added complications of structural interactions. If all of the individual component tests are predicted by the computational models with reasonable accuracy then it can be assumed that they are correct up to this point. Once the structure is assembled and tested, any discrepancies between the experimental results and the computational model are likely due to the connections between the components, thus giving the designer a starting location for debugging the code. First, the two blades were tested, each blade being composed of five separate sections composed of extruded aluminum, bent to the proper curvature. The blades were then tested in a free-free condition by suspending them by soft bungees. This condition was chosen because it is simple to create in the lab and relatively easy to simulate computationally. Following this, the tower and guy wires were attached and tested. This was done in situ to capture the effect that the unknown boundary condition at the base of the turbine represents. The theoretical model was well validated in this test with the exception of error generated from the structural supports (Carne et al., 1992).

Upon installation, 34 m test bed turbine was experimentally instrumented with permanent strain gauges and removable accelerometers on the blades, mast, and guy wires, and computationally modeled to determine its natural frequencies and mode shapes, thus generating a healthy state baseline against which further tests can be compared. Static, modal and operational tests of the turbine were carried out and showed good correlation between the two results demonstrating that the Finite Element Analysis (FEA) model accurately represented the turbine (Ashwill, 1988).

2.3.2 ATLAS

The ATLAS system consists of two or more DAQ's, one rotor based unit (RBU) and one or more ground based units (GBU) housed on the ground or in the nacelle of the turbine. Of vital importance to the success of this DAQ system, is the implementation of accurate time stamps in order to ensure that all collected data from the various DAQ systems can be precisely related to one another. Without this, the accuracy of the data and operations performed on the collected information becomes suspect. When using relatively high frequency rates, it was found that in one day, two DAQ systems could be out of step by one sample with each other. To solve this issue, SNL began the practice of utilizing Global Positioning System (GPS) receivers to ensure that separate subsystems, such a DAQ systems mounted on the turbine rotor, in the nacelle or tower, and on meteorological towers were in sync with each other. The signals transmitted by GPS satellites allow the disparate systems to remain in synch with each other. Depending on the system configuration, this can be achieved via the installation of a dedicated GPS card connected to a receiving antenna, or through a dedicated GPS unit connected through a serial port connection. Even should the satellite signal be lost for brief periods of time, the onboard clock in the DAQ is sufficiently accurate to allow the data to

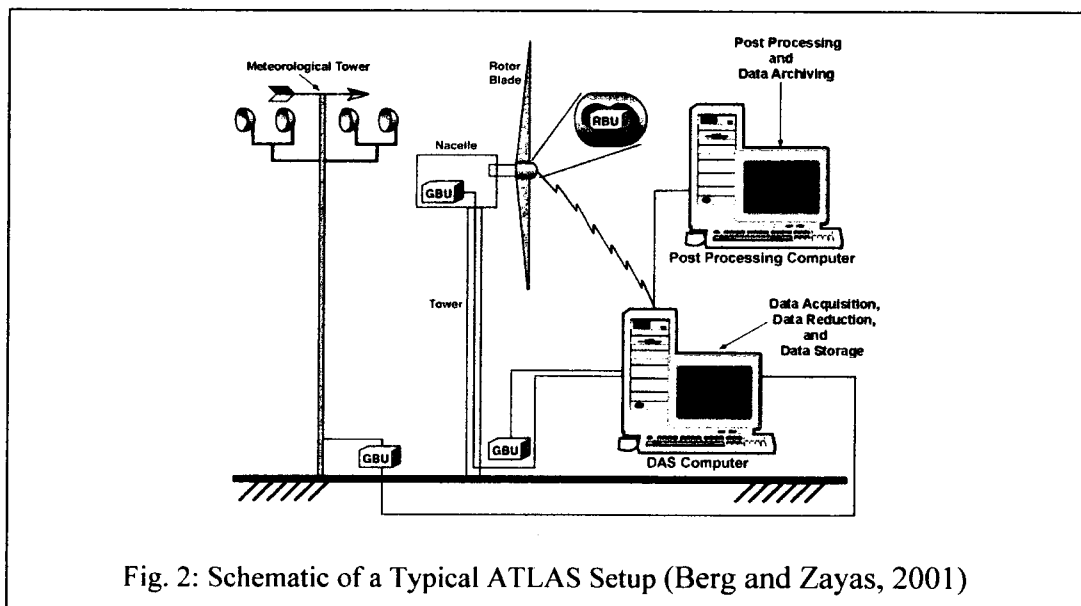


Fig. 2: Schematic of a Typical ATLAS Setup (Berg and Zayas, 2001)

remain in sync for brief periods of signal loss. The data from these remote units can then be transmitted and stored in a master computer either on or off site via spread spectrum radio modems for short range communication or cellular modems when greater distance is required (Berg and Robertson, 1998).

The above research soon developed into one of the best examples of a long term structural monitoring program that has been designed for commercial use. The Long-Term Inflow and Structural Test (LIST) Turbine is a program executed by SNL in Bushland, TX, on a 23 m modified Micon 65/13 turbine. A modal survey of the tower was conducted to locate the first two modes of the structure. The survey was not however, conducted with the nacelle installed and therefore, not indicative of the modal

response of the tower while in service (Sutherland et al., 2001).

The first generation of the data acquisition system is known as the Accurate Time-Linked Data Acquisition System (ATLAS). It employed a rotor based unit that utilized strain gauges to monitor the turbine blades, and another ground based unit to monitor the drive train as well as loading on the turbine tower. This first generation ATLAS system was installed in August of 1998 on an Atlantic Orient Corporation 50 kW turbine in Bushland, TX, seen in Figure 3 (Berg et al., 1999). The tower itself was only instrumented with strain gauges used to detect bending at 3.9 m above the base of the turbine. The remaining strain gauges as well as all of the accelerometers were distributed along the blades and in the nacelle (Sutherland

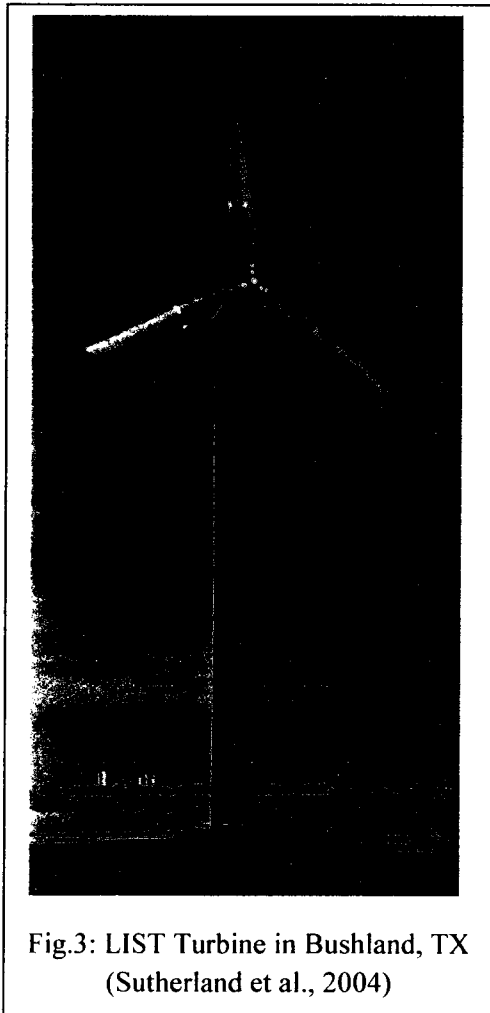


Fig.3: LIST Turbine in Bushland, TX (Sutherland et al., 2004)

et al., 2005).

The DAQ installed on the LIST turbine was designed to characterise the inflow, structural response, and turbine state with 60 sensors, 34, 19, and 7 sensors respectively, in order to develop the most complete picture of the affect that inflow has on the structural response of the turbine. They utilized a scanning rate of 30 Hz for the instrumentation, which yields a Nyquist frequency of 15 Hz that is sufficient to both capture the pertinent information of the turbine as well as prevent aliasing of the signals. This relatively high sampling rate was required to ensure sufficient resolution to capture events that had short time spans and low frequency of occurrence, such as gusts, as the traditional method of averaging out the wind speeds over the ten minute interval provides insufficient resolution to capture such events. They then broke the data into the industry standard of bins of 10 minute interval packages based on the mean wind speed, after discarding data that was below the cut in speed of the turbine determined the correlation of inflow with fatigue on the structure. Their results showed that if the data is captured with sufficient frequency, then a correlation between the inflow and the structural response of the turbine can be readily obtained (Sutherland, 2002).

The LIST program increased its scope with the implementation of a structural monitoring program on a 600 kW turbine located at the National Wind Technology Center (NWTC) near Boulder, CO. This area is a mountainous region meant to stand in contrast to the original turbine site in Bushland, TX, which is representative of a Great Plains site. This turbine was instrumented primarily to monitor flapwise and edgewise bending at the root of the turbine blades. While also incorporated an inertial measurement unit (IMU) installed in the nacelle, the paper presented dealt only with the measurements from the blade itself, and found that a good correlation could be reached between the inflow and the high end of the bending moment distribution (Sutherland and Kelley, 2003).

The ATLAS system was designed to be easily accessible to the public and private companies, and was constructed from off the shelf, commercially available parts. The

main thrust of this system was to monitor the vibrations and strain located in the nacelle and rotor as evidenced by the rotor based data acquisition unit (RBU) as well as the nacelle based data acquisition unit (NBU). One of the most important parts used in this system in the inclusion of separate GPS receivers integrated into each unit that allows all units to be accurately synced with one another (Berg and Zayas, 2001).

More recently, the ATLAS system has received minor upgrades to the to the hardware configuration in order to improve GPS reception among other issues, but the majority of the changes have been to the software component. The interface has recently been upgraded from a combination of the DOS/Windows software to a Windows system that utilizes National Instruments' LabView software. The change was made to make use of LabView's more fluid and easy to understand graphical programming language in order to facilitate that program's goal of creating a DAQ system that is simple to use and easy to implement (Berg et al., 2000).

In the past the major threat to the ATLAS system were lightning strikes(Sutherland et al., 2001). As turbines and requisite meteorological towers are often located in areas where they are the tallest structure, they tend to attract these events. As a result the system was shutdown within ten days of first becoming operational, and these events have been the major source of downtime. In order to remedy this situation, several layers of lightning protection have been implemented. These precautions include an extensive electrical grounding network, connecting all towers, guy wires buildings and electronics cabinets to ground in order to channel the energy away from sensitive electronics, as well as protecting circuits with high speed gas/diode lightning protection circuits and using fibre optics in place of electrical cable where necessary (Sutherland et al., 2001).

2.3.3 Meteorological Equipment

Due to their moving parts, cup anemometers have been found to be more susceptible to failure due to inclement weather; whereas sonic anemometers are less susceptible to damage from environmental conditions such as high wind and hail. To increase

reliability, sonic anemometers can be added to conventional systems, especially in areas subject to severe weather. Specifically, many of the cup anemometers at the site of the LIST turbine in Bushland, TX were destroyed during periods of severe weather (Sutherland et al., 2005).

Despite the apparent shortcomings of cup anemometers they are still useful to have on site. They have been heavily researched and have become the industry standard in the wind energy community, finding homes in various standards and methodologies. Conversely, sonic anemometers have made great strides in the last decade, and their inherent advantages over cup anemometers make them a possible successor. These strengths and shortcomings have both been investigated in the ACCUWIND project (Pedersen et al., 2006). This project attempts to bring emerging technology such as sonic anemometers, into line with industry standards to allow industry access to a broader range of instruments. As a result, it is beneficial to have both instruments on site in order to benefit from the capability of the sonic anemometers while having cup anemometers available to allow straightforward comparison of data between different test sites.

2.3.4 Strain Gauges

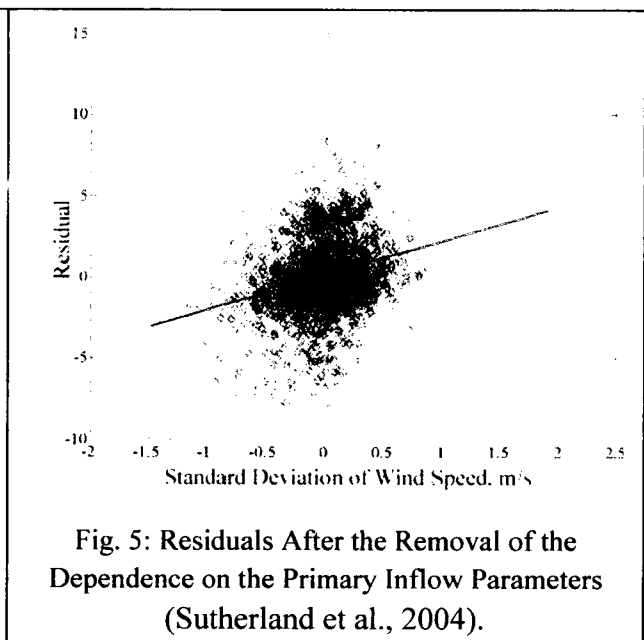
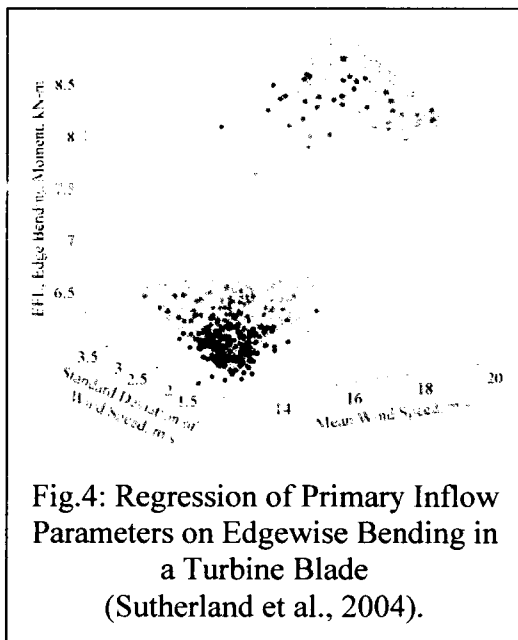
Studies involving the use of strain gauge monitoring of wind turbines can be found in the papers on the Variable Speed Test Bed wind turbines out of SNL. Tests to obtain damage estimates for a machine using a variable speed control algorithm were carried out on a ten meter downwind machine, using strain gauges installed on the turbine blades (Sutherland and Carlin, 1998). Further testing by Sandia was conducted to provide a comparison of different sensor types when used to detect structural damage to the blade during fatigue tests. The experiment used conventional piezoelectric accelerometers and strain gauges as well as micro-fibre composite (MFC) and acoustic sensors. They found that accelerometers and strain gauges were both effective in detecting damage while the acoustic and MFC sensors were notably less so. The acoustic gauges were likely less effective due to the sound attenuation because of the

composite nature of the turbine blade (Rumsey et al., 2008). Further investigation into this experiment yielded evidence that a method of determining optimal sensor locations needed to be found. The sensors on the turbine blade were not ideally arranged to detect and locate the areas in which damage occurred. The biggest challenge is properly locating sensors in a way that can pinpoint locations of damage while still being able to monitor the entire structure. (Rumsey and Paquette, 2008).

RISO National Laboratories launched a project with the goal of advancing wind turbine technology and reducing costs by outlining methods for the structural health monitoring of wind turbine blades. This project was executed in conjunction with the Sensor Technology Center, DELTA, InnospeXion, FORCE Technology and LM Glassfiber (Sorensen et al., 2002). In a way similar to the project conducted by SNL mentioned above, a portion of the project concerned itself with determining what instruments are best for different types of damage detection. They employed acoustic emission, fibre optic micro bend displacement transducers, and strain gauges. During test stops, ultra sonic and X-ray surveillance was employed to monitor the spread of damage. During this test artificial damage was inflicted on the turbine blade in the form of a notch in the laminate at the trailing edge of the blade followed by creating adhesive failure at the trailing edge. The strain gauges were capable of measuring the redistribution of strain in the system caused by the failures. Acoustic emissions were useful for detecting crack propagation before it became visible, as well as being able to determine the position and severity of the damaging events causing the sound. Fiber optic micro-bend displacement transducers can determine crack propagations, and show some promise for use in determining crack size. Finally both the X-ray and ultra-sonic imaging devices are useful in locating the size and location of damage to the blade (Kristensen et al., 2002).

The ATLAS/LIST structural monitoring program provided researchers with a great deal of data. This allowed them to not only monitor, but to also characterise the turbine extensively, and begin research into how various inflow parameters affect turbine component life. A sequential analysis, as opposed to traditional multivariate regression,

was carried out on the LIST test data to determine which of several different parameters may have an effect on component life. Two parameters were used as a basis, the mean wind speed and the standard deviation of the wind speed at hub height, and sixteen other variables were selected to determine their relative importance on turbine lifetime. The study found that the majority of these parameters did not have an appreciable impact on turbine fatigue, especially when compared with the impacts that both mean wind velocity and turbulence (Nelson et al., 2003). Further study into the importance of these variables using long term data gathered through the LIST program corroborated these results, and showed that the sixteen residual variables have almost no impact once removed from mean wind speed and turbulence, as seen in Figure 4 and the importance



of both turbulence and mean wind speed at hub height can be seen in Figure 5 (Sutherland et al., 2004).

RISO, under the Technical University of Denmark (DTU), has begun a commercial wind turbine monitoring program in the same spirit of the LIST project with the added mission of providing turbine data and operational experience to its students. A 36 m tall grid connected, stall regulated Nordtank, NTK 500/41 wind turbine has been installed on campus and instrumented with metrological tools describing inflow, structural

response sensors, control and power measurements and electrical measurements to measure interactions with the power grid. In order to monitor structural response, strain gauges have been placed on the blades, rotor hub, and the turbine tower. The turbine tower sensors consist of two instruments for measuring bending moments at the base of the shaft and one torsional sensor located at the top of the tower. This project has provided a variety of structural response measurements in a long term data set that has proven useful for research and education (Helgesen et al., 2008).

2.4 Computational Modeling

Early computational modeling was conducted on all the turbines worked on by SNL. The 34 m test bed, a darrieus style VAWT, was modeled several ways. While stationary the FEA code NASTRAN was used to determine the gravity loads via a static solution. As the rotor began to turn and speed up, the situation grew more complex and NASTRAN, along with a method developed by SNL, was required to adjust the stiffness matrix by including the effects of centrifugal softening and coriolis forces. This led to a change in the natural frequencies of the turbine as described in Section 2.2 (Ashwill, 1989).

Early experiments comparing FEA and experimental modal analysis techniques were performed at Sandia National Laboratories. Their early test specimen was a 2 m VAWT. They developed a FEA model of the turbine and then conducted modal tests on the specimen through modal impact testing during a standstill state, using a pretensioned cable for excitement for the rotating case, as well as using a combination of strain gauges and accelerometers to collect modal data. The experiment showed that good correlation between the experimental results from both the rotating and stationary tests, and computational results is possible (Carn et al., 1982).

One of the earliest referenced computer codes for determining damage and life expectancy was the Life2 computer code out of SLN. It was a system written in FORTRAN and concerned itself with determining the lifetime of a turbine component by determining when crack initiation and crack growth would occur (Sutherland, 1989).

Currently there are several different types of programs for simulating aeroelastic models of wind turbines available on the market. They range from simple procedures such as those developed by RISO National Laboratory and the International Electrotechnical Commission (IEC) Annex which model the structure as a simple one degree of freedom system that is useful for modeling the first natural frequency of the tower, to more complex full system models such as those put out by Garrad Hassan known as GH Bladed and the Fatigue, Aerodynamics, Structures, and Turbulence (FAST) program developed by the United States National Renewable Energy Laboratory (NREL) (Prowell and Veers, 2009).

RISO has tested a computational aeroelastic modeling software called HawC, a code specifically designed for horizontal axis wind turbines (HAWT). It is a FEA modeling software notable in that it has rotating substructures, such as the rotor and components within the nacelle, which is not satisfactorily handled in other FEA software. It is a code based on representing the structures as two dimensional prismatic elements and divides the structures into three substructures, the rotor, nacelle, and tower. This code has been verified through field tests, with the difference between the computational and experimental values accounted for through drift in the sensors (Larsen and Volund, 1998).

RISO has also investigated the loading case of a locked rotor during severe wind conditions in the KNOW-BLADE project. Currently such loading conditions are based on the Blade Element Momentum (BEM) or the lifting line method, both of which use tables for values of lift and drag for the airfoil. This work investigated the use of computational fluid dynamics to obtain these loads. This method of characterizing the loads on a parked turbine was quite successful at reproducing measured values from field experiments and it is hoped that this method can be used in the future to help refine design parameters for parked turbines (Sorensen et al., 2004).

Operational modal analysis using strain gauges has been performed on wind turbines in order to determine the structural damping of the system. They did not however

implement a long term monitoring system. The exciter methods used involved generating forced responses via generator torque, which is not a method capable of exciting modes above a certain frequency, they also used operational modal analysis (Hansen et al., 2006).

In a study aimed at simplifying aeroelastic models, researchers have attempted to extract equivalent beam properties from wind turbine blades. This procedure attempts to ease the construction of aeroelastic models by taking a structure as complex as a turbine blade and breaking it down into either a single beam element or several beam elements by using loading on the blade to generate a six by six stiffness matrix from which the equivalent beam or beams can be extracted. Currently the process is still in its infancy and relies on passing data between NuMAD, ANSYS, MATLAB, ADAMSpreprocessor, and Excel as well as separate code for each program (Malcolm and Laird, 2007).

Wind turbines have been modeled via FEA, in which the turbine tower, nacelle and blades are all subdivided into beam elements. A report out of RISO National Laboratories modeled the turbine using Timoshenko beam elements and computed aerodynamic forces by the BEM method. Through this method, they have managed to calculate natural frequencies, logarithmic decrements and mode shapes of the aeroelastic turbine modes. The study managed to find good agreement between the computed and experimentally measured damping from a stall regulated 600 kW turbine (Hansen, 2004).

2.5 Modal Modeling

This section deals with the creation of physical, aero-elastic models of various types for the purpose of studying modal properties of wind turbines.

When scaling down large structures, such as the Jindo Bridge in South Korea, mass and stiffness need to be carefully controlled via the selection of materials and placement of masses (Caetano et al., 2000). The Jindo model used an aluminum alloy in order to reduce the stiffness of beam elements. Similarly, masses were required to be added to the cable stays in order to compensate for the extremely light dead weight resulting from using piano wire as seen in Figure 6.

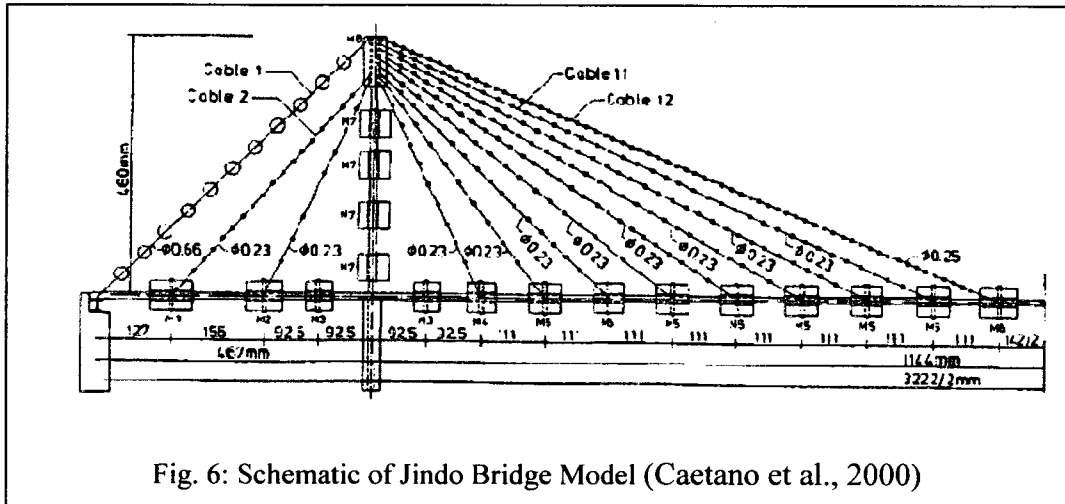


Fig. 6: Schematic of Jindo Bridge Model (Caetano et al., 2000)

When designing a physical model, special consideration must be given to any structure that has what is conventionally thought of as a fixed point. For normal structural analysis, a foundation can usually be considered as being a fixed support which would effectively turn a wind turbine into a cantilever beam. While this situation is extremely easy to simulate computationally, it cannot be easily replicated in an experimental situation. Far simpler to replicate experimentally, and as easy to recreate computationally is a free-free condition, in which the specimen can be suspended by soft springs (Ewins, 2000 and McConnell and Varoto, 2008).

Wind tunnel testing is expected to give good results when replicating the environmental conditions in the field. A study was conducted on a 2 m darrius wind turbine in order to investigate the effects of field conditions on a wind turbine, with an eye towards maintaining consistent Reynolds numbers. The experiment showed that the power coefficients, or C_p values, which are a standard method of evaluating the power output of a turbine, obtained in the field could be nearly replicated during wind tunnel

testing. The C_p for field values was 0.34 while that of the wind tunnel was 0.32 as long as the Reynolds numbers are kept constant (Sheldahl, 1980).

Further testing on this 2 m darrieus VAWT was conducted to determine the effect of rotation on the modal properties of the turbine (Carne and Nord, 1983). An unexpected result of the testing was that the stand that was added to the turbine in order to increase ground clearance greatly affected the turbine, complicating the modal properties of the overall system. This was despite the fact that the four foot steel channel stand was relatively stiff compared to the wind turbine. The steel stand was later dropped in favour of anchoring the structure directly to a concrete pad. The tests were then conducted and the results summarized below. As seen in Table 1, there is a trend for most of the modes to shift up the frequency spectrum as the rotor rpm increases. In some cases these shifts are quite large.

Mode Description	0 rpm		300 rpm		600 rpm	
	Frequency (Hz)	Damping (% of Critical)	Frequency (Hz)	Damping (% of Critical)	Frequency (Hz)	Damping (% of Critical)
1st antisymmetric flatwise	12.3	1.6	14.8	1.2	18.5	1.8
1st symmetric flatwise	12.5	1.6	14.2	1.4	17.7	0.4
1st rotor out-of-plane	15.3	0.7	10.8	1.7	5.9	2.9
1st rotor in-plane	15.8	0.6	21	0.4	25.7	0.3
Dumbbell	24.4	1.8	26.5	0.5	30.7	0.16
2nd rotor out-of-plane	26.2	0.5	24.2	1	19.6	0.7
2nd rotor in-plane	28.3	0.5	30.6	1.3	30.9	0.6
2nd symmetric flatwise	29.7	0.5	32.6	2	39.2	0.5
2nd antisymmetric flatwise	31.5	0.9	33.8	0.5	40	0.9
3rd rotor out-of-plane	36.5	1.1	38.2	1.1	41.4	1.5

Table 1: Modal Frequencies and Damping Ratios for a Stationary and a Rotating Darrieus Wind Turbine (Carne and Nord, 1983)

The testing of VAWT's continued with the creation of the 110 m tall EOLE wind turbine in Quebec Canada. Again, it was determined that due to the large size and relatively low frequencies that are expected in such a large structure, both natural excitation via ambient wind and step-relaxation would be used. It was concluded that as turbines became larger in size, step-relaxation, which in this case required the ability to

apply a 135 kN load to the turbine, becomes impractical. Thick cables, explosive cable cutters, expensive fixtures, significant ground support and a winch capable of exerting 135 kN are all required for a successful test. These materials are not only time consuming to install but are also extremely expensive and hazardous when in use (Carne et al., 1987).

3.0 Objectives

The goal of this thesis is the creation of a methodology to enable improved monitoring and design of commercial wind turbine masts. To this end there are three subsections. The first is the implementation of a short term data acquisition program that will assist in finding potential sensor positions for the instruments connected to the long term structural system. The second is development of a long term environmental and structural monitoring program developed with an eye towards monitoring environmental data and modal response of the mast. The final section deals with the creation of an aero-elastic model.

4.0 Data Acquisition System

The goals of the data acquisition is to adequately and economically determine the modal properties of the system, as well as to develop a database that can be used in future research into the health of the wind turbine. Two data acquisition systems will be implemented to collect and monitor this data. The experimental set-up for this project consists of two parts. A long term DAQ designed to remotely obtain both structural and environmental data, and a short term modal analysis system intended to conduct a modal survey of the turbine tower and obtain data regarding the structural properties via impact testing.

4.1 Short Term Data Acquisition System

The primary goal of short term modal impact testing is to provide a general view of the modal response of the mast in order to evaluate locations for the instrumentation to be used in the long term structural monitoring system. Additionally, it is used to evaluate the modal properties of the mast such as its natural frequencies, mode shapes, and damping ratios that will be used to assist in the design of the modal model. This data will be used to validate the model by comparing it to data that has been obtained from similar tests conducted on the model. This particular method of testing was selected in an attempt to combine ease of application with cost savings.

4.1.1 Objectives

The objective of this system is to rapidly, simply, and cost effectively conduct a modal survey of the tower in order to obtain data regarding the natural frequencies and mode shapes of the system in a simple and non-invasive manner.

4.1.2 Methodology

Standard practice for modal testing of large scale structures generally involve attachment of strain gauges and accelerometers to the structure and applying energy. The method of applying this energy usually takes place through the step relaxation method or a shaker. Both of these methods were explored and dismissed.

Step relaxation was not appropriate for the system due to the fact that a mounting block upon which to attach the cable of sufficient size did not exist on site. As well, the

expense of a large cable and winch of sufficient strength makes the procedure difficult. Additionally, suggesting a method that on the surface appears to put the structure at great risk would reduce confidence in the practitioner's ability. These reasons, compounded by the difficulty of attaching and reattaching the cable to the wind turbine between tests, make this procedure infeasible.

Shaker testing was discarded simply due to expense and logistics. Shakers of the size required are large, expensive, and driven hydraulically. In general these devices are not bought, but rented making it difficult to respond to the schedule of the wind farm. In addition to the cost, the mass and hydraulic power source of the shaker makes it difficult to move around the structure. Since the shaker must be solidly affixed to the turbine, there would be many restraints on its placement.

A large impact sledge was decided upon as the desired solution. This device is large enough to excite structures of this size, and is relatively inexpensive compared to other options. It also has the added benefit of being compact enough that the point of excitation can be moved about the tower.

In the choice between strain gauges and accelerometers, accelerometers were selected for this system. While strain gauges are cheaper per unit, the sheer number of strain gauges required to characterize the entire structure would make them cost prohibitive. Coupled with the time and difficulty of installing strain gauges while suspended from the access ladder, an accelerometer equipped with a simple magnetic base proves to be the best option.

4.1.3 Procedure

In order to determine mode shapes and natural frequencies, a roving accelerometer impact test was performed. For this test, two accelerometers were affixed to a magnetic base using hot glue. Two accelerometers were used in order to allow one to verify the other.

The accelerometers are placed at the base of the wind turbine. The structure is then excited at a location on the first platform, in a specific direction with the impact sledge equipped with a soft rubber tip affixed to a load cell attached to its head. At each

accelerometer location, the structure is struck five times and signals from the hammer and accelerometers are recorded, analyzed, and used to produce an frequency response function (FRF) curve. Finally the vibration in the mast is allowed to settle between strikes. The Supervisory Control and Data Acquisition System (SCADAS) generates feedback regarding the input, output, coherence and the FRF function allowing the user to determine whether or not to use each hit in the average FRF for that point. Following the five strikes, the accelerometers are moved up the side of the turbine, and this test is repeated at predetermined locations, as indicated in Figure 7 and Table 2. As seen from the figure, special attention was given to the flanged connections, and more samples were collected in these areas.

The selection of the number of sample locations is entirely dependent on the time available in the field. The more samples that are taken allow for a clearer picture of each mode shape of the turbine. This is especially important for higher natural frequencies where the mode shapes become more complex and require greater resolution to generate a clear and accurate picture. The sample locations are equally spaced which will help to generate a clear picture. Near the base of the turbine, this was not an option due to limited access to the tower due to generating and control equipment.

While the SCADAS system is capable of resolving natural frequencies and mode shapes up into the thousands of hertz, the focus will be on the low frequency spectrum between 0 and 50 Hz.

Name	Height (m)	Name	Height (m)
TurbineTower:1	0.3	TurbineTower:26	42.4
TurbineTower:2	0.8	TurbineTower:27	42.5
TurbineTower:3	5.0	TurbineTower:28	42.6
TurbineTower:4	8.0	TurbineTower:29	42.7
TurbineTower:5	10.0	TurbineTower:30	42.8
TurbineTower:6	12.0	TurbineTower:31	44.0
TurbineTower:7	15.3	TurbineTower:32	46.0
TurbineTower:8	15.4	TurbineTower:33	48.0
TurbineTower:9	15.5	TurbineTower:34	50.0
TurbineTower:10	15.6	TurbineTower:35	52.0
TurbineTower:11	15.6	TurbineTower:36	54.0
TurbineTower:12	15.8	TurbineTower:37	56.0
TurbineTower:13	15.9	TurbineTower:38	58.0
TurbineTower:14	16.0	TurbineTower:39	60.0
TurbineTower:15	18.0	TurbineTower:40	62.0
TurbineTower:16	20.0	TurbineTower:41	64.0
TurbineTower:17	23.0	TurbineTower:42	66.0
TurbineTower:18	25.0	TurbineTower:43	67.0
TurbineTower:19	28.0	TurbineTower:44	70.0
TurbineTower:20	31.0	TurbineTower:45	72.0
TurbineTower:21	33.0	TurbineTower:46	74.0
TurbineTower:22	36.0	TurbineTower:47	76.0
TurbineTower:23	39.0	TurbineTower:48	78.0
TurbineTower:24	42.2	TurbineTower:Hammer	6.6
TurbineTower:25	42.3		

Table 2: Accelerometer Locations on Wind Turbine

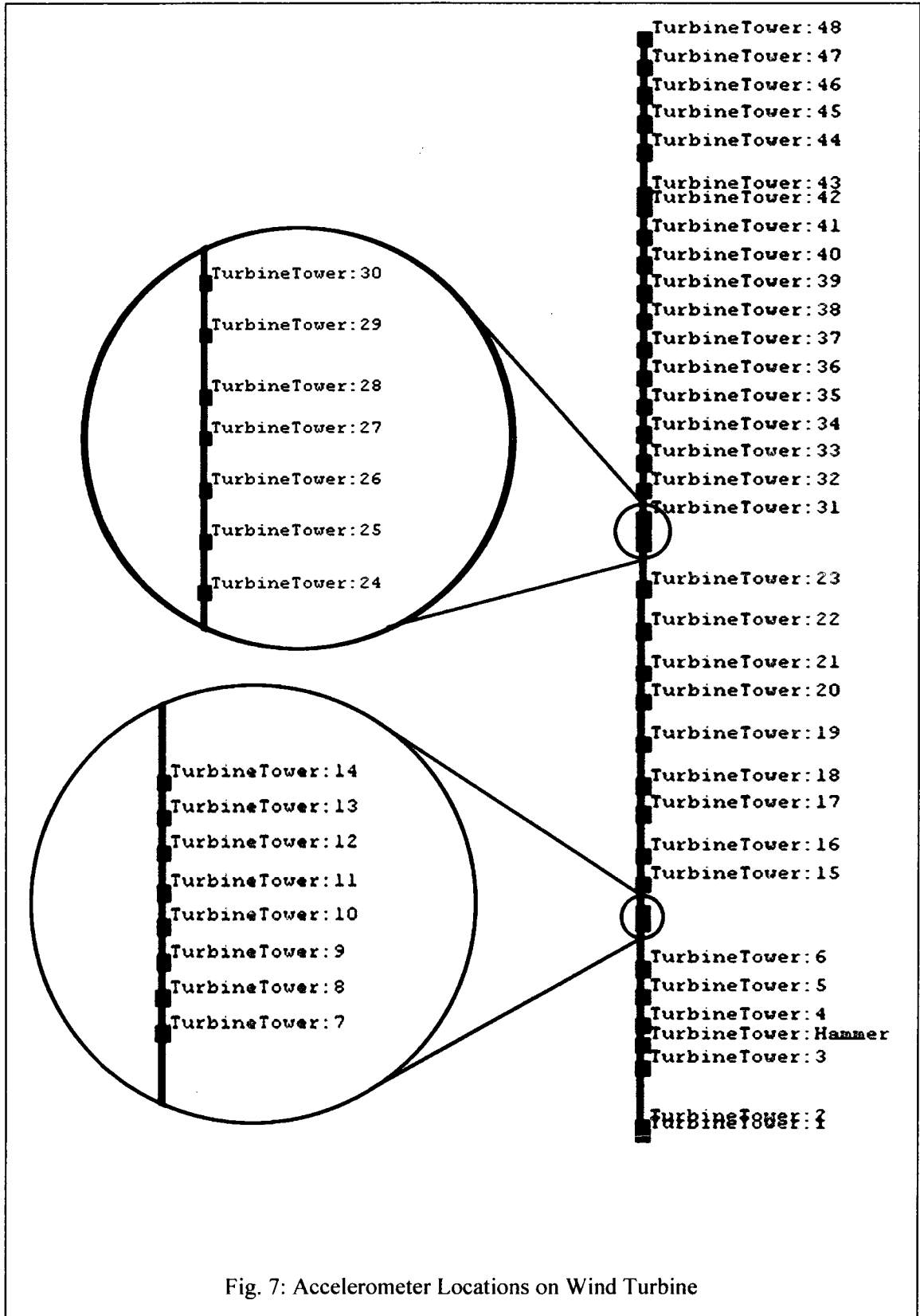


Fig. 7: Accelerometer Locations on Wind Turbine

4.1.4 Results

The roving accelerometer test of the field turbine identified a number of natural frequencies of the structure. These frequencies are determined from the locations of the peaks on the FRF curves in Figure 8 and Figure 9. The y axis is in units of g/N. This represents the acceleration observed in the structure when a 1N force is applied to it. This helps to normalize different readings taken from impact tests, to help allow for the fact that operators are unable to apply the same amount of force to the structure with every test. These peaks represent frequencies at which the response of the turbine per force input into the system increases. The results are also summarized in Table 3, which shows the correlation, as a percent, for each mode shape. Figure 10 is a graphical representation of Table 3.

When using the FRF curves to determine resonance frequencies of the system, extraneous results need to be eliminated. They were removed through two methods. The first was eliminating low level response peaks that can be seen dominating the lower portion of the graph. These peaks represent system noise as well as resonance frequencies that yield a low enough response that they can be considered trivial compared to the major frequencies, or are localized frequencies occurring due to resonance in nearby components. The other method involved correlation of mode shapes. The system often picks up several natural frequencies that are very close together both in frequency and mode shape. The “true” resonance frequency is selected by picking the shape that yields the highest response.

The FRF curves seen in Figures 8 and 9 were taken on two separate occasions and show close correlation to one another. This not only shows that the method is consistent, but also disputes the idea that environmental conditions have a substantial effect on the results of impact testing. Figure 8 is the result from the original attempt to characterize the turbine, and there is evidence of the first mode shape around 2.5 Hz, the area where we expect to see the first natural frequency for a structure of this size. For the rest of the peaks, there is clear agreement between the two charts. Figure 9 was the result of the second attempt to acquire modal data. In an attempt to better characterize the system,

the resolution was increased and this lead to poorer results as the instruments began to capture extraneous readings that lead to readings of false or inconsequential resonance, especially at very low frequencies.

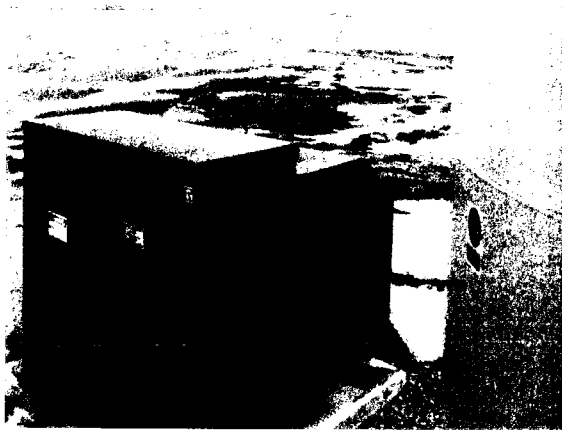


Fig. 8 Exterior of Field Turbine

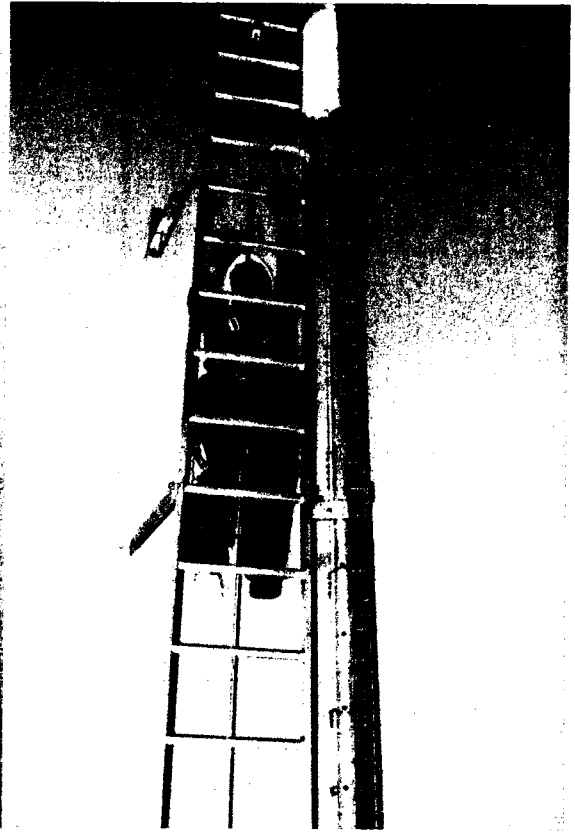


Fig.9 Interior of Field Turbine

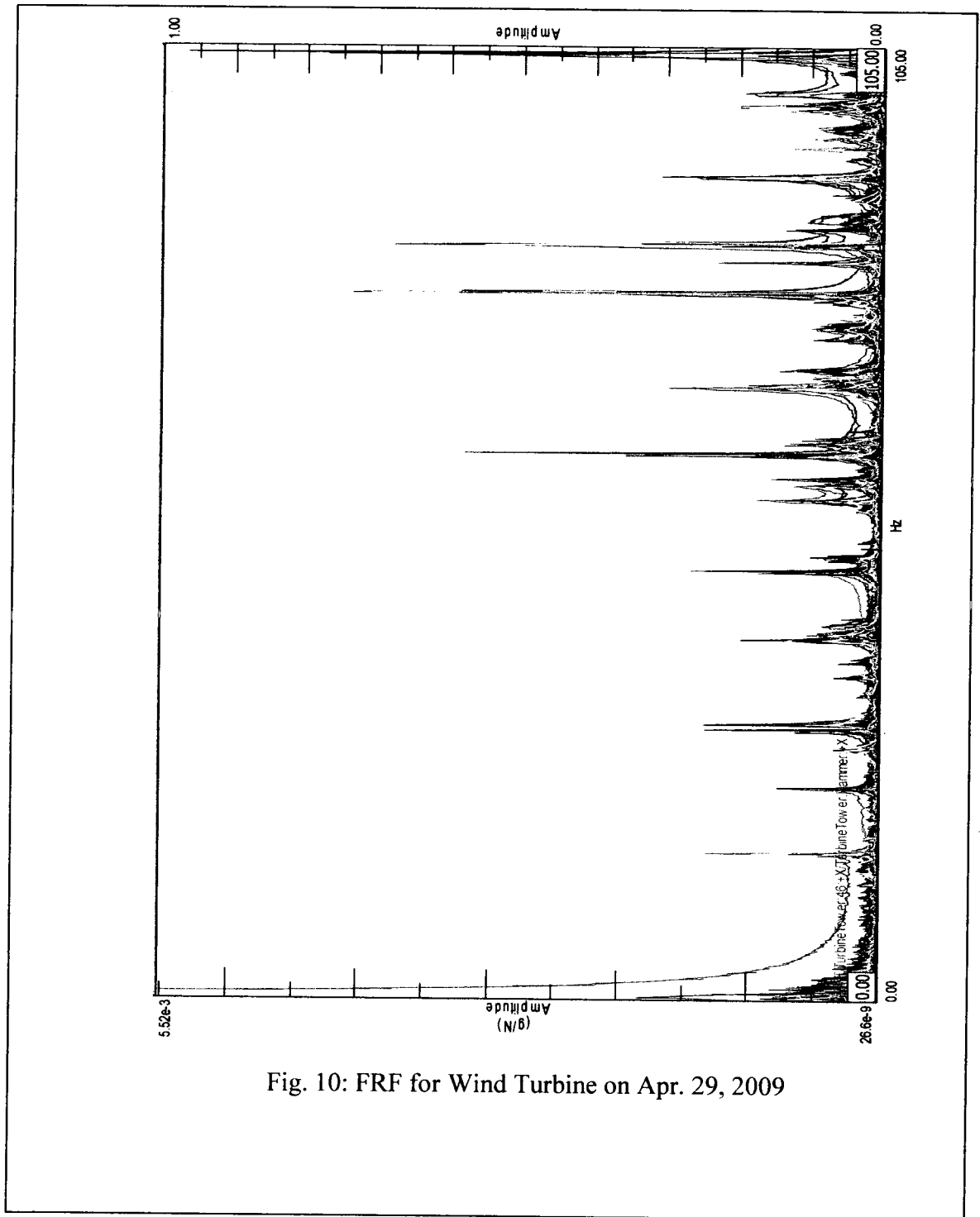


Fig. 10: FRF for Wind Turbine on Apr. 29, 2009

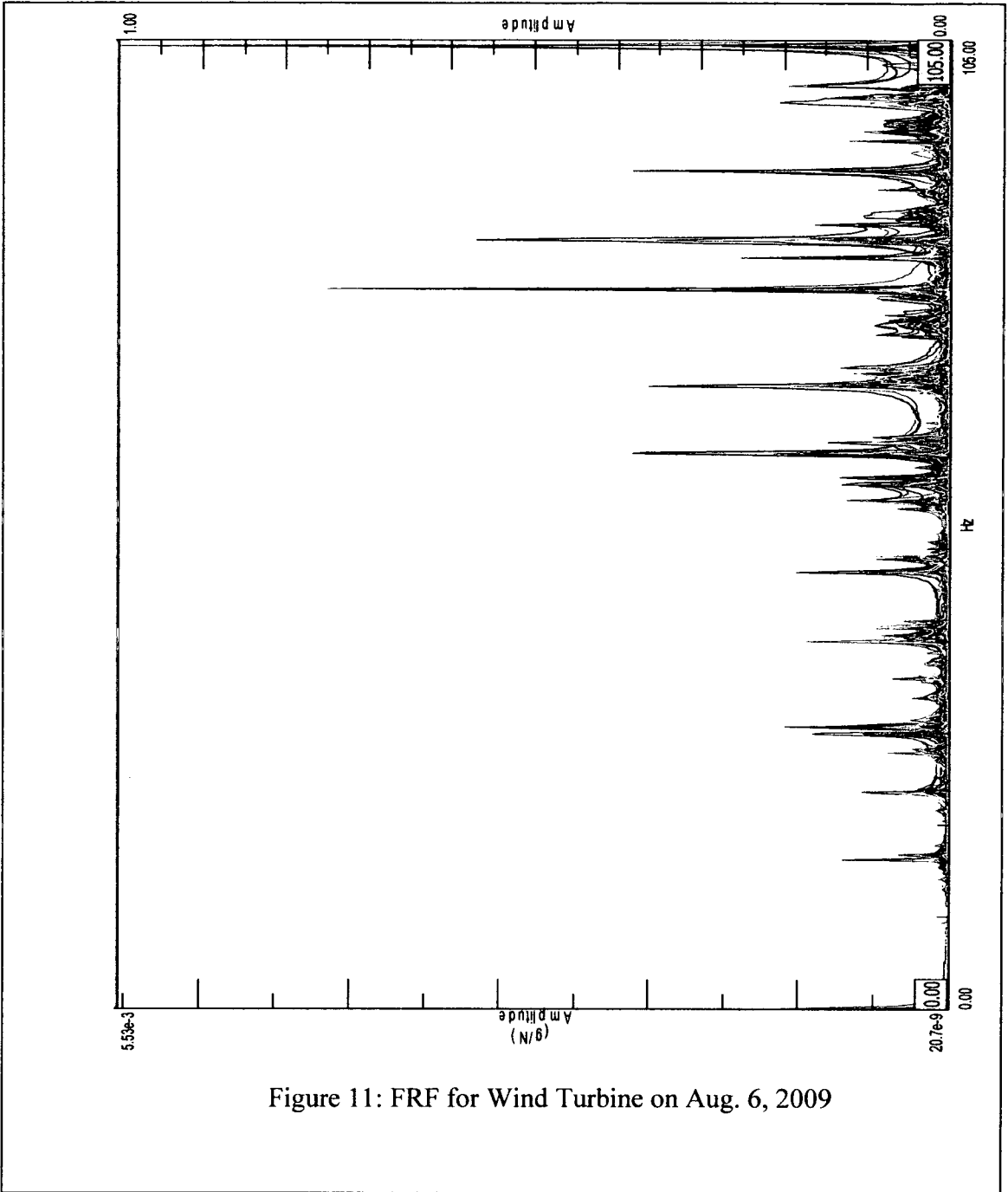


Figure 11: FRF for Wind Turbine on Aug. 6, 2009

Frequency (Hz)	Mode 1 16.2 Hz	Mode 2 30.5 Hz	Mode 3 60.3 Hz	Mode 4 78.1 Hz
Mode 1 16.2	100.0	4.1	0.3	7.0
Mode 2 30.5	4.1	100.0	0.1	9.8
Mode 3 60.3	0.3	0.1	100.0	37.3
Mode 4 78.1	6.9	9.8	37.3	100.0

Table 3: Modal Assurance Criterion

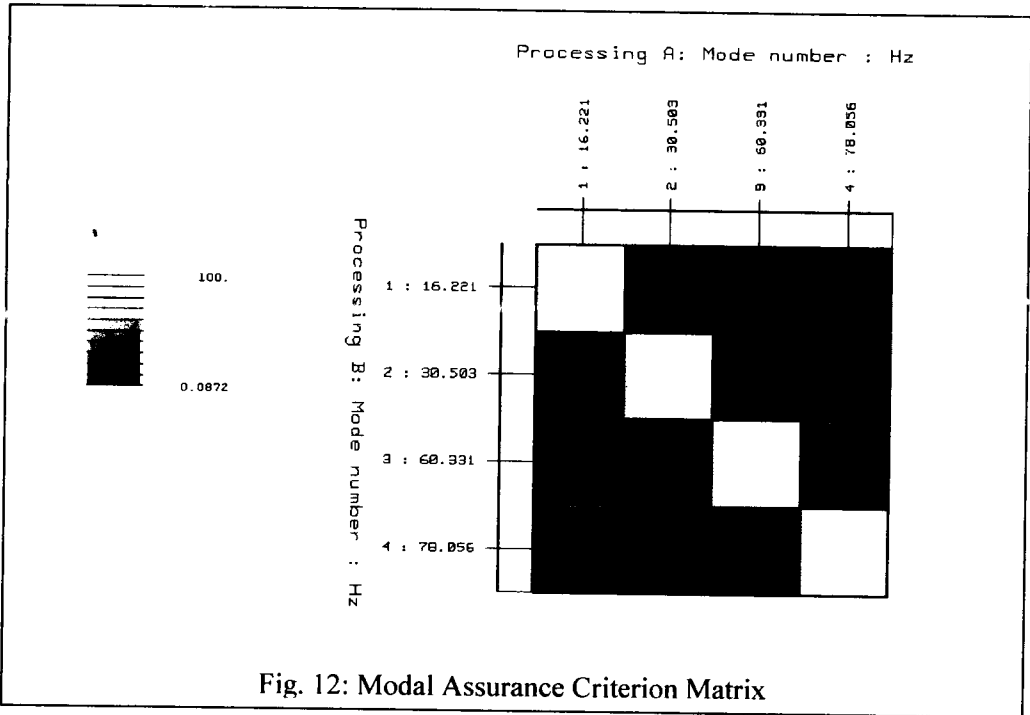


Fig. 12: Modal Assurance Criterion Matrix

4.2 Long Term Data Acquisition System

The long term DAQ was designed to utilize existing, onsite equipment, as well as allow integration of other instruments from different parties, and coordinate this equipment. Due to issues with installation and integration with the existing equipment, this plan was not implemented but it is the hope of the author that these plans will be put into action in future projects. Proof of concept has been obtained through the data acquisition system that has been installed.

4.2.1 Objectives

The long term structural response DAQ is intended to provide wind farm operators with an integrated system that can be easily applied in the field to monitor the response of the turbine mast and identify environmental conditions which have the possibility of exciting the resonance frequencies in the mast, exposing the turbine to conditions likely to cause structural damage.

4.2.2 Methodology

As with the short term modal testing method mentioned above, the methodology and components selected were chosen with cost savings and ease of application in mind to ensure that this remains a useful tool.

4.2.3 Procedure

The system for collecting long term structural data was designed to utilize existing equipment on site as well as keeping cost savings in mind. To this end, strain gauges were chosen over accelerometers. While a difficult to install initially, they are able to provide reliable, long term data acquisition, and are inexpensive. Strain gauges are capable of monitoring modal signals from large structures and have several advantages over accelerometers which are traditionally used for this purpose. Strain gauges are capable of detecting lower frequency responses than accelerometers, as accelerometers have a minimum frequency sensitivity beyond which their accuracy begins to quickly fall off. Additionally, strain gauges are more inexpensive than accelerometers, particularly speciality accelerometers that are designed for low frequency response needed in a large structure such as this.

The strain gages will be driven by 4-20 mA transmitters, a reliable device that has been used for decades to drive sensors over long distance with little signal loss. As well, 18 AWG (American Wire Gauge), shielded cable was selected to ensure good signal quality, as well as to reduce interference created by the generating equipment in the turbine nacelle and tower. To utilize existing equipment, two Campbell Scientific CR800 DAQ's are used in the design. Furthermore, monitoring of environmental data

needed to be addressed so that the structural signals can be related to wind conditions. Finally the need for coordination, and transmission of any data would need to be addressed.

4.2.4 Results

The final design of the long term data acquisition system is as follows. 350 Ohm strain gauges were selected as the sensors. The strain gauges are powered by 4-20 mA transmitters over an 18 AWG shielded cable. These transmitters are useful in this application due to their ability to attenuate the small changes in resistance and noise associated with long cables. The voltage drop occurring across a resistor is then read by the DAQ system. The gauges are installed in a vertical column along the inside of the

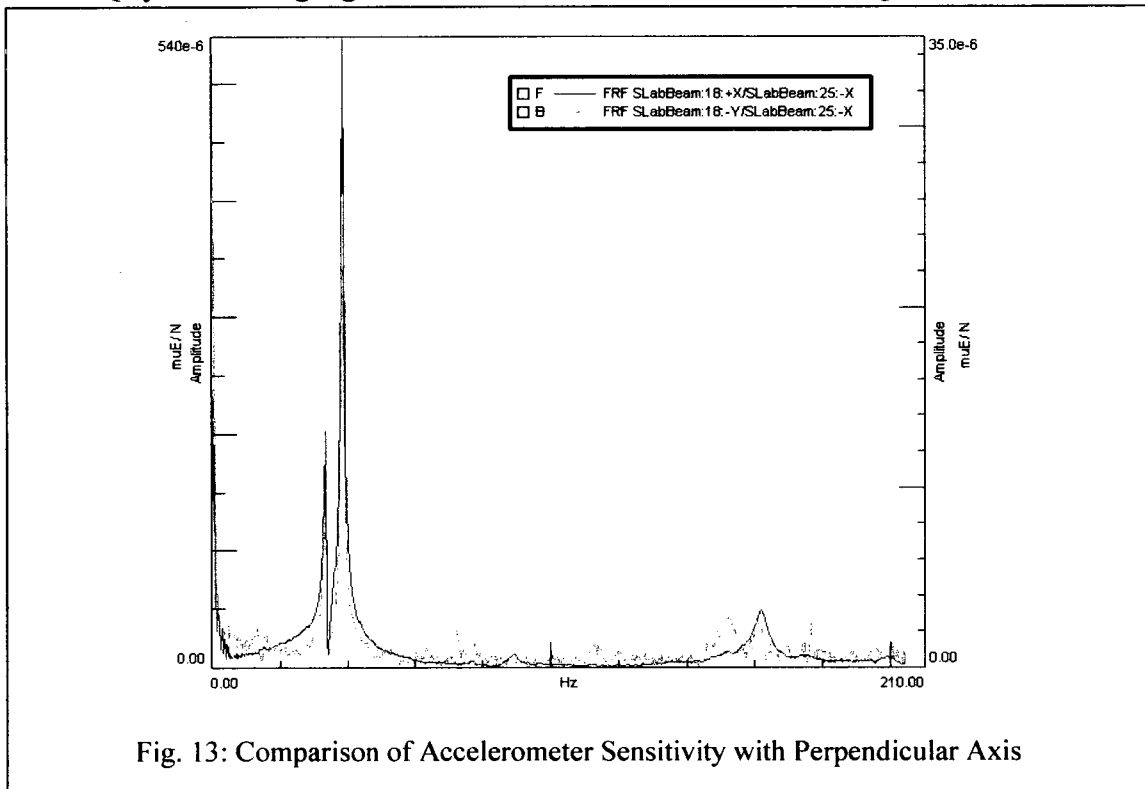


Fig. 13: Comparison of Accelerometer Sensitivity with Perpendicular Axis

mast. This was done to allow ease of installation, as the majority of the mast is inaccessible except for locations near the access ladder and tower platforms. This method is acceptable due to experiments that have shown that good response is still achieved even when the sensor is located 90 degrees from the direction of application of the exciting force acting on the structure; see Figure 11 Comparison of Sensor

Sensitivity, where the black line represents the response in the principal direction and the gray represents the response in the off direction.

The DAQ's intended for use in this system are two CR800 DAQ's from Campbell Scientific that were available for use onsite. Each CR800 will be responsible for monitoring up to five strain gauges. The CR800s have a maximum scanning rate of 100 Hz and cannot scan all channels simultaneously; meaning that the maximum frequency range will be limited to one half the maximum scanning rate to prevent aliasing, divided by the number of sensors monitored. For example, three strain gauges per DAQ would give a maximum range of $(100/2/3=16.67)$ 16.6 Hz. This allows some flexibility in the system, allowing to user to either monitor more or less strain gauges at the cost of frequency range.

These CR800's then pass their data on to a CR1000 DAQ. This system acts as a hub, responsible for receiving incoming signals from other DAQ systems, the structural response monitoring system, the environmental monitoring system, GPS signals and DAQ systems. It then packages the data and stores it until it can be transmitted to the University.

The GPS unit connected to the CR1000 is required for ensuring proper time stamping of all the data, thus ensuring that drift does not occur, which would cause the signals to move out of sync with each other.

Finally the CR1000 has two communication systems at its disposal. A spread spectrum radio modem allows communication with the meteorological instruments. The cellular modem enables users to dial up the system remotely and receive the data via the internet. This is necessary due to the remote location and inaccessibility of the system.

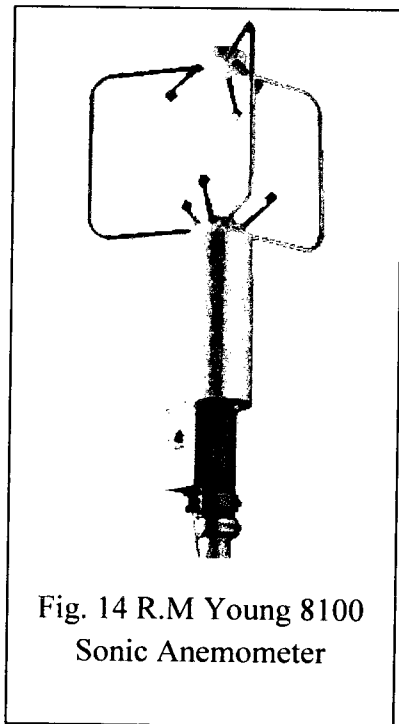


Fig. 14 R.M Young 8100
Sonic Anemometer

Weather conditions are monitored by instruments currently used by the wind farm to gather environmental data. These include a number of cup anemometers, wind veins, and sensors for rain fall and humidity. Additionally, a R.M. Young 81000 ultrasonic anemometer, Figure 12, was integrated with this system. This instrument has been calibrated by Campbell Scientific, and verified in the University of Windsor fluids lab wind tunnel with the cables that will be used during installation. This check shows that the device functions well despite the long cable required for installation on the metrological tower. Calibration and specification sheets have been included in Appendix A. The advantages of this instrument include the ability to sense short variations in wind speed, the capability to measure wind speed in all three directions. This data, along with information regarding the turbine operating state, will be gathered into ten minute interval data packs and shared with the University of Windsor.

5.0 Computational Modeling

5.1 Objective

The purpose of computational modeling is to serve as a design aid for the construction of a physical model of the wind turbine. This will be done in two ways. The first will be design and construction of a modal analysis program using a Matlab program that reads data from Microsoft Excel spreadsheets. The second is by using a commercially available structural analysis package, ANSYS 10.

5.2 Methodology

The computational model will be used to design a physical model of the test turbine at a scale of 1 to 53.33. The model will be based on the equation:

$$([k] - \omega^2[m])\hat{v} = 0 \quad [\text{Eq.1}]$$

where k and m are the stiffness and mass matrices, ω is the natural frequency of the undamped system, and \hat{v} is a vector representing the shape of the system. Through application of Cramer's rule, we see that the solution of the set of the simultaneous equations is of the form:

$$\hat{v} = \frac{0}{\| [k] - \omega^2[m] \|} \quad [\text{Eq.2}]$$

which leads to:

$$\| [k] - \omega^2[m] \| = 0 \quad [\text{Eq. 3}]$$

This is the equation that will be used to determine the natural frequencies of the test turbine and the model.

By iterating this equation over the desired frequency range, the values of ω that satisfy this equation and thus, the natural frequencies of the system can be found.

Matlab will be used to perform this iteration and the code for the program is included in Appendix B.

The mass matrix is of the form:

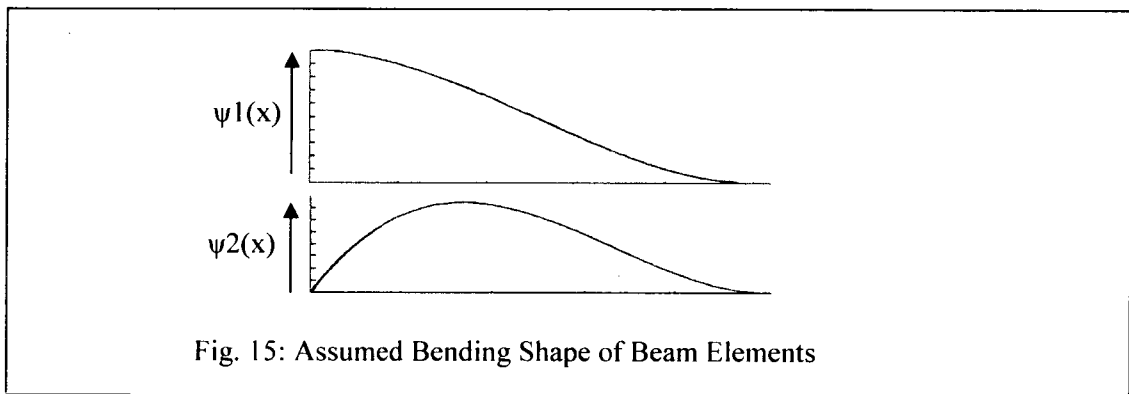
$$[m] = \bar{m}L[M] \quad [\text{Eq.4}]$$

where \bar{m} is the mass per unit length of the segment, L is the length of the segment and $[M]$ is a diagonal N by N symmetric matrix, identical for all structures having N degrees of freedom.

The stiffness matrix is of the form:

$$[k] = \frac{EI}{L^3}[K] \quad [\text{Eq.5}]$$

where E is the modulus of elasticity of the material, I is the moment of inertia of the cross sectional area, and $[K]$ is a N by N symmetric matrix that is identical for all structures having N degrees of freedom and similar boundary conditions. The matrices are constructed by assuming that each beam element has four degrees of freedom, one translational and one rotational at each end, and that it will deform in the manner of a uniform beam that has been subjected to nodal displacements and rotations. The assumed shape is that of a cubic hermitian polynomial as shown in Figure 13:



These shape functions for a unit translation or rotation applied to the left side of the beam element respectively are the following:

$$\psi_1(x) = 1 - 3\left(\frac{x}{L}\right)^2 + 2\left(\frac{x}{L}\right)^3 \quad [\text{Eq.6}]$$

$$\psi_3(x) = x\left(1 - \frac{x}{L}\right)^2 \quad [\text{Eq.7}]$$

The shape functions for a unit displacement or rotation applied to the right side of the beam element are:

$$\psi_2(x) = 3\left(\frac{x}{L}\right)^2 - 2\left(\frac{x}{L}\right)^3 \quad [\text{Eq.8}]$$

$$\psi_4(x) = \frac{x^2}{L}\left(\frac{x}{L} - 1\right) \quad [\text{Eq.9}]$$

This method assumes that each beam element has uniform properties of mass, stiffness, and moment of inertia. Agreement between the natural frequencies of the test turbine and the model will be achieved by adjusting the properties of mass, stiffness, and moment of inertia of the model.

Absent from the above calculations is the damping matrix. The damping matrix will not be calculated, the damping ratios will be used in its place. The damping from both the model and full scale structures will be determined experimentally through the use of the LMS system, and will be used to adjust the natural frequency that is obtained from the computational model to properly represent the natural frequency desired from the modal model.

The effect of damping on the natural frequencies of a structure is shown by the following equation:

$$\omega_D = \omega \sqrt{1 - \xi^2} \quad [\text{Eq.10}]$$

where ω_D is the damped natural frequency, ω is the undamped natural frequency, and ξ is the damping ratio of the structure. The desired natural frequencies will be calculated through theory and then adjusted by the damping ratio. As we see from equation 10 the damping ratio may not have a significant effect on the overall frequency. A damping ratio of 20%, relatively high for a civil structure, will only cause a change in the natural frequency of approximately 2%.

5.3 Procedure

Both the model and the field turbine are modeled using a Matlab program the author has designed for this purpose. The model will be simulated three ways. The first will be by modeling each of its three sections individually in a free-free condition. This will allow the sections to be experimentally tested and verified independently from each other. Secondly, the entire assembled model will be simulated in a free-free condition. This allows the structure as a whole to be verified. If there are no discrepancies in any of the first tests, we can assume that the individual pieces have been properly constructed. If after the second test, in which the pieces have been assembled, discrepancies are found, it can be surmised that there are problems resulting from the connections between the sections. The entire model will then be simulated with a fixed base connection, and the experimental model will be tested against this condition. Finally the field turbine will be modeled. The Matlab program designed by the author will be verified computationally by comparing the results obtained to those obtained by a commercial software program, ANSYS, and then by comparing the results determined experimentally through the use of the LMS SCADAS system. The test specimen used is a stainless steel pole that will be modeled with free-free and fixed-free boundary conditions.

5.3.1 Matlab

The method using Matlab to solve the natural frequencies of the system consists of two parts. The first is a spreadsheet created in Microsoft Excel. This is a series of seven sheets that calculate the mass and stiffness matrices for each of the three sections as well as an input sheet that allows the user to manipulate the other six by adjusting a several fields on a single screen. Once the mass and stiffness matrices are calculated, the spreadsheets are read into a Matlab program. A sample of this program used to calculate the complete model in with a fixed base has been included in Appendix D. Here the mass and stiffness matrices first assembled and are then operated on according to the method outlined in Section 5.2, and the natural frequencies are determined based on what frequencies a value of 0 is obtained for the determinant.

5.3.2 ANSYS

ANSYS is used to verify the Matlab program. The same modeling conditions were used for these models as in the Matlab program. A test specimen was modeled in a free-free and fixed-free boundary conditions, and the bottom two sections of the model were modeled in a free-free boundary condition. The mesh was created using a hex dominated method. Though as suitable as using tetrahedrons for a shape such as the one modeled here, it was necessary in order to keep the number of elements under that restricted by the student version of ANSYS.

5.4 Results

5.4.1 Matlab

The Matlab program was used to generate tables from which the user can determine the natural frequencies of each of the systems modeled. The results are summarized in Table 4. The 25 degree of freedom (DOF) calculations are provided to show the expected results from the model. This model required weights to be attached to it at certain points, this process is further explained in section 6.0. Due to this, the model will exhibit characteristics that would more closely resemble the results generated in the 25 DOF results. It can be seen that at lower frequencies, there is a greater correlation

between the results of the two models. This is satisfactory for our purposes, as the frequencies of interest are lower, between 0 and 100 Hz.

Section 1		Section 2		Section 3		Free-Free		Fixed-Free		Field Turbine
22 DOF	78 DOF	42 DOF	78 DOF	54 DOF	78.0 DOF	118 DOF	234 DOF	118 DOF	234 DOF	234.0 DOF
98.1	103.7	33.2	35.3	15.4	13.8	0.6	0.6	3.4	3.7	3.6
268.7	290.2	91.8	98.8	42.3	41.5	2.0	2.0	13.3	13.4	9.9
522.7	568.6	179.6	193.5	82.8	82.5	10.4	10.7	17.0	18.4	18.9
848.9	940.0	296.7	320.0	137.0	137.4	14.6	14.6	39.2	44.0	32.7
		442.9	478.0	204.6	206.2	27.3	29.5	49.9	54.2	48.1
		617.4	667.9	285.6	288.5	48.3	52.0	68.7	84.3	68.4
		819.9	889.4	380.0	384.6	54.4	57.9	77.1	93.5	89.5
						69.6	86.2	113.6	122.3	117.5

Table 4: Computed Resonance Frequencies of Model at 25 and 365 Degrees of Freedom

6.0 Aeroelastic Model

The final component of this thesis will be the design and creation of an aeroelastic modal model for use as a tool in wind tunnel testing. The model can be used as a standalone tool to investigate the effect of different wind conditions on the mast, or it can be combined with many other models to study the effect of wake interactions that occur when many turbines are placed in close proximity. In this manner, the possibility of harmful effects occurring in the wind farm can be studied and minimized.

6.1 Objectives

The author has constructed an aero-elastic model suitable for use in a commercial wind tunnel. The hope is to develop a tool that can be used to test this wind turbine in extreme wind conditions outside of its normal operating range. This approach is of interest given that the turbine mast undergoes a great deal of excitation in this state, suggesting that natural frequencies could be excited to the point of causing damage. Additionally, under these conditions the turbine will be in a stalled state, which eliminates extraneous readings due to rotor imbalance or generating equipment. This also allows for the gathering of data that will hopefully serve as a base to build further models that will model the turbine under normal operating conditions.

6.2 Methodology

The model was created with two main goals in mind, aerodynamic similarity to the field turbine in order to allow the model to experience the same scaled loadings that wind exerts on the structure, as well modal similarity, allowing the model to exhibit the same natural frequencies and mode shapes of the

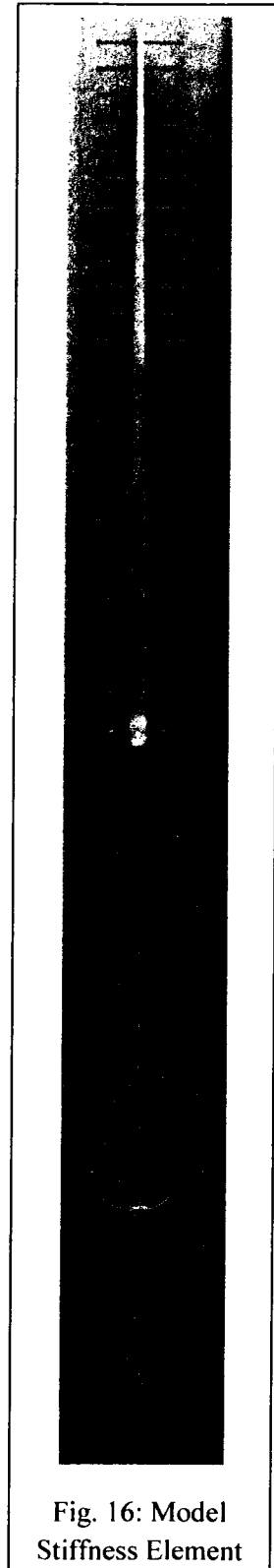


Fig. 16: Model Stiffness Element

wind turbine in modal testing as well as when it is exposed to similar wind conditions to those found in the field.

The model's mast will consist of three sections bolted together in much the same way that the field turbine is. Each section consists of a rectangular aluminum spine, around which a thin, cylindrical, aluminum shell is attached to the spine via steel machine screws set into the sides of the spine.

The purpose of the aluminum spine, seen in Figure 14, is to provide structural stiffness to the model, and is responsible for the accurately recreating this property according to the stiffness matrix. It will be constructed out of 7075 aluminum due to its high strength. The cylindrical shells attached to the spine are responsible for recreating the aerodynamic properties of the turbine in order to allow it to faithfully respond to simulated conditions in the wind tunnel. As the shells are not structural members, they will be constructed out of less expensive standard aluminum. Additionally, the shells will replicate the mass that is needed in the model. The spine itself is too light when compared to the wind turbine, and thus the shells, with the assistance of weights attached to them, will simulate the inertial properties. The shells will be screwed into the sides of the spine at two points. This is done to reduce the effect that the shells will have on the stiffness of the spine. The small gap between each shell allows them to float over each other and not contribute to the stiffness of the system.

In order to ensure modal similarity, both the field turbine and the model have been simulated using Matlab to determine their natural frequencies. As discussed, the creation of a "fixed" point is extremely difficult to produce in the real world from a model standpoint, and extremely easy to reproduce computationally. With this in mind the testing will need to be broken down into several sections.

First each of the three sections composing the aluminum spines will undergo impact testing and simulated in Matlab using free-free boundary conditions. The free-free condition is simulated in the lab by suspending the specimen from a solid frame using very soft springs or bungees. When the three sections have been independently tested and verified against the Matlab simulation, they will then be assembled and tested once

more in the free-free condition. In this way the construction of the model sections as well as the connections can be independently looked at and verified away from the difficulties a fixed point can cause. In this way, when the final modal test is performed on the assembled and fixed structure any discrepancies in the modal testing can be attributed to a specific component of the model depending on what stage the error occurs.

The model is scaled by a factor of 53.33, giving a total model height of 2.3m in order to allow it to fit within the Boundary Layer Wind Tunnel at the University of Western Ontario. This height was chosen in order to keep the model as large as possible to keep the weight of the model down, relative to the size of the model. The blockage ratio of this model will be less than 4 percent.

Fluid dynamic scaling will be executed via Reynolds number scaling. To ensure dynamic similarity, the model tests should be run so that $Re_m = Re$ where:

$$Re = \frac{\rho V l}{\mu} \quad [\text{Eq. 11}]$$

ρ = density of the fluid

V = velocity of the fluid

l = a characteristic length

μ = viscosity of the fluid

Choosing the characteristic length as the diameter of the mast, using air as the fluid and with a velocity range of between 10 and 15m/s, it is expected that the Reynolds number for the structure will be between 2.9×10^6 to 4.3×10^6 . This places the structure strictly within the turbulent boundary layer flow regime, characterized by a turbulent boundary layer with a narrow turbulent wake and separation points above ninety degrees. In order to reach this value in the wind tunnel requires wind speeds of between 533 and 800 m/s, not values easily obtainable in standard wind tunnels.

This is problematic as a traditional wind tunnel will generally be only able to generate speeds up to 100 m/s. The solution used will be to not match the Reynolds number exactly, but instead to match the flow patterns, so that the model is representative of the structure. As the Reynolds number will be lower in the model test,

owing the reduced wind velocity, it will be necessary to prematurely trip the boundary layer into turbulence as well as to control the separation angle on the model. This is done by perturbing the flow as it approaches the structure via screens or tripwires, or by adding tripwires to the model, or adjusting the surface roughness to force the flow into a turbulent state.

Using wind speeds obtainable in a commercial wind tunnel, 50 m/s, the Reynolds number of the model becomes 268×10^3 . This value places the model between the boundaries of the precritical and single bubble flow regimes. By adding trip wires or sufficient surface roughness, the laminar boundary layer can be forced into a turbulent state, imparting the energy required for it to pass into the same flow regime as seen in the field.

6.3 Results

The result of this process is a structural spine that makes up the stiffness element of the model. Attached to this spine are masses that complete the model. It is now expected that the complete model with mass and stiffness elements attached, will behave in a manner representative of the field turbine during modal testing. Ideally the model will exhibit similar natural frequencies as well as the mode shapes associated with these frequencies.

With the addition of the rings, nacelle and rotor to the structure, the model will then exhibit geometric similarity to the field turbine. This allows it to be used in wind tunnel tests in order to further explore the response of the field turbine in varying wind conditions.

7.0 Results

This section contains a presentation and discussion of the results of the long and short term field data acquisition, computational results, as well as a comparison of the model to the field turbine.

7.1 Validation of Computational Modeling

The resonance frequencies of a 1 m long, stainless steel pole were determined using the author's Matlab program, ANSYS, as well as experimentally via the SCADAS Mobile system. It was tested in free-free condition by suspending it on soft bungees and in the fixed-free condition by clamping it firmly at the base and securing it to a stable structure as seen in Figures 15 and 16. Table 5 shows the modal properties of the test specimen for the free-free and fixed-free conditions.

Test Specimen Properties		
	Free-Free	Fixed-Free
Mass (kg)	4.084	3.6554
Length (m)	1.095	0.98
E (Pa)	1.93E+11	1.93E+11
I (m ⁴)	1.14E-07	1.14E-07

Table 5: Modal Properties of Stainless Steel Test Specimen

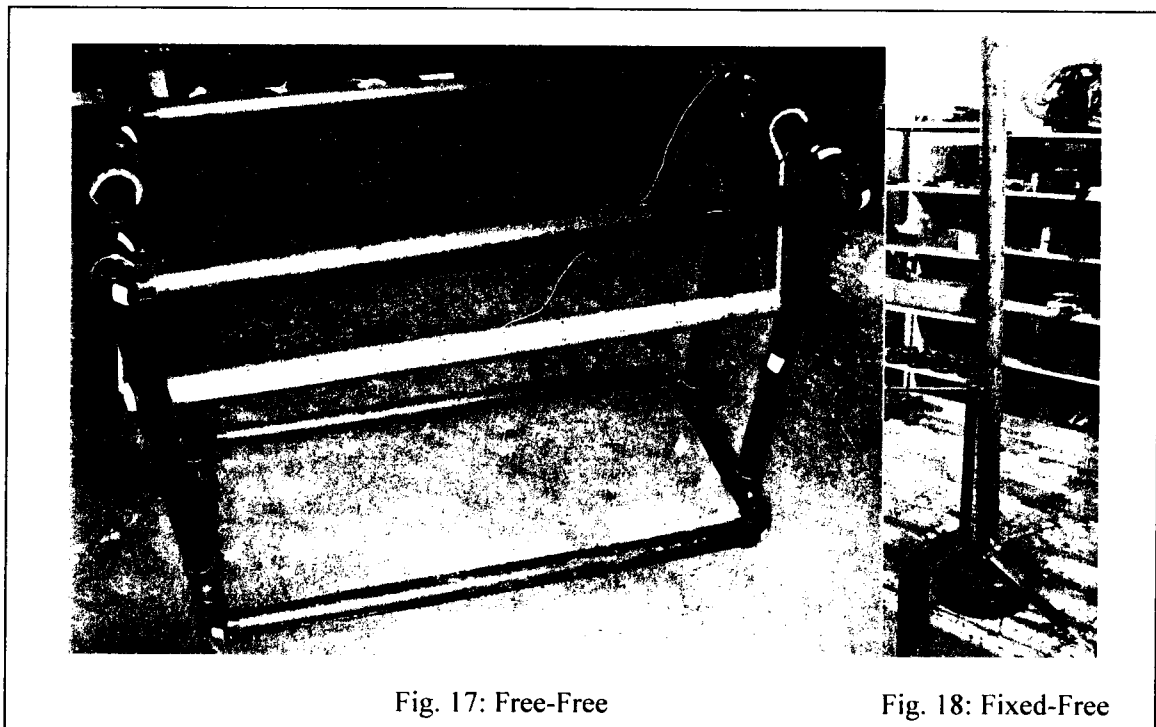


Fig. 17: Free-Free

Fig. 18: Fixed-Free

The results for the three tests of the two different boundary conditions are presented in Table 6. The frequency results are given in Hz and the percent error relative to the Matlab results are presented in the brackets.

Mode	Free-Free Boundary Condition			Fixed-Free Boundary Condition		
	Matlab	ANSYS	Experimental	Matlab	ANSYS	Experimental
1	233.5 Hz	224.9 Hz (3%)	275.4 Hz (2%)	48.2 Hz	46.2 Hz (4%)	32.4 Hz (33%)
2	642.7 Hz	607.8 Hz (5%)	733.3 Hz (1%)	303.1 Hz	285.1 Hz (6%)	215.8 Hz (29%)
3	1260.1 Hz	1158.6 Hz (8%)	1388.4 Hz (10%)	848.4 Hz	776.7 Hz (8%)	635.3 Hz (25%)

Table 6: Comparison of Results for Resonance Frequencies of Stainless Steel Specimen

As can be seen from Table 6, there is a good correlation between the two computational methods and the experimental method. This demonstrates that the simplified method of determining natural frequencies of a system employed is sufficient for the purposes of this study.

7.2 Modeling of the Full Scale Wind

Turbine

The results of the field turbine modeling are presented in Table 7. As can be seen, there is close similarity between the computational results determined through the authors Matlab program and the experimental results. The lack of the first two mode shapes at approximately 1 and 7 Hz, is of some concern. It is hoped that the use of strain gauges in future measurement campaigns will

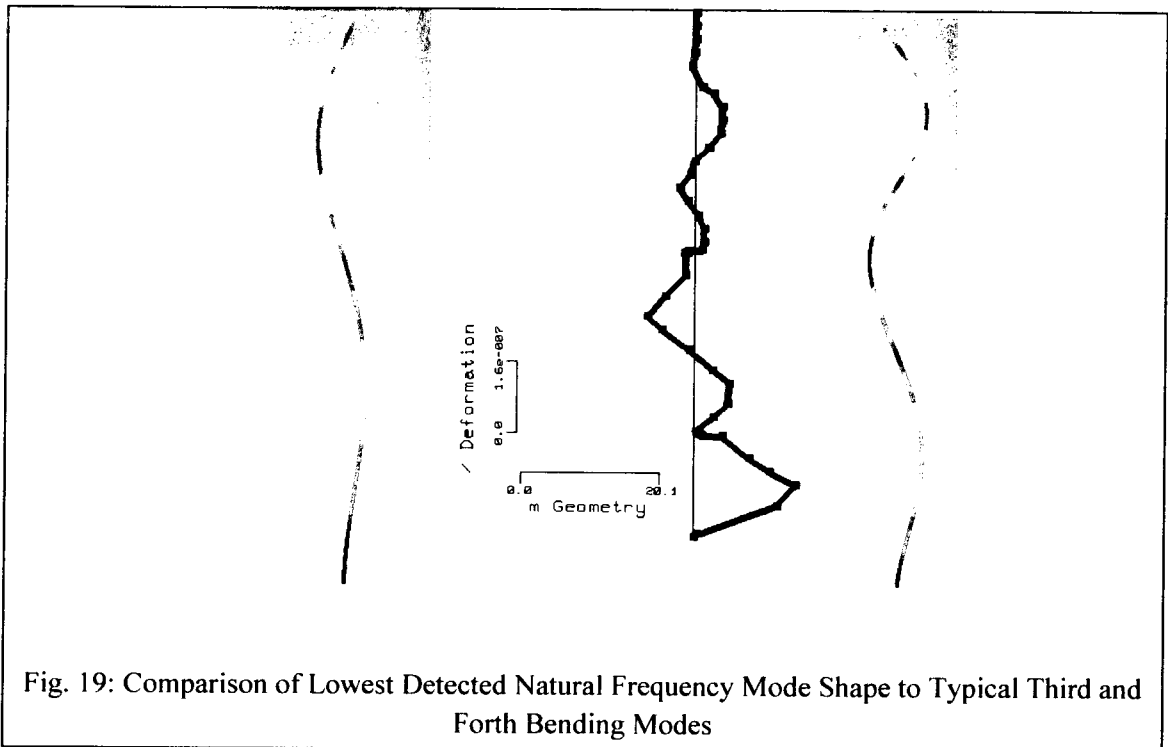
remedy this issue. Also of note is that the author had expected that a lower resonant frequency would be present that is absent from both results. The first natural frequency should occur at approximately 0.5 Hz. The sway of this frequency was noted by the author while working on the turbine during an exceptionally windy day. Additionally it would be expected that a structure of this size would have a lower first natural

Matlab	Field
1.2 Hz	
7.6 Hz	
17.9 Hz	16.16 Hz
33.2 Hz	30.52 Hz
56.6 Hz	60.37 Hz
82.8 Hz	78.04 Hz

Table 7: Comparison of Results for Resonance Frequencies for the Wind Turbine

frequency. Support this is the fact that the experimental mode shape result at a frequency of 16.16 Hz closely resembles the shape of a forth bending mode, not a third bending mode as would be assumed by the results. This comparison is given in Figure 17. If we compare the experimental result from the turbine, pictured middle, to the image of a typical third bending mode, seen left, we can see that the experimental result has more peaks. The middle image more closely resembles on the one on the right, an example of a typical forth bending mode for a structure with a fixed base. The differences are accounted for by the mass of the bolted connections in the turbine, as well as the mass of the nacelle and rotor. These masses act to dampen out movement, and remain nearly stationary when compared to the rest of the structure.

In an attempt to pick up this first mode, the degrees of freedom in the Matlab model were doubled. This made no appreciable change to the results and failed to detect this frequency.



In order to ensure the environmental conditions did not affect the modal impact measurement campaign, a test was conducted in a wind tunnel. The middle section of the model was removed and secured to the bed of the tunnel. A modal impact test was conducted on it, yielding natural frequencies and corresponding mode shapes. Then a second test was conducted with the wind tunnel producing a wind speed of 7 m/s. During this run the flexible model was visibly shaken by the wind produced by the tunnel. A second modal impact test was then conducted. The results of this test are provided in Appendix E, but there was no significant change from the test conducted in still air to when the wind tunnel was engaged.

7.2.1 Data Acquisition System

Acquisition of modal data for wind turbines presents challenges not normally encountered in standard environments. By adapting traditional systems and methods, the author has created a robust system capable of monitoring modal data of large structures in remote locations. The system uses cheap and effective materials to keep down costs, along with remote control and expandability that allows the system to be adapted and modified as the needs of the project change. The results of this effort are summarized below in schematic form in Figure 18.

It is however, important to note that due to the restriction of the 100 Hz scanning rate, the frequency range available would be capped at 25 Hz for this set up. The best compromise would be to use only two sensors, one located at 15.86 m another located at 66 m, raising the maximum frequency range to 50 Hz, while still maintaining the ability to monitor all the resonance frequencies in this range, as well as retaining redundancy in the system to allow for data checking and sensor failure.

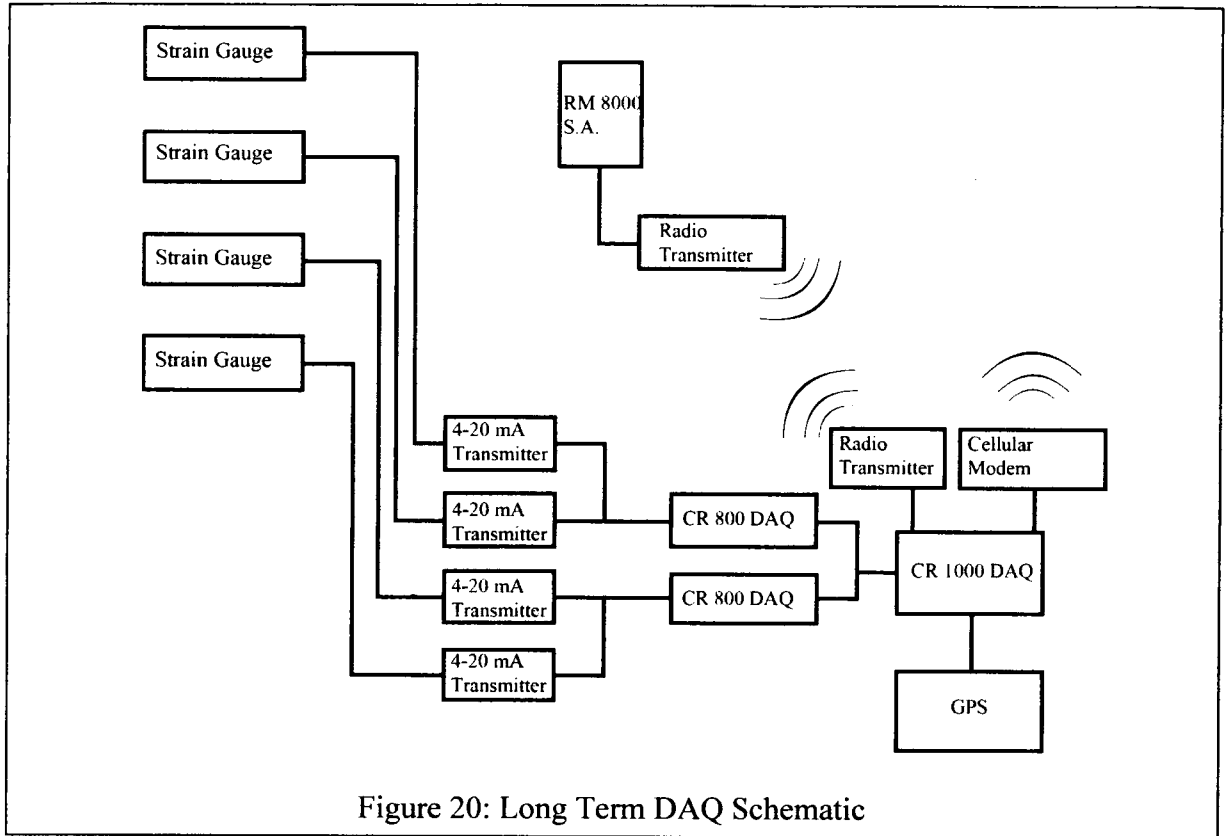


Figure 20: Long Term DAQ Schematic

as the long term DAQ, is short term modal testing. Without this, a practitioner would be unable to determine the optimal sensor locations for monitoring the excitation of natural frequencies. A system using a large impact sledge and two accelerometers equipped with a magnetic base is an ideal method for determining these locations. This setup has the benefits of being light weight and portable allowing it to be employed in remote sites, or locations without power available to them. Additionally only two investigators are needed to employ this system.

The mast can be monitored with only four strain gauges buy using the data that is generated from this roving accelerometer test. By placing sensors at the specified locations, the natural frequencies of interest can be monitored. This is done by carefully selecting a few points on the turbine which are sensitive to the majority of the natural frequencies of interest. These are the locations that undergo the greatest amount of movement due to the mode shape associated with these natural frequencies. As can be

seen in Figures 19-22, the combination of the four points that are selected are sensitive to all the natural frequencies of interest, as well as providing redundancy in the system to allow for sensor failure and double checking of the data.

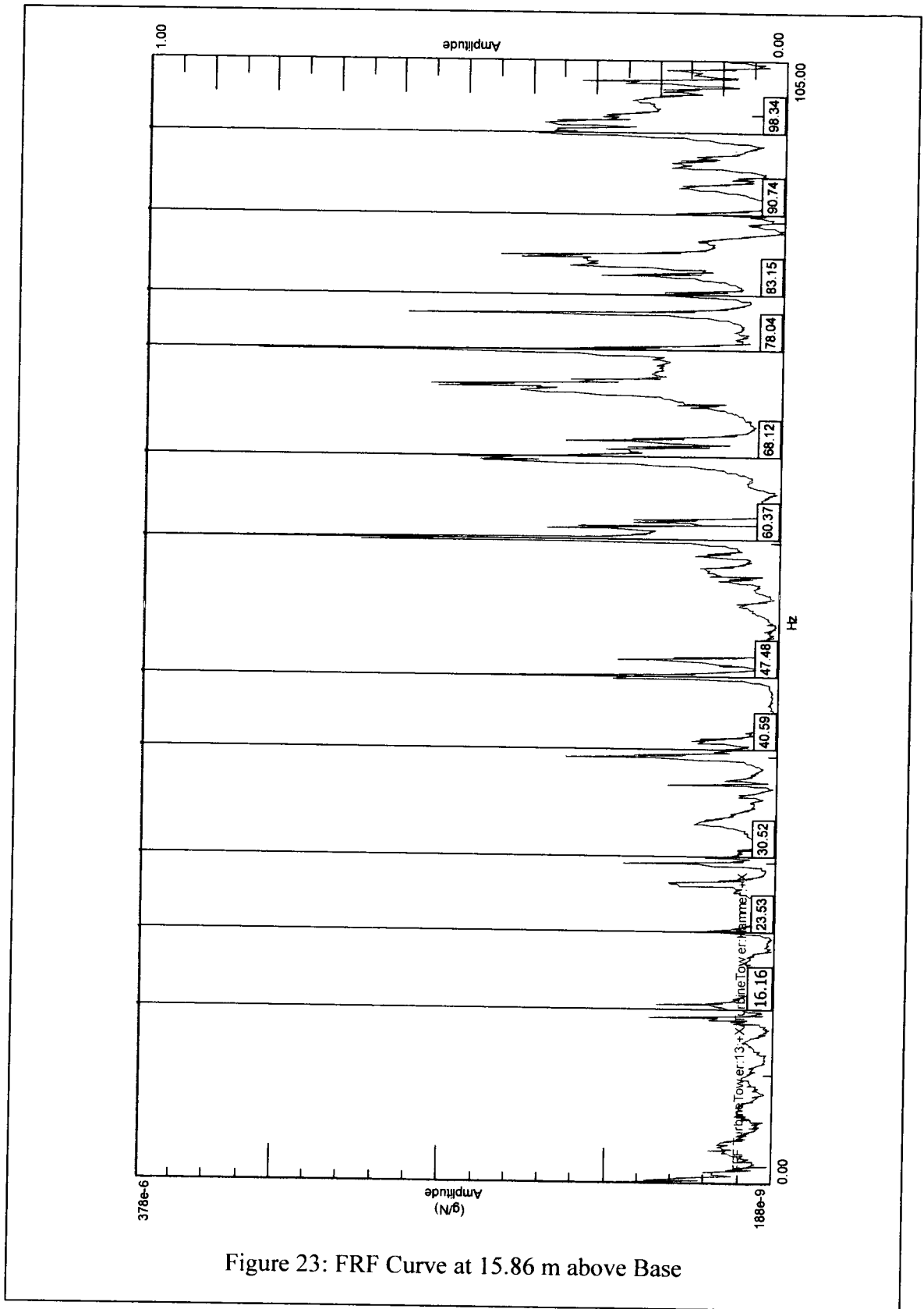


Figure 23: FRF Curve at 15.86 m above Base

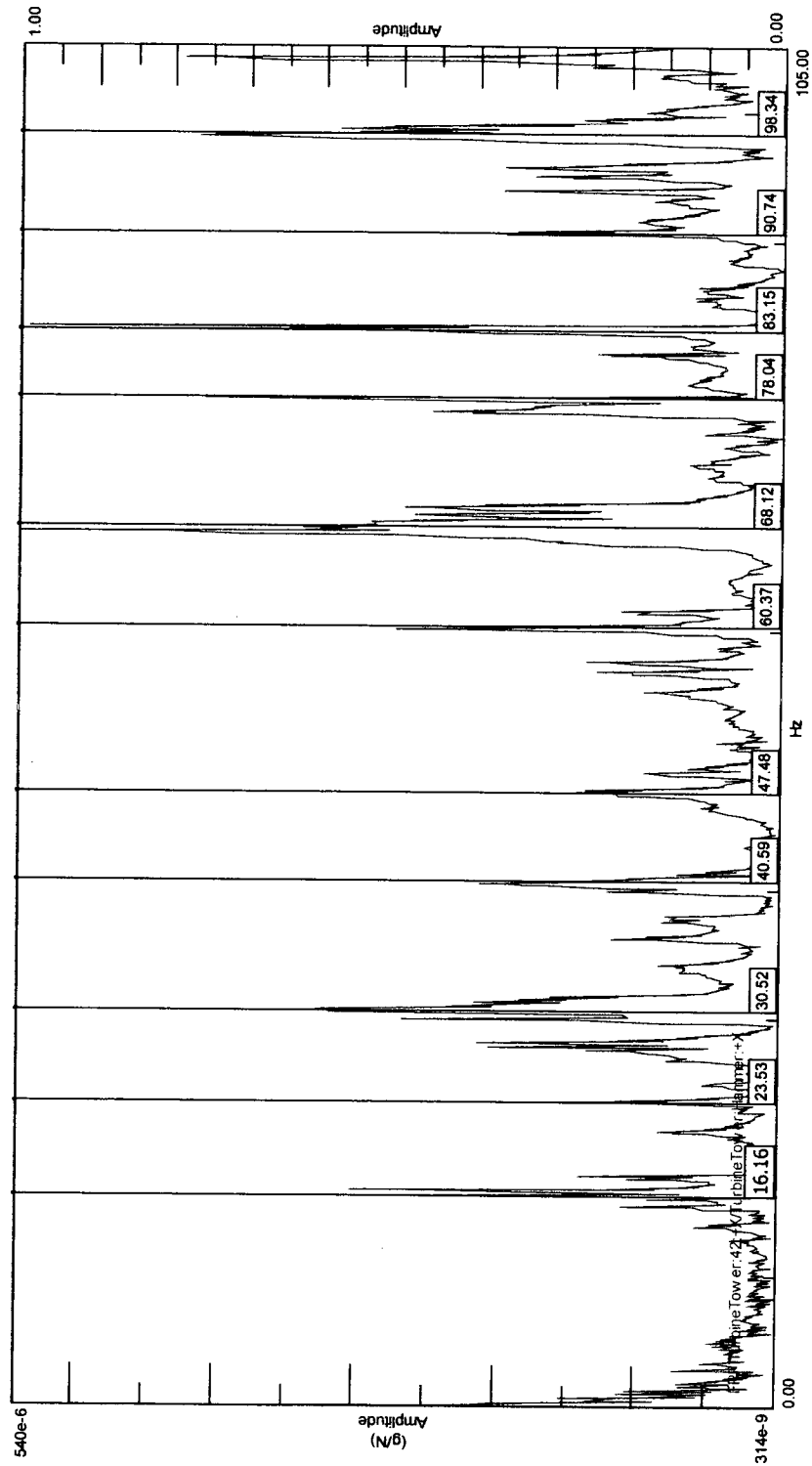


Figure 24: FRF Curve at 66.00 m above Base

7.3 Modal Model

The physical model is constructed of three aluminum sections, bolted together at their bases. When all three sections are joined, and the mass of each is adjusted to be representative of that of the wind turbine, the model will behave in a manner representative of the structure. By adding the aerodynamic elements to the model, it can then be employed in wind tunnel tests. This allows investigators to look into how the turbine could be expected to perform in severe wind conditions, test it in varying surrounding environments, and use the model in conjunction with others to determine if there would be any interference effects between many turbines grouped together in a relatively small area.

8.0 Future Work

Work for future investigators will consist mainly of three parts, testing and validation the modal model, validation of the model in a wind tunnel, and finally a complete deployment and refining of the data acquisition system.

Validation of the modal model would take place in three phases, testing the individual sections with free-free boundary conditions, testing of the assembled structure with free-free boundary conditions, and finally testing of the assembled structure with a fixed base. As previously discussed, these three tests should be conducted for ease of trouble shooting the components as they are assembled.

It is likely that adjustments will need to be made to the top section of the model before it can be employed. Foremost, the masses and aerodynamic elements will need to be fabricated and attached to the structure in order to properly scale the mass and geometry. Secondly, issues regarding the stiffness of the topmost section of the model need to be addressed. During fabrication, it was noted that the top section was too long to be machined as a single piece. Because of this, it was created in two parts and then assembled using two brass pins. This changed the stiffness in the area of the joint. The author suggests that the two sections be separated by a small gap causing this point to be supported by only the two pins. To make up remaining stiffness required, two plates would be welded in place on the outside of the joint. Barring this, there are no further problems anticipated with any of the free-free boundary condition testing. During wind tunnel testing, special care will be needed to differentiate the excitation of the desired natural frequencies which simulate the response of the wind turbine from those generated by the off axis direction. This is due to the fact that the aluminum spine that makes up the stiffness element of the model is rectangular, leading to two different sets of natural frequencies. This can be monitored by locating an accelerometer in the off axis direction during testing.

Finally the long term monitoring system will need to be employed. In order to do this, location of the low resonance frequencies at 7.96, 1.19, and less than 1 Hz that

were not detected by the modal impact testing will need to be resolved in order to ensure that a complete picture of the wind turbine is captured. It is the hope that the use of strain gauges will assist in their location in future measurement campaigns.

9.0 Concluding Remarks

The author has presented a method for monitoring of resonance frequencies in the mast of wind turbines. By first conducting a measurement campaign, proper positioning of permanent sensors can be located in as little as a single day when performed by an experienced, two man crew utilizing the proper equipment and techniques. Once located, a relatively simple and inexpensive long term DAQ system can be installed on site, allowing the range of resonance of the structure can be easily measured via two strain gauges when. The installation complicated only through the remote nature of the structure, which is easily solved though modern communication devices, allowing users to access this information worldwide.

Using this experimental data, the author was able to validate the theoretical model used to calculate the resonance frequencies of the wind turbine. Using this data, the structure was then scaled down to a size that is satiable in wind tunnel testing, providing future researchers with a tool to continue investigations into the nature of resonance in commercial wind turbine masts.

References

- Abdulrehem M.M. and Ott E. "Low Dimensional Description of Pedestrian-Induced Oscillation of the Millennium Bridge" Chaos 19 (2009)
- Ashebo, D.B., Chan, T.H.T and Yu, L. "Evaluation of dynamic loads on a Skew box girder continuous bridge Part I: Field test and modal analysis" Engineering Structures 29 (2007) 1052-1063
- Ashwill, T.D. "Initial Structural Response Measurements and Modal Validation for the Sandia 34-Meter VAWT Test Bed" SAND88-0633 (1988)
- Ashwill, T.D. "Initial Structural Response Measurements for the Sandia 34-Meter Test VWAT Test Bed." Selected Papers on Wind Energy Technology (1992): 47-54
- Ashwill, T.D. and Veers, P.S. "Structural Response Measurements and Predictions for the Sandia 34-Meter Test BED." Selected Papers on Wind Energy Technology (1992): 101-108
- Avitabile, P. "Experimental Modal Analysis: A Simple Non-Mathematical Presentation" Sound and Vibration Draft Document (2001)
- Berg, D.E., and Robertson, P.J., "Precise Time Synchronization Data Acquisition with Remote Systems" SAND98-1690C (1998)
- Berg, D.E., Robertson, P., and Zayas, J., "ATLAS: A Small, Light Weight, Time-Synchronized Wind-Turbine Data Acquisition System" AIAA-99-0050 (1999)
- Berg, D.E., Rumsey, M.A., Zayas, J.R., "Hardware and Software Developments for the Accurate time-Linked Data Acquisition System" AIAA-2000-0052 (2000)
- Berg, Dale and Zayas, Jose. "Accurate Time-Linked Data Acquisition System Field Deployment and Operational Experience." AIAA-2001-0038 (2001)
- Billah, K.Y. and Scanlan, R.H. "Resonance, Tacoma Narrows bridge failure, and undergraduate physics textbooks" American Association of Physics Teachers 59 (1991): 118-124
- Caetano, E., Cunha, A. and Taylor, C.A. "Investigation of dynamic cable-deck interaction in a physical model of a cable-stayed bridge. Part I: modal analysis" Earthquake Engineering and Structural Dynamics 29 (2000): 481-498
- Carne, T.G., Lobitz, D.W., Nord, A.R., and Watson, R.A. "Finite Element Analysis and Modal Testing of a Rotating Wind Turbine" SAND82-0345 (1982)

Carne, T.G., and Nord, A.R. "Modal Testing of a Rotating Wind Turbine" SAND82-0631(1982)

Carne, T.G., Lauffer, J.P., Gomez, A.J., and Benjannet, H. "Modal Testing the EOLE" SAND87-1506 (1987)

Carne, T.G., Lauffer, J.P., Gomez, A.J., and Ashwill, T.D., "Model Validation of the Sandia 34-Meter Test Bed Turbine Using Substructured Modal-Testing." Selected Papers on Wind Energy Technology (1992): 39-45

Chellini, G., De Roeck, G.D., Nardini, L., and Salvatore, W., "Damage detection of a steel-concrete composite frame by a multilevel approach: Experimental measurements and modal identification" Earthquake Engng Struct. Dyn. (2008): 37:1763-1783

Ewins, D.J. Modal Testing theory, practice and application Second Edition. Research Studies press LTD., 2000

Gross. E., Simmermacher, T., and Zadoks. R.I., "Application of Damage Detection Techniques using Wind Turbine Modal Data" AIAA 99-0047 (1998)

Hansen, M.O.L., Sorensen, J.N., Voutsinas, S., Sorensen, N., and Madsen, H.A. "State of the art in wind turbine aerodynamics and aeroelasticity" Progress in Aerospace Sciences 42 (2006): 285-330

Hansen, M.H. "Aeroelastic Stability Analysis of Wind Turbines Using an Eigenvalue Approach" Wind Energy (2004): 7:133-143

Hansen, M.H. "Aeroelastic Instability Problems for Wind Turbines" Wind energy 10 (2007): 551-577

Hansen, M.H., Fuglsang, P. and Kundsen, T. "Two Methods for Estimating Aeroelastic Damping of Operational Wind Turbine Modes from Experiments" Wind Energy 9 (2006): 179-191

James, G., Mayes, R., Carne, T., Simmermacher, T., and Goodding, J. "Health Monitoring of Operational Structures-Initial Results" SAND95-0345C (1995)

Kristensen, O.J.D., McGuan, M., Sendrup, P., Rheinlander, J., Rusborg, J., Hansen, - A.M., Debel, C.P., and Sorensen, B.F. "Health Monitoring of Wind Turbine Blades-a Preproject Annex E – Full-Scale Test of Wind Turbine Blade, Using Sensors and NDT" RISO-R-1333(En) (2002)

Larsen, G.C. and Volund, P. "Validation of an Aeroelastic Model of Vestas V39" RISO-R-1051(EN) (1998)

- Lauffer, J.P., Carne, T.G., and Ashwill, T.D. "Modal Testing in the Design Evaluation of Wind Turbines" SAND87-2461 (1987)
- Malcolm, D.J., and Laird, D.L. "Extraction of Equivalent Beam Properties from Blade Models" Wind Energ. (2007): 10:135-157
- Mahmoud, M.A. and Ott, E. "Low dimensional description of pedestrian-induced oscillation of the Millennium Bridge" American Institute of Physics (2009)
- McConnell, K.G. and Varoto, P.S. Vibration Testing Theory and Practice. John Wiley & Sons, Inc. 2008
- Nelson, L.D., Manuel, L., Sutherland, H.J. and Veers, P.S. "Statistical Analysis of Inflow and Structural Response Data from the LIST Program" AIAA-2003-0867 (2003)
- Pendersen, H.B. and Kristensen, O.J.D., "Applied Modal Analysis of Wind Turbine Blades" RISO-R-1388(EN) (2003)
- Pendersen, K.O.H, Hansen, K.S., Paulsen, U.S. and Sorensen, P. "Wind Turbine Measurement Technique-and Open Laboratory for Educational Purposes" Wind Energy (2008): 11:281-295
- Pedersen, T. F., Dahlberg, J., Cuerva, A., Mouzakis, F., Busche, P., Eecen, P., Sanz-Andres, A., Franchini, S. and Petersen, S.M. "ACCUWIND-Accurate Wind Speed Measurements in Wind Energy" RISO-R-1563(EN) 2006
- Prowell, I. and Veers. V., "Assessment of Wind Turbine Seismic Risk: Existing Literature and Simple Study of Tower Moment Demand" SAND2009-1100 (2009)
- Rasmussen, F., Hansen, M.H., Thomsen, K., Larsen, T.J., Bertagnolio, F., Johansen, J., Madsen, H.A., Bak, C. and Hansen, A.M. "Present Status of Aeroelasticity of Wind Turbines" Wind Energy (2003): 6:213-228
- Rumsey, M.A., Paquette, J., White, J.R., Werlink, R.J., Beattie, A.G., Pitchford, C.W. and Dam, J.V. "Experimental Results of Structural Health Monitoring of Wind Turbine Blades" American Institute of Aeronautics and Astronautics Paper (2008)
- Rumsey, M.A. and Paquette, J. "Structural health Monitoring of Wind Turbine Blades" Sandia National Laboratories Paper (2008)
- Sheldahl, R.E., "Comparison of Field and Wind Tunnel Darrieus Wind Turbine Data" SAND80-2469 (1980)

Sorensen, B.F., Lading, L., Sendrup, P., McGugan, M., Debel, C.P., Kristensen O.J.D., Larsen, G., Hansen, A.M., Rheinlander, J., Rusbork, J. and Vestergaard, J.D. "Fundamentals for Remote Structural Health Monitoring of Wind Turbine Blades-a Preproject" RISO-R-1336(EN)

Sorensen, J.D., Frandsen, S. and Tarp-Johansen, N.J., "Effective turbulence models and fatigue reliability in wind farms" Probabilistic Engineering Mechanics 23 (2008): 531-538

Sorensen, N.N., Johansen, J. and Conway, S., "CFD Computations of wind Turbine Blade Loads During Standstill Operation KNOW-BLADE TASK 3.1 Report" RISO-R-1465(EN) (2004)

Strogatz, S.H., Abrams, D.M., McRobie, A., Eckhardt, B., Ott, E. "Crowd synchrony on the Millennium Bridge" Nature Vol. 438 (2005): 43-44

Sutherland, H. J. "Damage Predictions for Wind Turbine Components using the LIFE2 Computer Code." Selected Papers on Wind Energy Technology (1992)

Sutherland, H.J. and Carlin, P.W. "Damage Measurements on the NWTTC Direct-Drive Variable-Speed Test Bed" AIAA-98-0064 (1998)

Sutherland, H.J., Jones, P.L. and Neal, B.A., "The Long-Term Inflow and Structural Test Program" AIAA-2001-0039 (2001)

Sutherland, H.J. "Inflow and the Fatigue of the LIST Wind Turbine" AIA-2002-0065 (2002)

Sutherland, H.J., Kelley, N.D. and Hand, M.M. "Inflow and Fatigue Response of the NWTTC Advanced Research Turbine" AIAA-2003-0862 (2003)

Sutherland, H.J., Zayas, J.R. and Sterns, A.J. "Update of the Long-Term Inflow and Structural Test Program" AIAA-2004-0500 (2004)

The Highways Agency, Scottish Executive Development Department, The National Assembly for Wales Cynulliat Cendlaethol Cymru, The Department for Regional Development "Design Rules for Aerodynamic Effects on Bridges" (2001)

Vand Den Avyle, J.A., Sutherland H.J. "Fatigue Characterization of a VAWT Blade Material." Selected Papers on Wind Energy Technology (1992): 19-23

Varma, R.K., Auddy, S., and Semsedini, Y. "Mitigation of Subsynchronous Resonance in a Series-Compensated Wind Farm Using FACTS Controllers." IEEE Transactions on power Delivery, Vol. 23, No. 3 (2008): 1645-1654

Veers, P.S. "Simplified Fatigue Damage and Crack Growth Calculations for Wind Turbines." Selected Papers on Wind Energy Technology (1992): 25-32

Zhang, X., Brownjohn, J.M.W., Wang, Y. and Pan, T. "Direct observations of non-stationary bridge deck aeroelastic vibration in wind tunnel" Journal of Sound and Vibration 291 (2006): 202-214

Zhu, Z., Gu, M. and Chen, Z. "Wind Tunnel and CFD Study on Identification of Flutter Derivatives of a Long-Span Self-Anchored Suspension Bridge" Computer-Aided civil and Infrastructure Engineering 22 (2007): 541-554

Appendix A Calibration and Specification Sheets

Accelerometer Calibration Sheets

~ Calibration Certificate ~

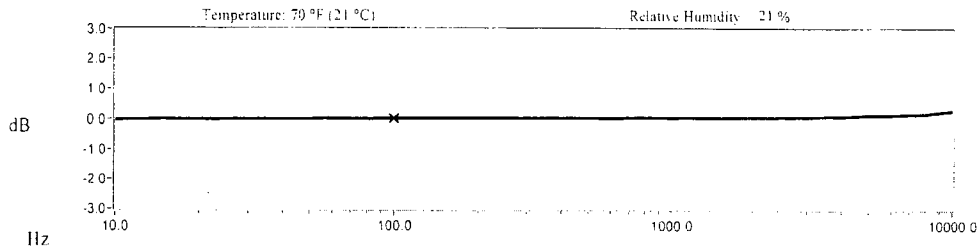
Per ISO 15063-21

Model Number: 352B10
 Serial Number: 91289
 Description: ICP® Accelerometer Method: Back-to-Back Comparison
 Manufacturer: PCB

Calibration Data

Sensitivity @ 100.0 Hz: **10.68 mV/g** Output Bias: 9.9 VDC
(1.089 mV/m/s²) Transverse Sensitivity: 2.2 %
 Discharge Time Constant: 0.4 seconds Resonant Frequency: 77.6 kHz

Sensitivity Plot



Data Points

Frequency (Hz)	Dev. (%)	Frequency (Hz)	Dev. (%)	Frequency (Hz)	Dev. (%)
10.0	-0.6	300.0	0.2	7000.0	1.7
15.0	-0.2	500.0	0.1	10000.0	3.1
30.0	-0.2	1000.0	0.2		
50.0	-0.3	3000.0	0.5		
REF. FREQ.	0.0	5000.0	1.3		

Mounting Surface: Tempcon Adapter Fastener - Curacao/Gate Adhesive Fixture Orientation: Vertical
 Acceleration Level (rms): 10.0 ± 0.1 m/s²
 The acceleration level may be limited by shaker displacement at low frequencies. If the listed level cannot be obtained, the calibration system uses the following formula to set the vibration amplitude: Acceleration Level (g) = 0.05(1 + 0.001f)². The gravitational constant used for calculations by the calibration system is: 1 g = 9.80665 m/s².

Condition of Unit

As Found: n/a
 As Left: New Unit, In Tolerance

Notes

1. Calibration is NIST Traceable thru Project 822/274086 and PTB Traceable thru Project 1060.
2. This certificate shall not be reproduced, except in full, without written approval from PCB Piezotronics, Inc.
3. Calibration is performed in compliance with ISO 9001, ISO 10012-1, ANSI/NCSL Z540-1-1994 and ISO 17025.
4. See Manufacturer's Specification Sheet for a detailed listing of performance specifications.
5. Measurement uncertainty (95% confidence level with coverage factor of 2) for frequency ranges tested during calibration are as follows: 5-9 Hz: +/- 2.0%, 10-99 Hz: +/- 1.5%, 100-1999 Hz: +/- 1.0%, 2-10 kHz: +/- 2.5%.

Technician: Robert Zsebezhay R. Z Date: 02/29/08



Headquarters: 3425 Walden Avenue, Depew, NY 14043
 Manufacturing and Calibration Facility: 10869 Highway 903, Halifax, NC 27839
 TEL: 888-684-0013 FAX: 716-685-3886 www.pcb.com

0485-235158109-02



~ Calibration Certificate ~

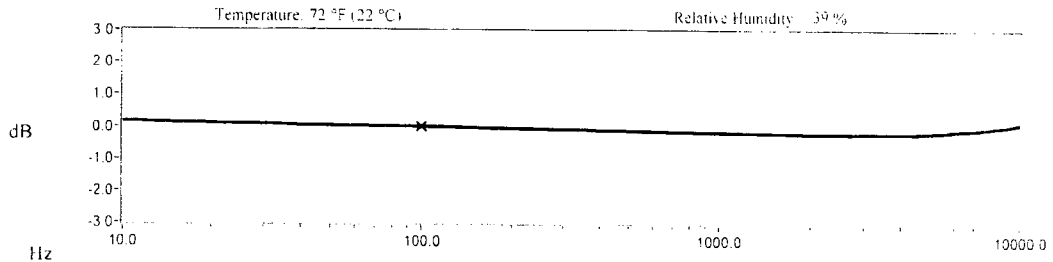
Per ISO 15063-21

Model Number: 352C34
 Serial Number: 101574
 Description: ICP® Accelerometer Method: Back-to-Back Comparison (AT401-3)
 Manufacturer: PCB

Calibration Data

Sensitivity @ 100.0 Hz **100.0** mV/g Output Bias 11.2 VDC
 (10.20 mV/m/s²) Transverse Sensitivity 0.3 %
 Discharge Time Constant 1.8 seconds Resonant Frequency 57.1 kHz

Sensitivity Plot



Data Points

Frequency (Hz)	Dev. (%)	Frequency (Hz)	Dev. (%)	Frequency (Hz)	Dev. (%)
10.0	1.8	300.0	-1.0	7000.0	-1.2
15.0	1.2	500.0	-1.5	10000.0	1.2
30.0	0.9	1000.0	-2.1		
50.0	0.2	3000.0	-2.5		
REF. FREQ.	0.0	5000.0	-2.1		

Measuring Surface: Stainless Steel w/ Silicone Grease Coating Fastener: Stud Mount Fixture Orientation: Vertical
 Acceleration Level (rms): 10 Hz @ 0.81 m/s²
 The acceleration level may be limited by shaker displacement at low frequencies. If the listed level cannot be obtained, the calibration system uses the following formula to set the vibration amplitude: Acceleration Level (g_{rms}) = 0.039 * sqrt(freq)
 The gravitational constant used for calculations by the calibration system is: 1 g = 9.80665 m/s²

Condition of Unit

As Found: n/a
 As Left: New Unit, In Tolerance

Notes

1. Calibration is NIST Traceable thru Project 822/277342 and PTB Traceable thru Project 1254.
2. This certificate shall not be reproduced, except in full, without written approval from PCB Piezotronics, Inc.
3. Calibration is performed in compliance with ISO 9001, ISO 10012-1, ANSI/NCSL Z540-1-1994 and ISO 17025.
4. See Manufacturer's Specification Sheet for a detailed listing of performance specifications.
5. Measurement uncertainty (95% confidence level with coverage factor of 2) for frequency ranges tested during calibration are as follows: 5-9 Hz: +/- 2.0%, 10-99 Hz: +/- 1.5%, 100-1999 Hz: +/- 1.0%, 2-10 kHz: +/- 2.5%.

Technician: Brian Kemp Date: 02/02/09



ACCREDITED
 CALIBRATION CERT #1862.02



Headquarters 3425 Walden Avenue, Depew, NY 14043
 Calibration Performed at: 10869 Highway 903, Halifax, NC 27839
 TEL: 888-684-0013 FAX: 716-685-3886 www.pcb.com

PAGE 1 of 1

DATE: 02/02/09



~ Calibration Certificate ~

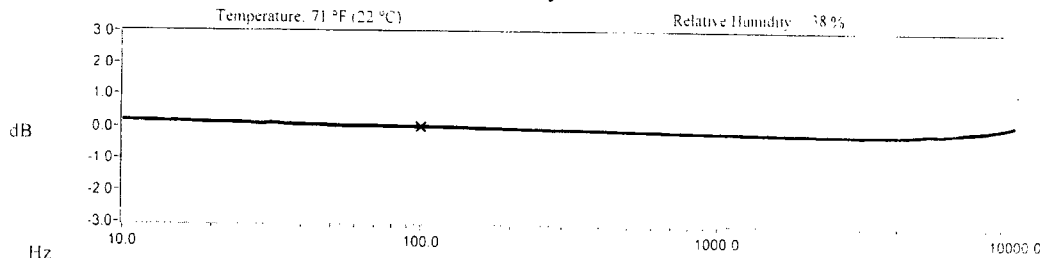
Per ISO 16063-21

Model Number: 352C34
 Serial Number: 101808
 Description: ICP® Accelerometer Method: Back-to-Back Comparison (A1401-3)
 Manufacturer: PCB

Calibration Data

Sensitivity @ 100.0 Hz	98.9 mV/g	Output Bias	10.7 VDC
	(10.08 mV/m/s ²)	Transverse Sensitivity	2.3 %
Discharge Time Constant	1.8 seconds	Resonant Frequency	56.8 kHz

Sensitivity Plot



Data Points

Frequency (Hz)	Dev. (%)	Frequency (Hz)	Dev. (%)	Frequency (Hz)	Dev. (%)
10.0	2.1	300.0	-1.0	7000.0	-1.2
15.0	1.7	500.0	-1.5	10000.0	1.3
30.0	1.0	1000.0	-2.1		
50.0	0.5	3000.0	-2.8		
REF. FREQ.	0.0	5000.0	-2.0		

Mounting Surface: Stainless Steel w/ Silicone Grease Coating Fastener: Stud Mount Fixture Orientation: Vertical
 Acceleration Level (rms): 10.0 g (98.1 m/s²)
 *The acceleration level may be limited by shaker displacement at low frequencies. If the listed level cannot be obtained, the calibration system uses the following formula to set the vibration amplitude: Acceleration Level (g) = 0.010 * (v/freq)²
 †The gravitational constant used for calculations by this calibration system is: 1 g = 9.80665 m/s²

Condition of Unit

As Found: n/a
 As Left: New Unit, In Tolerance

Notes

1. Calibration is NIST Traceable thru Project 822/277342 and PTB Traceable thru Project 1254.
2. This certificate shall not be reproduced, except in full, without written approval from PCB Piezotronics, Inc.
3. Calibration is performed in compliance with ISO 9001, ISO 10012-1, ANSI/NCSL Z540-1-1994 and ISO 17025.
4. See Manufacturer's Specification Sheet for a detailed listing of performance specifications.
5. Measurement uncertainty (95% confidence level with coverage factor of 2) for frequency ranges tested during calibration are as follows: 5-9 Hz: +/- 2.0%, 10-99 Hz: +/- 1.5%, 100-1999 Hz: +/- 1.0%, 2-10 kHz: +/- 2.5%.

Technician: Joseph Rogerson Date: 02-03-09



ACCREDITED
 CALIBRATION CERT #1862.02



Headquarters: 3425 Walden Avenue, Depew, NY 14043
 Calibration Performed at: 10869 Highway 903, Halifax, NC 27839
 TEL: 888-684-0013 FAX: 716-685-3886 www.pcb.com



Impulse Hammer Calibration Certificate

~Calibration Certificate~

Model No.: 086D50 Customer: _____

Serial No.: 26873 _____

Description: Impulse Force Hammer PO No.: _____

Manufacturer: PCB Calibration Method: Impulse (at-303-1)

Data

Output Bias: **9.6** Temperature: **74 °F** **23 °C** Relative Humidity: **36 %**

HAMMER SENSITIVITY:

Tip		Medium (Red)		
Hammer Configuration		Extender	None	
Hammer Sensitivity	mV/lb		1.03	
	(mV/N)		0.23	


Above data is valid for all supplied tips.

Condition of Unit:

As Found *N/A*.
As Left New unit in tolerance.

Notes:

1. Calibration is N.I.S.T traceable through project No. 822/274086 and PTB Traceable thru Project 1060.
2. This certificate may not be reproduced, except in full, without written approval from PCB Piezotronics, inc
3. Calibration is performed in compliance with ISO 10012-1, ANSI/NCSL Z540-1-1994.
4. See Manufacturer's specification sheet for a detailed listing of performance specifications.
5. Measurement uncertainty (95% confidence level with a coverage factor of 2) is +/- 3.8%.

Technician: Jose Ramos 

Date: 2/18/2009



7208441, 1.5, 2001.1, 100.00



3425 Walden Avenue
Depew, N.Y. 14043

TEL: 716-684-0001


FAX: 716-684-0987

www.pcb.com

Page 1 of 1

Revision: 02

Impact Hammer Specification Sheet

Model Number 086DS0	IMPACT HAMMER, ICP®		Revision D ECN # 27899										
<p>Performance</p> <p>Sensitivity (±15 %) ±5000 lbf/pk Resonant Frequency Non-Linearity</p> <p>Electrical</p> <p>Excitation Voltage Constant Current Excitation Output Impedance Output Bias Voltage Discharge Time Constant</p> <p>Physical</p> <p>Sensing Element Sealing Hammer Mass Head Diameter Tip Diameter Hammer Length Electrical Connection Position Electrical Connector</p>	<p>ENGLISH</p> <p>1 mV/lbf ±5000 lbf/pk ≥5 KHZ ≤1 %</p> <p>18 to 30 VDC 2 to 20 mA <100 ohm 8 to 12 VDC ≥2000 sec</p> <p>Quartz Hermetic 12.1 lb 3.0 in 3.0 in 35 in Bottom of Handle BNC Jack</p>	<p>SI</p> <p>0.23 mV/N ±22240 N/pk ≥5 KHZ ≤1 %</p> <p>18 to 30 VDC 2 to 20 mA <100 ohm 8 to 12 VDC ≥2000 sec</p> <p>Quartz Hermetic 5.5 kg 7.6 cm 7.6 cm 89 cm Bottom of Handle BNC Jack</p>	<p>Optional Versions (Optional versions have identical specifications and accessories as listed for standard model except where noted below. More than one option may be used.) T - TEDS Capable of Digital Memory and Communication Compliant with IEEE P1451.4</p> <p>Output Bias Voltage 8.5 to 13 VDC 8.5 to 13 VDC</p> <p>Notes [1] Typical</p> <p>Supplied Accessories 084A31 Tip - soft plastic, brown (1) 084A32 Tip - hard plastic, red (1) HCS 2 Calibration of Series 086 instrumented impact hammers (1)</p>										
<p><i>All specifications are at room temperature unless otherwise specified in the interest of constant product improvement, we reserve the right to change specifications without notice ICP® is a registered trademark of PCB group, Inc.</i></p>													
		<table border="1" style="width: 100%; border-collapse: collapse;"> <tr> <td>Entered: LLH</td> <td>Engineer: CCL</td> <td>Sales: RJL</td> <td>Approved: EB</td> <td>Spec Number:</td> </tr> <tr> <td>Date: 01/02/2008</td> <td>Date: 12/14/2007</td> <td>Date: 12/19/2007</td> <td>Date: 12/19/2007</td> <td>12993</td> </tr> </table>		Entered: LLH	Engineer: CCL	Sales: RJL	Approved: EB	Spec Number:	Date: 01/02/2008	Date: 12/14/2007	Date: 12/19/2007	Date: 12/19/2007	12993
Entered: LLH	Engineer: CCL	Sales: RJL	Approved: EB	Spec Number:									
Date: 01/02/2008	Date: 12/14/2007	Date: 12/19/2007	Date: 12/19/2007	12993									
		 <p>3425 Walden Avenue Depew, NY 14043 UNITED STATES Phone: 888-684-0013 Fax: 716-685-3886 E-mail: vibration@pcb.com Web site: www.pcb.com</p>											

Accelerometer Specification Sheets

Model Number 352B10	ICP® ACCELEROMETER	Revision D ECN # 24842										
Performance Sensitivity (± 10 %) Measurement Range Frequency Range (± 5 %) F. Frequency Range (± 10 %) Resonant Frequency Broadband Resolution (1 to 10,000 Hz) Non-Linearity Transverse Sensitivity Environmental Overload Limit (Shock) Temperature Range (Operating) Electrical Excitation Voltage Constant Current Excitation Output Impedance Output Bias Voltage Discharge Time Constant Settling Time (within 10% of bias) Spectral Noise (1 Hz) Spectral Noise (10 Hz) Spectral Noise (100 Hz) Spectral Noise (1 kHz) Physical Sensing Element Sensing Geometry Housing Material Sealing Size (Height x Diameter) Weight Electrical Connector Electrical Connection Position Cable Termination Cable Length Cable Type Mounting	ENGLISH 10 mV/g ± 500 g pk 2 to 10,000 Hz 1 to 17,000 Hz ± 65 kHz 0.003 g rms ± 1 % ± 5 % ± 10,000 g pk -65 to +250 °F See Graph 18 to 30 VDC 2 to 20 mA ± 200 ohm 7 to 11 VDC 0.3 to 1.0 sec <3 sec 1000 µg/√Hz 300 µg/√Hz 80 µg/√Hz 25 µg/√Hz Ceramic Shear Titanium Hermetic 0.32 in x 0.24 in 0.03 oz Top 10-32 Coaxial Plug 10 ft 030 Coaxial Adhesive Solder pins with attached cable Solder pins with attached cable Top 10-32 Coaxial Plug 3 m 030 Coaxial Adhesive	SI 1.02 mV/(m/s²) ± 4005 m/s² pk 2 to 10,000 Hz 1 to 17,000 Hz ± 65 kHz 0.03 m/s² rms ± 1 % ± 5 % ± 98,100 m/s² pk -64 to +121 °C See Graph 18 to 30 VDC 2 to 20 mA ± 200 ohm 7 to 11 VDC 0.3 to 1.0 sec <3 sec 9810 (µm/s²)/√Hz 2843 (µm/s²)/√Hz 785 (µm/s²)/√Hz 308 (µm/s²)/√Hz Ceramic Shear Titanium Hermetic 8.1 mm x 6.1 mm 0.7 gm Solder pins with attached cable Solder pins with attached cable Top 10-32 Coaxial Plug 3 m 030 Coaxial Adhesive	OPTIONAL VERSIONS Optional versions have identical specifications and accessories as listed for the standard model except where noted below. More than one option may be used. HT - High temperature, extends normal operation temperatures Temperature Range (Operating) -65 to 325 °F -54 to 163 °C W - Water Resistant Cable Temperature Range (Operating) -20 to 220 °F -28 to 104 °C Electrical Connector Sealed Integral Cable Cable Type 018 Coaxial 018 Coaxial									
NOTES: [1] Typical. [2] 250° F to 325° F data valid with HT option only. [3] Zero-based, least-squares, straight line method.												
SUPPLIED ACCESSORIES: Model 080A109 Petro Wax (1) Model 080A90 Quick Bonding Gel (1) Model ACS-1 INST traceable frequency response (10 Hz to upper 5% point). (1)												
<table border="1" style="width: 100%; border-collapse: collapse;"> <tr> <td>Entered: <i>JR</i></td> <td>Engineer: <i>PKH</i></td> <td>Sales: <i>WJ</i></td> <td>Approved: <i>[Signature]</i></td> <td>Spec Number:</td> </tr> <tr> <td>Date: 8-18-04</td> <td>Date: 8/2/06</td> <td>Date: 8/2/06</td> <td>Date: 8/2/06</td> <td>16312</td> </tr> </table>			Entered: <i>JR</i>	Engineer: <i>PKH</i>	Sales: <i>WJ</i>	Approved: <i>[Signature]</i>	Spec Number:	Date: 8-18-04	Date: 8/2/06	Date: 8/2/06	Date: 8/2/06	16312
Entered: <i>JR</i>	Engineer: <i>PKH</i>	Sales: <i>WJ</i>	Approved: <i>[Signature]</i>	Spec Number:								
Date: 8-18-04	Date: 8/2/06	Date: 8/2/06	Date: 8/2/06	16312								
<p style="text-align: center;">Typical Sensitivity Deviation vs Temperature</p>												
All specifications are at room temperature unless otherwise specified. In the interest of constant product improvement, we reserve the right to change specifications without notice. ICP® is a registered trademark of PCB Group, Inc.												

Phone: 716-684-0001
 Fax: 716-685-3888
 E-Mail: vibration@pcb.com

PCB PIEZOTRONICS™
 VIBRATION DIVISION
 3425 Warden Avenue, Depew, NY 14043

ACCELEROMETER, ICP®

Optional Versions (Optional versions have identical specifications and accessories as listed for standard model except where noted below. More than one option may be used.)

HT - High temperature, extends normal operation temperatures

Frequency Range (5%) 6 to 10000 Hz

Frequency Range (10%) 4.5 to 15000 Hz

Broadband Resolution (1 to 10000 Hz) 0.0009 g rms

Temperature Range (Operating) -65 to +325 °F

Excitation Voltage 22 to 30 VDC

Discharge Time Constant 0.07 to 0.15 sec

Spectral Noise (1 Hz) 107 µg/√Hz

Spectral Noise (10 Hz) 58 µg/√Hz

Spectral Noise (100 Hz) 41 µg/√Hz

Spectral Noise (1000 Hz) 9.8 µg/√Hz

Output Bias Voltage 10 to 15 VDC

Supplied Accessory, Model ACS-68 Single Axis Amplitude Response Calibration from 5 Hz to upper 5% plotted on dB scale replaces Model ACS-1

J - Ground Isolated

Frequency Range (5%) 0.5 to 9000 Hz

Frequency Range (10%) 0.3 to 14000 Hz

Resonant Frequency ≥40 kHz

Electrical Isolation (Base) >10³ ohm

Size (Hex x Height) 0.44 in x 0.93 in

Weight 0.21 oz

Weight 6.0 gm

T - TEDS Capable of Digital Memory and Communication Compliant with IEEE P1451.4

TLA - TEDS LMS International - Free Format

TLB - TEDS LMS International - Automotive Format

TLC - TEDS LMS International - Aeronautical Format

TLD - TEDS Capable of Digital Memory and Communication Compliant with IEEE 1451.4

Temperature Range -10 to +200 °F

Excitation Voltage 20 to 30 VDC

Output Bias Voltage 7.5 to 13 VDC

W - Water Resistant Cable

Electrical Connector Sealed Integral Cable

Electrical Connection Position Sealed Integral Cable Top

Notes
 [1] Typical.
 [2] TEDS option adds 1.0 VDC to bias voltage.
 [3] 200°F to 325°F data valid with HT option only.
 [4] Zero-based, least-squares, straight line method.
 [5] See PCB Declaration of Conformance PS023 for details.

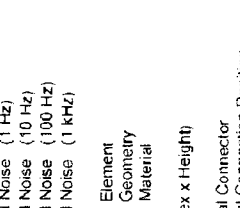
Supplied Accessories
 080A Adhesive Mounting Base (1)
 080A109 Petro Wax (1)
 081B05 Mounting Stud (10-32 to 10-32) (1)
 ACS-1 NIST traceable frequency response (10 Hz to upper 5% point), (1)
 M081B05 Mounting Stud 10-32 to M6 X 0.75 (1)

Performance	ENGLISH	SI
Sensitivity (±10%)	100 mV/g	10.2 mV/(m/s ²)
Measurement Range	±50 g pk	±490 m/s ² pk
Frequency Range (±5%)	0.5 to 10000 Hz	0.5 to 10000 Hz
Frequency Range (±10%)	0.3 to 15000 Hz	0.3 to 15000 Hz
Resonant Frequency	≥50 kHz	≥50 kHz
Broadband Resolution (1 to 10000 Hz)	0.00015 g rms	0.0015 m/s ² rms
Non-Linearity	≤1%	≤1%
Transverse Sensitivity	≤5%	≤5%

Environmental		
Overload Limit (Shock)	±5000 g pk	±49000 m/s ² pk
Temperature Range (Operating)	-65 to +200 °F	-54 to +93 °C
Temperature Response	See Graph	See Graph
Base Strain Sensitivity	0.003 g/µε	0.029 (m/s ²)/µε

Electrical		
Excitation Voltage	18 to 30 VDC	18 to 30 VDC
Constant Current Excitation	2 to 20 mA	2 to 20 mA
Output Impedance	≤200 ohm	≤200 ohm
Output Bias Voltage	7 to 12 VDC	7 to 12 VDC
Discharge Time Constant	1.0 to 2.5 sec	1.0 to 2.5 sec
Settling Time (within 10% of bias)	<10 sec	<10 sec
Spectral Noise (1 Hz)	39 µg/√Hz	380 (µm/s ²)/√Hz
Spectral Noise (10 Hz)	11 µg/√Hz	110 (µm/s ²)/√Hz
Spectral Noise (100 Hz)	3.4 µg/√Hz	33 (µm/s ²)/√Hz
Spectral Noise (1 kHz)	1.4 µg/√Hz	14 (µm/s ²)/√Hz

Physical		
Sensing Element	Ceramic	Ceramic
Sensing Geometry	Shear	Shear
Housing Material	Titanium	Titanium
Sealing	Hermetic	Hermetic
Size (Hex x Height)	0.44 in x 0.88 in	11.2 mm x 22.4 mm
Weight	0.20 oz	5.8 gm
Electrical Connector	10-32 Coaxial Jack	10-32 Coaxial Jack
Electrical Connection Position	Top	Top
Mounting Thread	10-32 Female	10-32 Female
Mounting Torque	10 to 20 in-lb	113 to 226 N-cm



All specifications are at room temperature unless otherwise specified in the interest of constant product improvement, we reserve the right to change specifications without notice. ICP® is a registered trademark of PCB group, Inc.

Entered: BLS	Engineer: JJB	Sales: WDC	Approved: BAM	Spec Number
--------------	---------------	------------	---------------	-------------

Appendix B ANSYS Reports

Test Specimen Free-Free Condition

First Saved	Tuesday, November 10, 2009
Last Saved	Monday, January 11, 2010
Product Version	11.0 SP1 Release

Units

Unit System	Metric (m, kg, N, °C, s, V, A)
Angle	Degrees
Rotational Velocity	rad/s

Model

Geometry

Model > Geometry

Object Name	Geometry
State	Fully Defined
Definition	
Source	Unnamed.agdb
Type	DesignModeler
Length Unit	Millimeters
Element Control	Program Controlled
Display Style	Part Color
Bounding Box	
Length X	4.7e-002 m
Length Y	4.7e-002 m
Length Z	1.095 m
Properties	
Volume	5.2375e-004 m ³
Mass	4.059 kg
Statistics	
Bodies	1
Active Bodies	1
Nodes	29968
Elements	4523
Preferences	
Import Solid Bodies	Yes
Import Surface Bodies	Yes
Import Line Bodies	Yes

Parameter Processing	Yes
Personal Parameter Key	DS
CAD Attribute Transfer	No
Named Selection Processing	No
Material Properties Transfer	No
CAD Associativity	Yes
Import Coordinate Systems	No
Reader Save Part File	No
Import Using Instances	Yes
Do Smart Update	No
Attach File Via Temp File	No
Analysis Type	3-D
Mixed Import Resolution	None
Enclosure and Symmetry Processing	Yes

Model > Geometry > Parts

Object Name	<i>Solid</i>
State	Meshed
Graphics Properties	
Visible	Yes
Transparency	1
Definition	
Suppressed	No
Material	Stainless Steel
Stiffness Behavior	Flexible
Nonlinear Material Effects	Yes
Bounding Box	
Length X	4.7e-002 m
Length Y	4.7e-002 m
Length Z	1.095 m
Properties	
Volume	5.2375e-004 m ³
Mass	4.059 kg
Centroid X	8.0565e-019 m
Centroid Y	9.0636e-019 m
Centroid Z	0.5475 m
Moment of Inertia Ip1	0.4019 kg·m ²
Moment of Inertia Ip2	0.4019 kg·m ²
Moment of Inertia Ip3	1.8889e-003 kg·m ²
Statistics	
Nodes	29968
Elements	4523

Mesh

Model > Mesh

Object Name	<i>Mesh</i>
State	Solved
Defaults	
Physics Preference	Mechanical
Relevance	0
Advanced	
Relevance Center	Coarse
Element Size	6.e-003 m
Shape Checking	Standard Mechanical
Solid Element Midside Nodes	Program Controlled
Straight Sided Elements	Yes
Initial Size Seed	Part
Smoothing	Low
Transition	Fast
Statistics	
Nodes	29968
Elements	4523

Model > Mesh > Mesh Controls

Object Name	<i>Body Sizing</i>	<i>Hex Dominant Method</i>
State	Fully Defined	
Scope		
Scoping Method	Geometry Selection	
Geometry	1 Body	
Definition		
Suppressed	No	
Type	Element Size	
Element Size	Default	
Edge Behavior	Curv/Proximity Refinement	
Method	Hex Dominant	
Element Midside Nodes	Use Global Setting	
Control Messages	No	

Modal

Model > Analysis

Object Name	<i>Modal</i>
State	Fully Defined
Definition	
Physics Type	Structural
Analysis Type	Modal
Options	
Reference Temp	22. °C

Model > Modal > Initial Condition

Object Name	<i>Initial Condition</i>
State	Fully Defined
Definition	
Initial Condition Environment	None

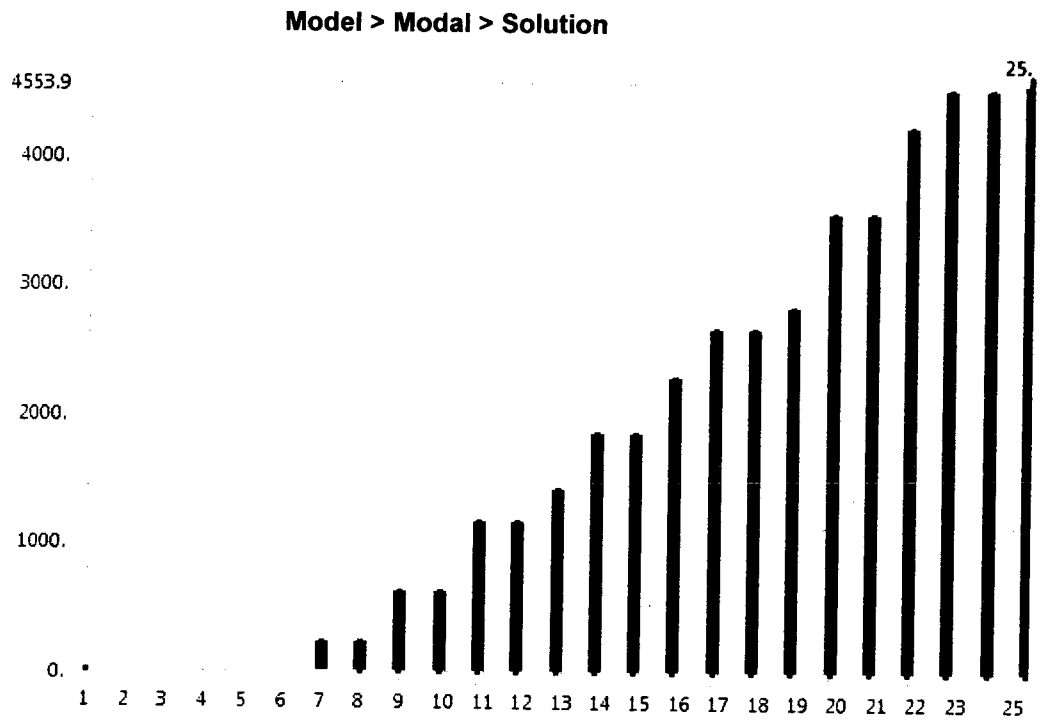
Model > Modal > Analysis Settings

Object Name	<i>Analysis Settings</i>
State	Fully Defined
Options	
Max Modes to Find	25
Limit Search to Range	No
Solver Controls	
Solver Type	Program Controlled
Output Controls	
Calculate Stress	No
Calculate Strain	No
Analysis Data Management	
Solver Files Directory	E:\Thesis Archive\Thesis Backup Nov. 6\Thesis Results\Pole\Free Free\Ansys\Free Free Pole Simulation Files\Modal\
Future Analysis	None
Save ANSYS db	No
Delete Unneeded Files	Yes

Solution

Model > Modal > Solution	
Object Name	Solution
State	Solved
Adaptive Mesh Refinement	
Max Refinement Loops	1.
Refinement Depth	2.

The following bar chart indicates the frequency at each calculated mode.



Model > Modal > Solution

Mode	Frequency [Hz]
1.	0.
2.	
3.	1.7634e-004
4.	4.2372e-004
5.	1.012e-003
6.	1.9568e-003
7.	224.93
8.	224.94
9.	607.82
10.	607.83
11.	1158.6
12.	1158.7
13.	1407.8
14.	1849.5
15.	1849.6
16.	2278.3
17.	2654.1
18.	2654.2
19.	2815.5
20.	3547.8
21.	
22.	4223.3
23.	4508.9
24.	
25.	4553.9

Model > Modal > Solution > Solution Information

Object Name	<i>Solution Information</i>
State	Solved
Solution Information	
Solution Output	Solver Output
Newton-Raphson Residuals	0
Update Interval	2.5 s
Display Points	All

Model > Modal > Solution > Results

Object Name	Total Deformation 11	Total Deformation 12
State	Solved	
Scope		
Geometry	All Bodies	
Definition		
Type	Total Deformation	
Mode	11	12
Results		
Frequency	1158.6 Hz	1158.7 Hz
Minimum	4.286e-003 m	3.1258e-003 m
Maximum	0.97978 m	0.97971 m

Material Data

Stainless Steel

TABLE 15
Stainless Steel > Constants

Structural	
Young's Modulus	1.93e+011 Pa
Poisson's Ratio	0.31
Density	7750. kg/m ³
Thermal Expansion	1.7e-005 1/°C
Tensile Yield Strength	2.07e+008 Pa
Compressive Yield Strength	2.07e+008 Pa
Tensile Ultimate Strength	5.86e+008 Pa
Compressive Ultimate Strength	0. Pa
Thermal	
Thermal Conductivity	15.1 W/m·°C
Specific Heat	480. J/kg·°C
Electromagnetics	
Relative Permeability	10000
Resistivity	7.7e-007 Ohm·m

Test Specimen Fixed-Free Condition

First Saved	Monday, January 11, 2010
Last Saved	Monday, January 18, 2010
Product Version	11.0 SP1 Release

Units

Unit System	Metric (m, kg, N, °C, s, V, A)
Angle	Degrees
Rotational Velocity	rad/s

Model

Geometry

Model > Geometry	
Object Name	Geometry
State	Fully Defined
Definition	
Source	E:\Single Beam\Single Beam Fixed.agdb
Type	DesignModeler
Length Unit	Meters
Element Control	Program Controlled
Display Style	Part Color
Bounding Box	
Length X	4.8e-002 m
Length Y	4.8e-002 m
Length Z	0.98 m
Properties	
Volume	4.7952e-004 m ³
Mass	3.7163 kg
Statistics	
Bodies	1
Active Bodies	1
Nodes	28446
Elements	14091
Preferences	
Import Solid Bodies	Yes
Import Surface Bodies	Yes
Import Line Bodies	Yes
Parameter Processing	Yes
Personal Parameter Key	DS
CAD Attribute Transfer	No

Named Selection Processing	No
Material Properties Transfer	No
CAD Associativity	Yes
Import Coordinate Systems	No
Reader Save Part File	No
Import Using Instances	Yes
Do Smart Update	No
Attach File Via Temp File	No
Analysis Type	3-D
Mixed Import Resolution	None
Enclosure and Symmetry Processing	Yes

Model > Geometry > Parts

Object Name	<i>Solid</i>
State	Meshed
Graphics Properties	
Visible	Yes
Transparency	1
Definition	
Suppressed	No
Material	Stainless Steel
Stiffness Behavior	Flexible
Nonlinear Material Effects	Yes
Bounding Box	
Length X	4.8e-002 m
Length Y	4.8e-002 m
Length Z	0.98 m
Properties	
Volume	4.7952e-004 m ³
Mass	3.7163 kg
Centroid X	-1.7495e-018 m
Centroid Y	1.1795e-018 m
Centroid Z	0.49 m
Moment of Inertia Ip1	0.29494 kg·m ²
Moment of Inertia Ip2	0.29494 kg·m ²
Moment of Inertia Ip3	1.8093e-003 kg·m ²
Statistics	
Nodes	28446
Elements	14091

Mesh

Model > Mesh

Object Name	<i>Mesh</i>
State	Solved
Defaults	
Physics Preference	Mechanical
Relevance	0
Advanced	
Relevance Center	Coarse
Element Size	Default
Shape Checking	Standard Mechanical
Solid Element Midside Nodes	Program Controlled
Straight Sided Elements	No
Initial Size Seed	Active Assembly
Smoothing	Low
Transition	Fast
Statistics	
Nodes	28446
Elements	14091

Model > Mesh > Mesh Controls

Object Name	<i>Body Sizing</i>	<i>Patch Conforming Method</i>
State	Fully Defined	
Scope		
Scoping Method	Geometry Selection	
Geometry	1 Body	
Definition		
Suppressed	No	
Type	Element Size	
Element Size	Default	
Edge Behavior	Curv/Proximity Refinement	
Method	Tetrahedrons	
Algorithm	Patch Conforming	
Element Midside Nodes	Use Global Setting	
Expansion Factor	1	

Modal

Model > Analysis

Object Name: *Modal*
 State: Fully Defined

Definition

Physics Type: Structural
 Analysis Type: Modal

Options

Reference Temp: 22. °C

Model > Modal > Initial Condition

Object Name: *Initial Condition*
 State: Fully Defined

Definition

Initial Condition Environment: None

Model > Modal > Analysis Settings

Object Name: *Analysis Settings*

State: Fully Defined

Options

Max Modes to Find: 10

Limit Search to Range: No

Solver Controls

Solver Type: Program Controlled

Output Controls

Calculate Stress: No

Calculate Strain: No

Analysis Data Management

Solver Files Directory: E:\Finalized Ansys Reluts 2\Fixed Pole\Single Beam Fixed Simulation Files\Modal\

Future Analysis: None

Save ANSYS db: No

Delete Unneeded Files: Yes

Model > Modal > Loads

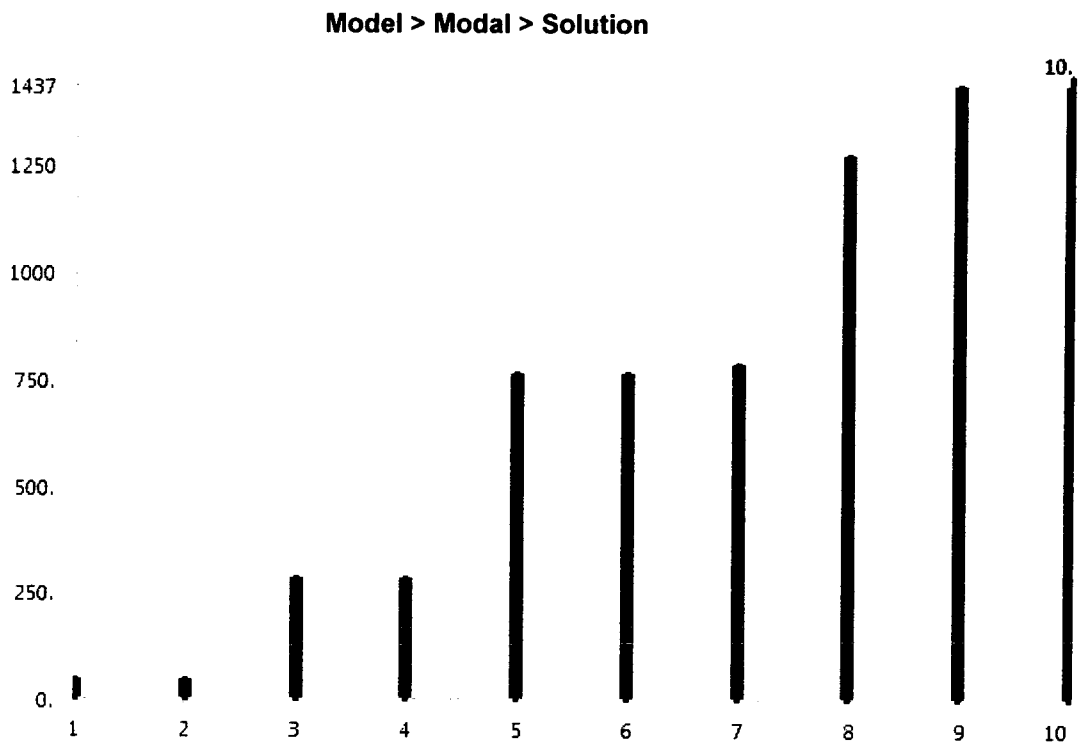
Object Name	<i>Fixed Support</i>
State	Fully Defined
Scope	
Scoping Method	Geometry Selection
Geometry	1 Face
Definition	
Type	Fixed Support
Suppressed	No

Solution

Model > Modal > Solution

Object Name	<i>Solution</i>
State	Solved
Adaptive Mesh Refinement	
Max Refinement Loops	1.
Refinement Depth	2.

The following bar chart indicates the frequency at each calculated mode.



Model > Modal > Solution

Mode	Frequency [Hz]
1.	45.797
2.	45.798
3.	281.22
4.	281.22
5.	763.85
6.	763.87
7.	786.52
8.	1274.1
9.	1274.1
10.	1437.3

Model > Modal > Solution > Solution Information

Object Name	<i>Solution Information</i>
State	Solved
Solution Information	
Solution Output	Solver Output
Newton-Raphson Residuals	0
Update Interval	2.5 s
Display Points	All

Material Data

Stainless Steel

Stainless Steel > Constants

Structural	
Young's Modulus	1.93e+011 Pa
Poisson's Ratio	0.31
Density	7750. kg/m ³
Thermal Expansion	1.7e-005 1/°C
Tensile Yield Strength	2.07e+008 Pa
Compressive Yield Strength	2.07e+008 Pa
Tensile Ultimate Strength	5.86e+008 Pa
Compressive Ultimate Strength	0. Pa
Thermal	
Thermal Conductivity	15.1 W/m·°C
Specific Heat	480. J/kg·°C
Electromagnetics	
Relative Permeability	10000
Resistivity	7.7e-007 Ohm·m

Appendix C Mode Shapes

Test Specimen Mode Shapes, Free-Free Boundary Conditions

ANSYS Mode Shapes



Fig. C1: Mode 1: 224 Hz

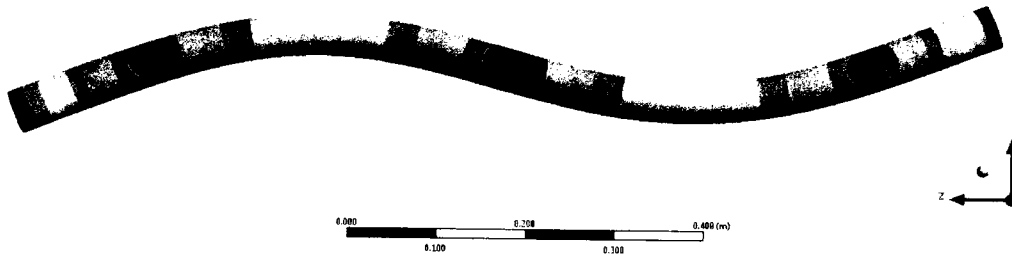


Fig. C2: Mode 2: 607 Hz

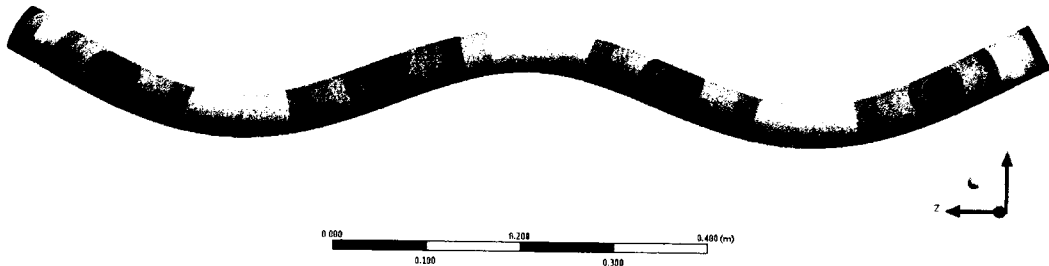


Fig. C3: Mode 3: 1158.6 Hz

Experimentally Determined Mode Shapes

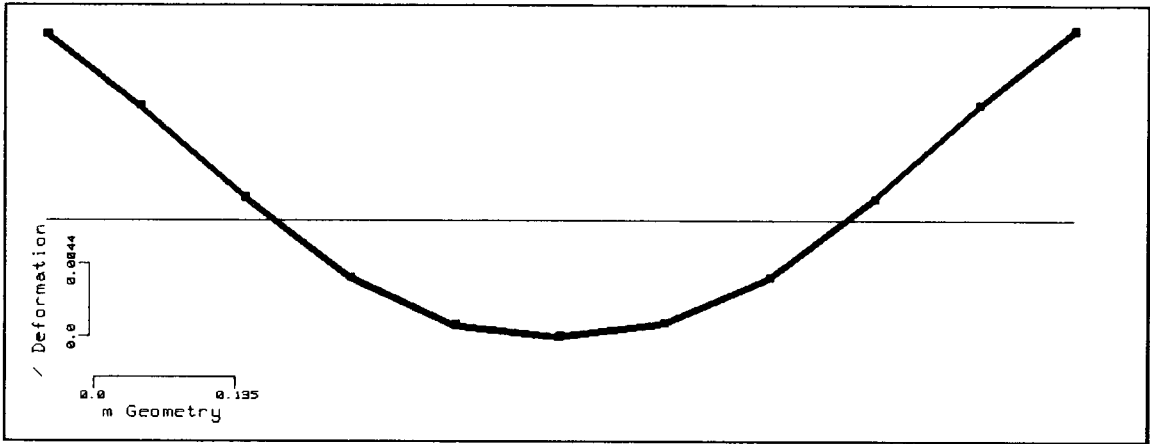


Fig. C4: Mode 1: 271.37 Hz

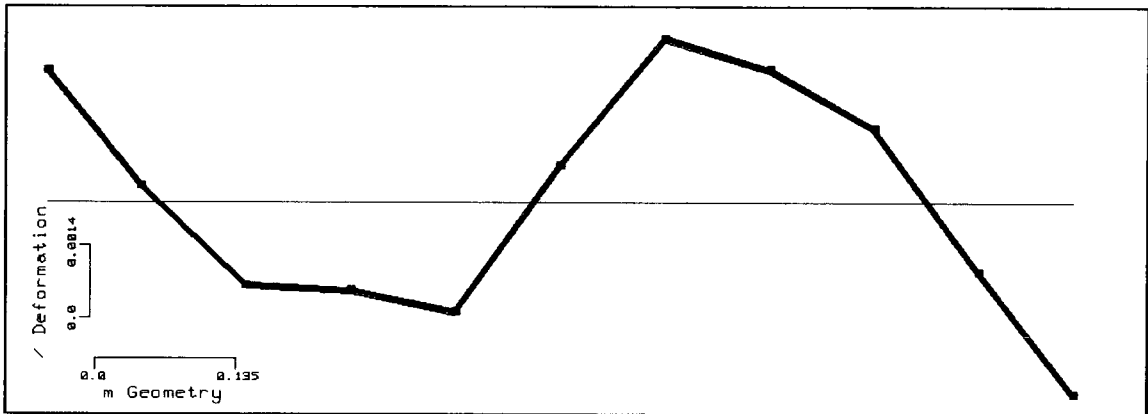


Fig. C5: Mode 2: 732.44 Hz

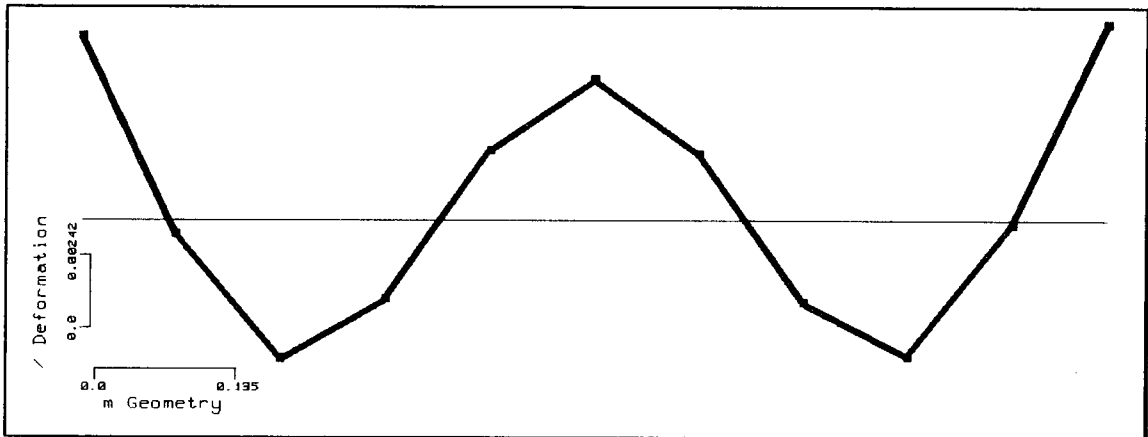


Fig. C6: Mode 3: 1389.62 Hz

Test Specimen Mode Shapes, Fixed-Free Boundary Conditions

ANSYS Mode Shapes

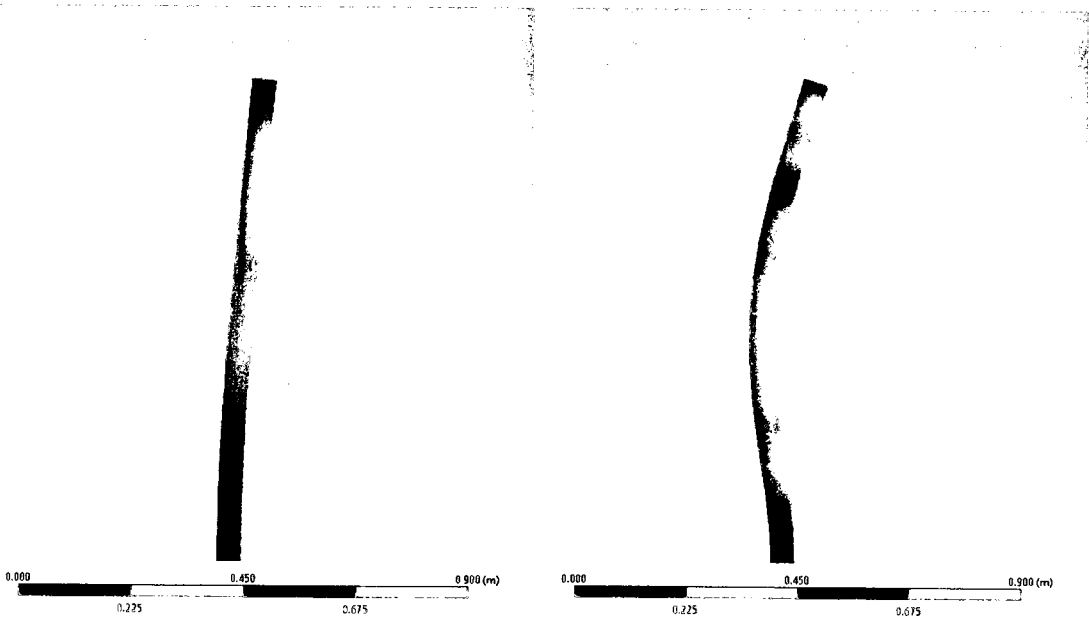


Fig. C7: Mode 1: 46.21 Hz

Fig. C8: Mode 2: 285 Hz

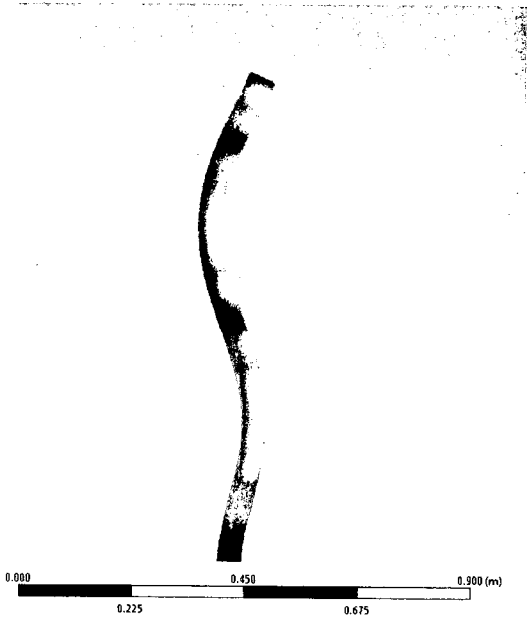


Fig. C9: Mode 3: 776.68 Hz

Experimental Mode Shapes

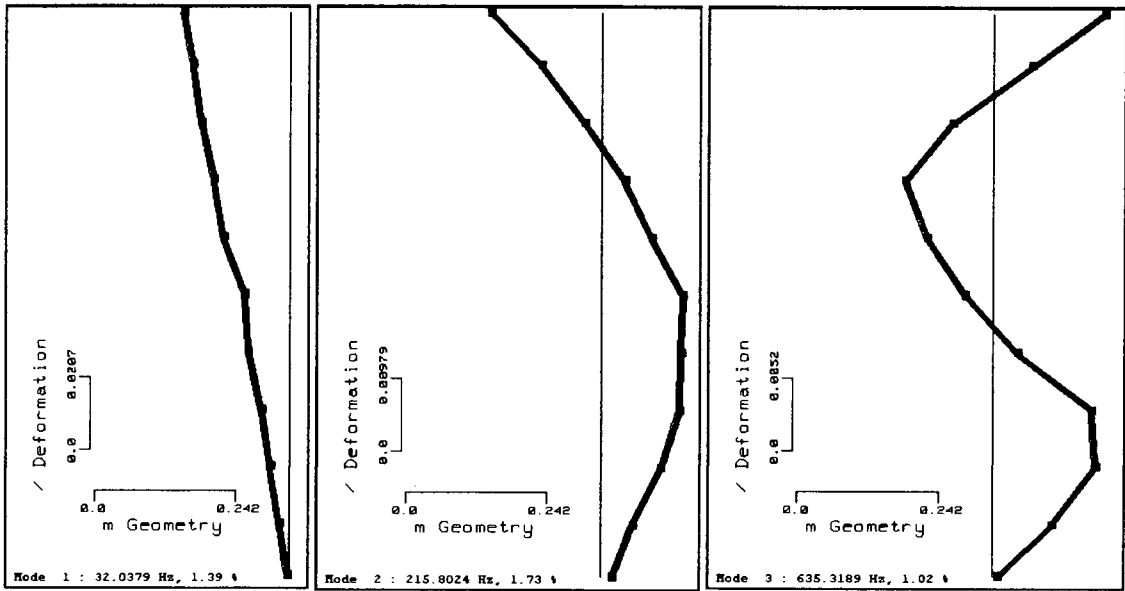


Fig. C10: Mode 1:
32.04 Hz

Fig. C11: Mode 2:
215.80 Hz

Fig. C12: Mode 12:
635.32 Hz

Experimental Wind Turbine Mode Shapes

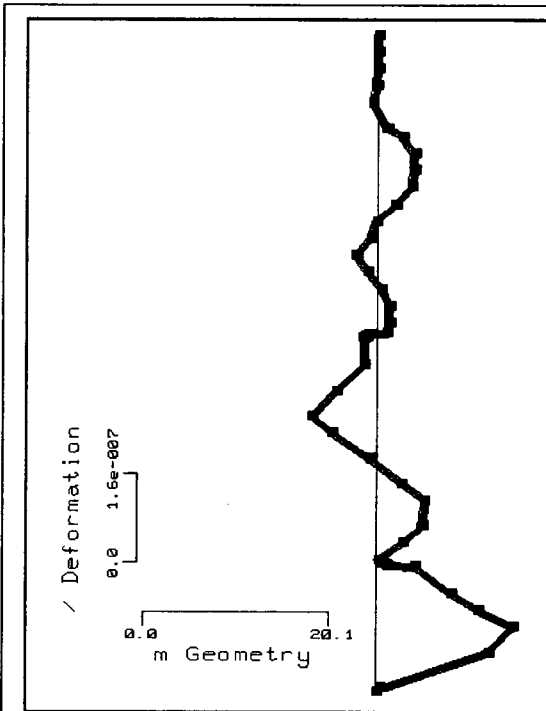


Fig. C23: Mode 1: 16.23

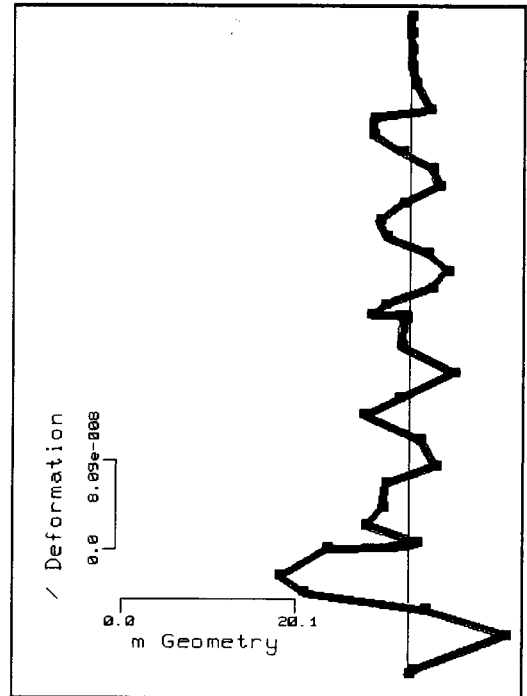


Fig. C24: Mode 2: 30.53

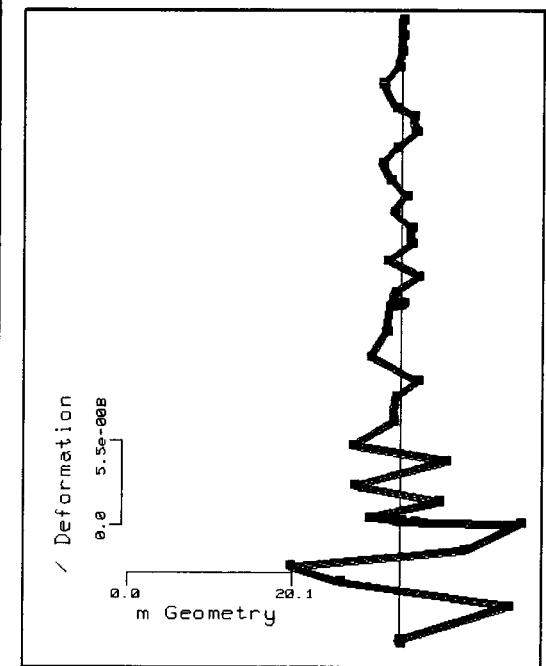


Fig. 25: Mode 3: 60.33

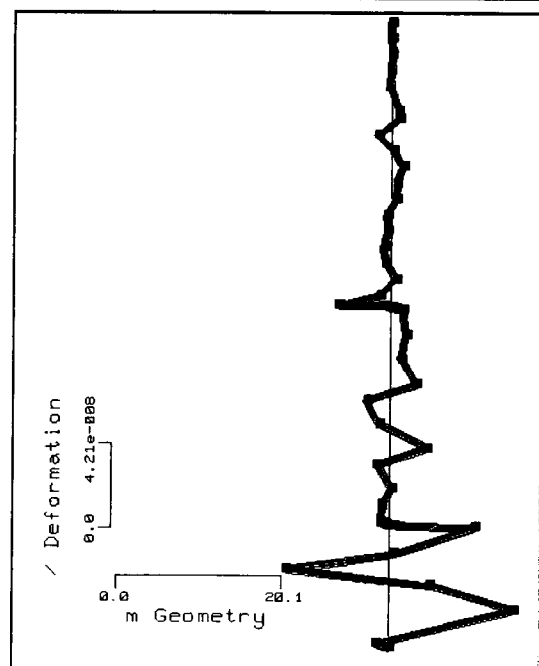


Fig. C26: Mode 4: 78.04

Appendix D

Matlab Program

%%%% Assigning the Three Base Matrices for the Stiffness Calculations %%%%

```
BaseMatrix1=xlsread('C:\Users\Adam\Desktop\Finalized Thesis
Results\Model\Complete Fixed Free\Complete 356 DOF\Complete Model 356
DOF','1st Stiff','G159:CH314');
BaseMatrix2=xlsread('C:\Users\Adam\Desktop\Finalized Thesis
Results\Model\Complete Fixed Free\Complete 356 DOF\Complete Model 356
DOF','2nd Stiff','G159:CH314');
BaseMatrix3=xlsread('C:\Users\Adam\Desktop\Finalized Thesis
Results\Model\Complete Fixed Free\Complete 356 DOF\Complete Model 356
DOF','3rd Stiff','J159:CK318');
```

%%%% Assigning the Base Mass Matrices %%%%

```
MassMatrix1=xlsread('C:\Users\Adam\Desktop\Finalized Thesis
Results\Model\Complete Fixed Free\Complete 356 DOF\Complete Model 356
DOF','1st Mass','B80:CA157');
MassMatrix2=xlsread('C:\Users\Adam\Desktop\Finalized Thesis
Results\Model\Complete Fixed Free\Complete 356 DOF\Complete Model 356
DOF','2nd Mass','B80:CA159');
MassMatrix3=xlsread('C:\Users\Adam\Desktop\Finalized Thesis
Results\Model\Complete Fixed Free\Complete 356 DOF\Complete Model 356
DOF','3rd Mass','D83:CC160');
```

%%%% Assigning Other Variables %%%%

```
ModalMatrix=0;
Stiffness=0;
StiffnessRowCounter=1;
StiffnessColumnCounter=1;
ColumnCounter=3;
RowCounter=1;
LowerRowCounter=RowCounter+1;
RowMover=1;
BaseMatrixRow=0;
DoubleRowMover=0;
```

%%%% Assembling Aggregate Matrix %%%%

```

Aggegrate(1:156,1:80)=BaseMatrix1;
Aggegrate(157:312,79:158)=BaseMatrix2;
Aggegrate(313:472,157:236)=BaseMatrix3;

%First Block%
PreStiffness(1,1)=Aggegrate(1,1)*2;
PreStiffness(1,2)=0;
PreStiffness(2,1)=0;
PreStiffness(2,2)=Aggegrate(2,2)*2;

%Second Bock%
PreStiffness(3,1)=Aggegrate(3,1);
PreStiffness(3,2)=Aggegrate(3,2);
PreStiffness(4,1)=Aggegrate(4,1);
PreStiffness(4,2)=Aggegrate(4,2);

for BigColumnCounter=(3:2:236)

for ColumnCounter=(0:1:1)
    RowCounter=1+DoubleRowMover;
    %Top Block%
    PreStiffness(RowCounter,BigColumnCounter+ColumnCounter)=Aggegrate(Base
MatrixRow+RowCounter,BigColumnCounter+ColumnCounter);
    RowCounter=RowCounter+1;
    PreStiffness(RowCounter,BigColumnCounter+ColumnCounter)=Aggegrate(Base
MatrixRow+RowCounter,BigColumnCounter+ColumnCounter);
    RowCounter=RowCounter+1;

    %Middle Block%
    PreStiffness(RowCounter,BigColumnCounter+ColumnCounter)=Aggegrate(Base
MatrixRow+RowCounter,BigColumnCounter+ColumnCounter)+Aggegrate(BaseMatri
xRow+RowCounter+2,BigColumnCounter+ColumnCounter);
    RowCounter=RowCounter+1;
    PreStiffness(RowCounter,BigColumnCounter+ColumnCounter)=Aggegrate(Base
MatrixRow+RowCounter,BigColumnCounter+ColumnCounter)+Aggegrate(BaseMatri
xRow+RowCounter+2,BigColumnCounter+ColumnCounter);
    RowCounter=RowCounter+1;

    %Bottom Block%
    PreStiffness(RowCounter,BigColumnCounter+ColumnCounter)=Aggegrate(Base
MatrixRow+RowCounter+2,BigColumnCounter+ColumnCounter);
    RowCounter=RowCounter+1;
    PreStiffness(RowCounter,BigColumnCounter+ColumnCounter)=Aggegrate(Base
MatrixRow+RowCounter+2,BigColumnCounter+ColumnCounter);
    RowCounter=RowCounter+1;

```

```

end
ColumnCounter=0;
DoubleRowMover=DoubleRowMover+2;
BaseMatrixRow=BaseMatrixRow+2;
end

for StiffnessRowCounter=(1:1:234)
    for StiffnessColumnCounter=(1:1:234)
        Stiffness(StiffnessRowCounter,StiffnessColumnCounter)=PreStiffness(StiffnessR
owCounter,StiffnessColumnCounter);
    end
    StiffnessColumnCounter=1;
end

%%%%%% Mass Matrices %%%%%%

Mass(1:78,1:78)=MassMatrix1;
Mass(79:156,79:156)=MassMatrix2;
Mass(157:234,157:234)=MassMatrix3;

%%%%%% Code to Find the Natural Frequencies %%%%%%

output=0;
output1=0;
output2=0;
w=0;
Det=0;
DetMatrix=0;

for w=0:1:7000
    output1=output1+1;
    output2=output2+1;
    DetMatrix=(Stiffness-(w^2)*Mass)/1000000;
    Det=det(DetMatrix);
    output(output1,1)=w/2/pi;
    output(output2,2)=Det;
end

```


Appendix E

Comparison of Impact Testing In Still and Moving Air

The results presented in this section were generated by securing a specimen to the base of a wind tunnel and then conducting two sets of impact tests on it, one in still air and one in moving air. The specimen used was the middle section of the model, a 504 mm long aluminum bar, 11 mm wide by 9 mm deep.

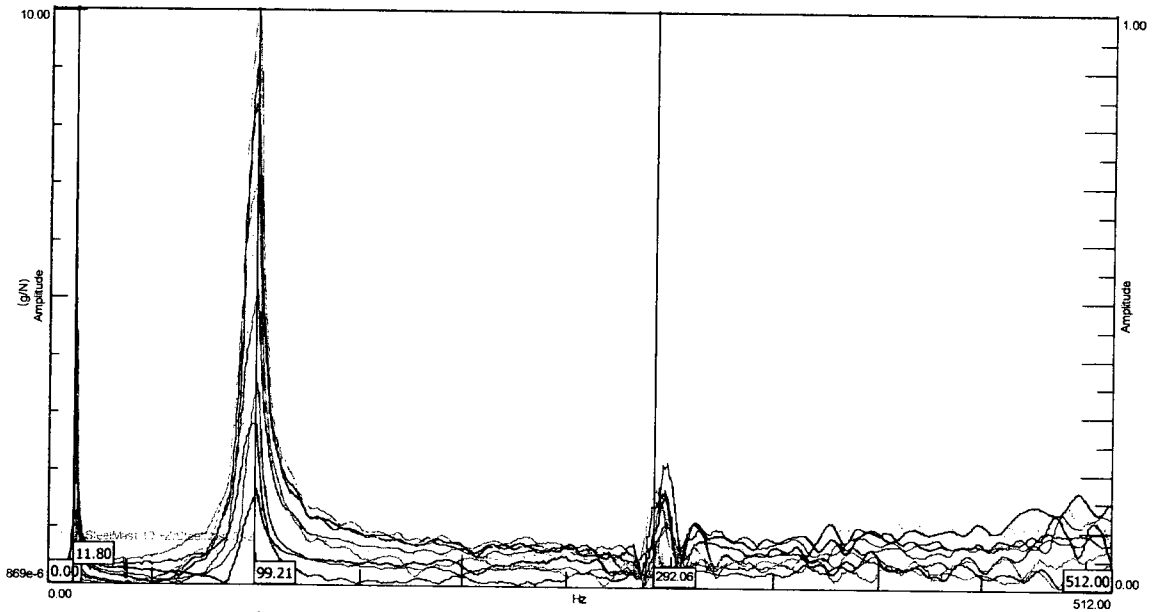


Fig. E1: Resonance Frequencies of Test Specimen in Still Air

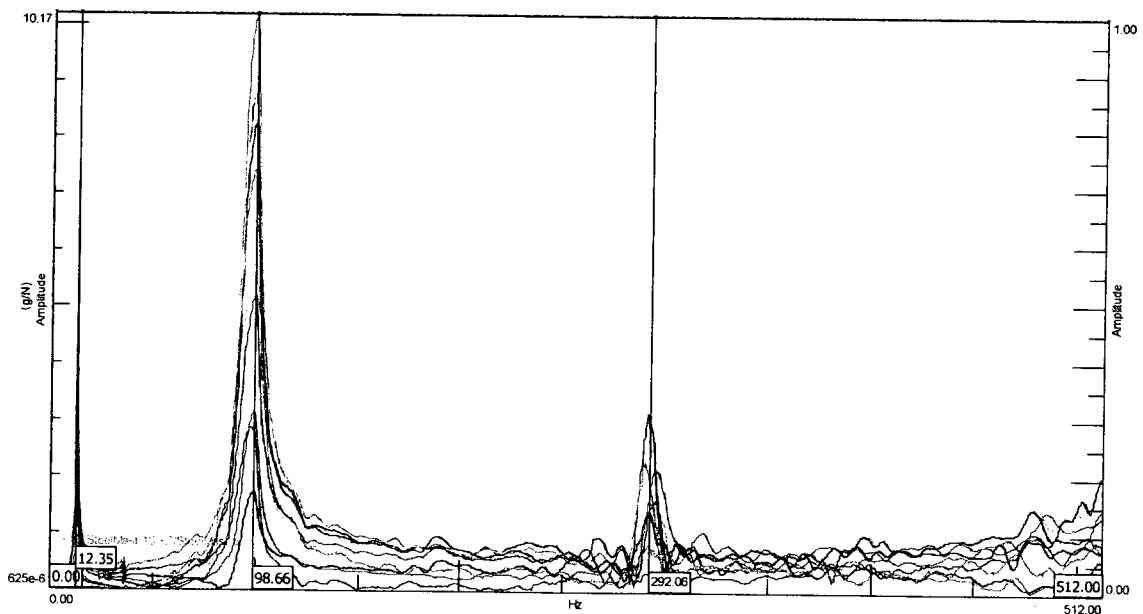


Fig. E2: Resonance Frequencies of Test Specimen in 7 m/s Wind

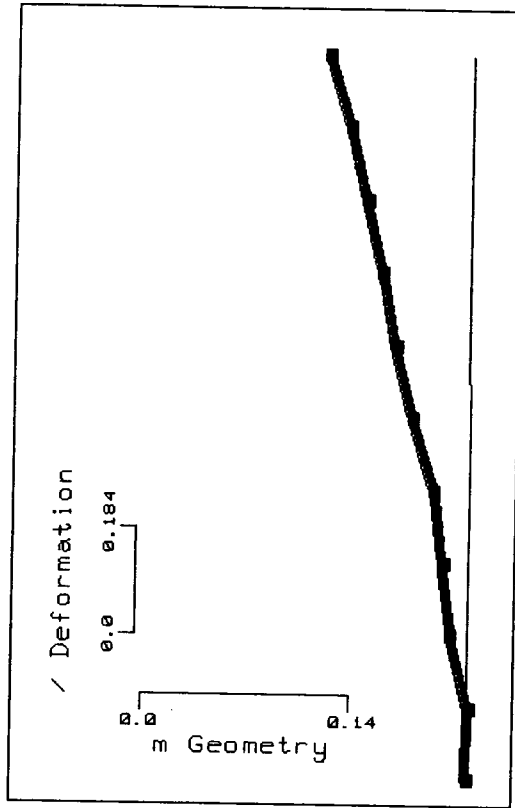


Fig. E3: Mode 1, 12.23 Hz: Still Air

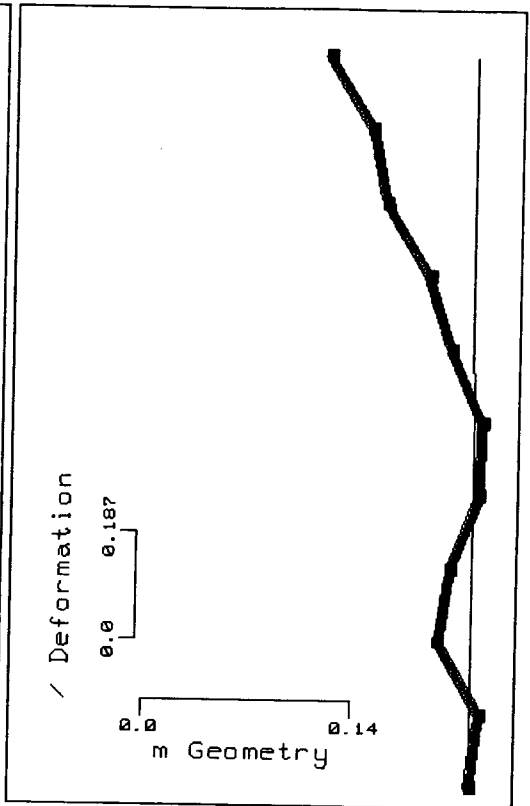


Fig. E4: Mode 1, 12.55 Hz: 7 m/s Wind

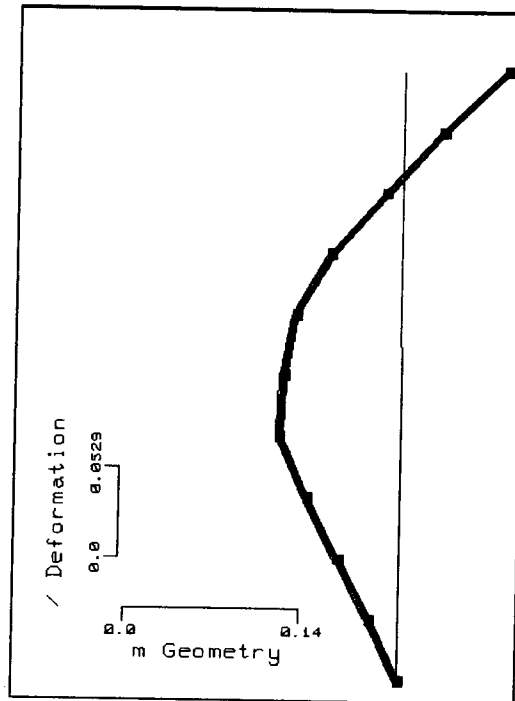


Fig. E5: Mode 2, 99.16 Hz: Still Air

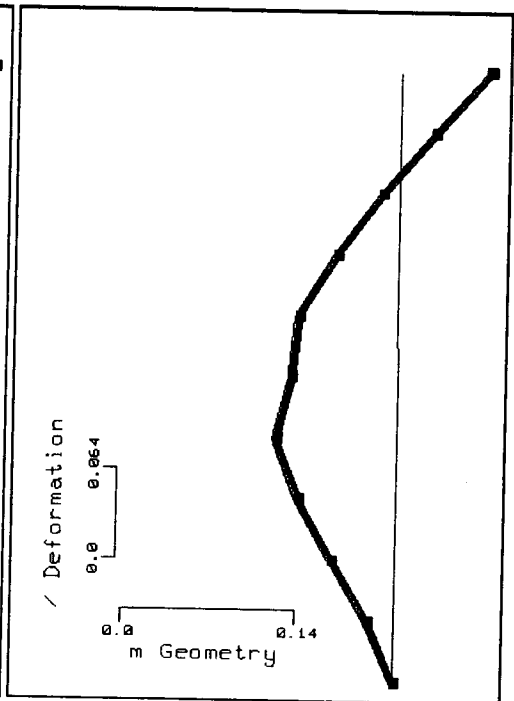


Fig. E6: Mode 2, 98.41 Hz: 7 m/s Wind



Fig. E7: Mode 3, 291.71 Hz: Still Air

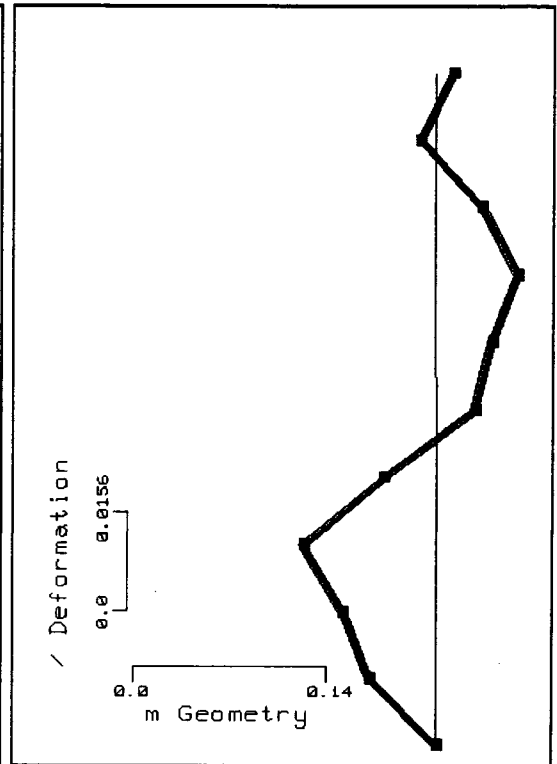


Fig. E8: Mode 3, 293.61 Hz: 7 m/s Wind

Vita Auctoris

Name: Adam Mourad
Place of Birth: Windsor, Ontario
Year of Birth: 1984
Education: Bell River District High School
1998-2003

University of Windsor
2003-2007 B.A.Sc.

University of Windsor
2007-2010 M.A.Sc.